TABLE 8-7
24-HOUR SOURCE BREAKDOWN BASED ON CHEMICAL ELEMENT BALANCE (a)

	Pasadena 9-20-72	Pomona 10-24-72	Riverside 9-20-72	Fresno 9-1-72	San Jose. 10-20-72
Sea Salt	0.7 ± 0.06	5.7 ± 0.6	1.3 ± 0.1	0(c) ± 0.4	19.4 ± 0.5
Soil Dust	19.8 ± 0.1	15.1 ± 0.5	28.5 ± 0.9	51.1 ± 2.8	29.6 ± 1.1
Auto Exhaust	5.1 ± 0.15	7.2 ± 0.3	3.9 ± 0.15	2.2 ± 0.1	8.3 ± 0.33
Cement Dust	1.4 ± 0.15	3.3 ± 0.6	2.3 ± 0.15	0.5 ± 0.14	4.5 ± 1.3
Fly Ash	0.1 ± 0.01	0.2 ± 0.01	0.1 ± 0.01	<0.1 ± 0.01	0.1 ± 0.01
Diesel Exhaust (d)	1.4	1.9	0.9	0.6	2.2
Tire Dust (f)	0.5	0.7	0.4	0.2	0.8
Industr. & Agric. (d)	4.7	6.6	20.5	37.8	27.6
Aircraft (d)	1.3	1.8	7.4	0.9	4.9
$SO_4^=$ (b)	2.9 ± 0.7	19 5	5.9 ± 1.5	4.2 ± 1.0	16.6 ± 3.3
NO_3^- (b)	4.9 ± 0.4	36.4 ± 2.7	12.9 ± 1.0	7.9 ± 0.6	12.3 ± 0.9
NH_4^+ (b)	2.3 ± 0.1	16.3 ± 0.8	5.7 ± 0.3	3.1 ± 0.15	7.2 ± 0.72
Organics (e)	29.6	29.3	24.8	U	U
Water (b)	12 ± 6	18 ± 9	U	U	U
Total Mass	86.7	161.5	114.6	108.5	133.5
Measured Mass	64 7	180 ± 20	125 ± 14	207 ± 23	189 ± 21

(a) Values in $\mu gm/m^3$. Errors associated with sea salt, soil dust, auto exhaust, cement dust and fly ash are standard errors from the least squares fit for the chemical element balance; errors associated with SO_4, NO_3, NH_4, water and measured total mass concentrations are analytical errors.
(b) Measured values.
(c) Value actually found to be slightly negative.
(d) Scaled to auto exhaust based on relative inputs (Table 8.5).
(e) Based on carbon balance (Table 8.6).
(f) Assumed 10% of auto exhaust component.
U = unknown

TABLE 8-8

2-HOUR SOURCE BREAKDOWN BASED ON CHEMICAL ELEMENT BALANCE (a)

	Pasadena 9/20/72 1200 - 1400	Pomona 10/24/72 1200 - 1400
Sea Salt w/$SO_4^=$ replacement (c)	1.1 ± 0.4 (1.3)	2.9 ± 0.4 (3.5)
Soil Dust	7.5 ± 0.5	10.6 ± 0.44
Auto Exhaust	6.0 ± 0.26	6.8 ± 0.4
Cement Dust	1.4 ± 1.3	0.6 ± 0.6
Fly Ash	0.1 ± 0.01	0.1 ± 0.01
Diesel Exhaust (b)	1.6	1.8
Tire Dust (b)	0.6	0.7
Indust. and Agric. (b)	5.5	6.2
Aircraft (b)	1.5	1.7
$SO_4^=$ (e)	3.0 ± 0.6	23 ± 4.5
less replacement (d)	(2.3)	(20.1)
NO_3^- (f)	4.0	46.0
NH_4^+ (e)	U	18 ± 3.7
Organics (g)	33.5	42.0
Water (e)	13 ± 7	U
Total Mass	78.8	160.4
Measured Mass	65 ± 7	227 ± 20

(a) Values in $\mu gm/m^3$, errors as in Table 8.7.

(b) Tire dust assumed to be 10% of auto exhaust component; diesel, aircraft, industrial and agriculture emission scaled to auto exhaust using Table 8.5.

(c) $SO_4^=$ has been assumed to replace Cl^- in sea salt, and these values reflect the mass increase.

(d) $SO_4^=$ left after Cl^- replacement.

(e) Measured values.

(f) Fraction of nitrate assumed equal to 24-hour average.

(g) Based on carbon balance.

U = unknown

Table 8-9 compares measured concentrations of the elements with concentrations calculated from the concentrations of soil dust, sea salt, auto exhaust, flyash and cement dust obtained from the chemical element balance. The species on which the calculation was based, aluminum, sodium, lead, calcium, vanadium, magnesium and potassium, are listed first in the table and show generally good agreement between measured and calculated values. The results are not normalized to specific species so the good agreement adds confidence that the sources identified are the major ones for this set of elements.

A chemical element breakdown was not carried out for the industrial sources. Hence the calculated concentrations for elements in the industrial sources would be expected to be smaller than the measured concentrations. This probably explains the deviations between measured and calculated concentrations for copper, chromium and zinc in Table 8-9. The discrepancy would not appear in the material balance (Tables 8-7 and 8-8) since these species would be included, on a mass basis, in the industrial contribution. Except at Fresno, chlorine was present in smaller concentrations than calculated because it is lost from the aerosol by chemical reactions (Miller et al.,1972; Friedlander, 1973).

The results for the mass contribution calculations for 1973 data are shown in Table 8-10. The agreement is acceptable in all cases. It is interesting to note that the sea salt contribution is larger for the twenty-four hour samples than for the two hour midday samples, indicating that the peak in the marine contribution does not occur at midday. West Covina, Pomona, and Dominguez Hills are dominated by a mixture of secondary organics, ammonium and sulfate contributions while Rubidoux contains a small secondary organic contribution and is dominated by nitrate and sulfate.

Table 8-11 compares measured concentrations of several elements with those predicted from the results of the chemical element balance. Sodium, aluminum, lead, calcium, and vanadium agree quite well; magnesium and potassium show poorer agreement although they were also used in the chemical element balances. The measured concentrations of the magnesium and potassium

TABLE 8-9A

MEASURED AND CALCULATED ELEMENT CONCENTRATION (a)

Element	Pasadena 9/20/72 Calculated	Pasadena 9/20/72 Measured	Pomona 10/24/72 Calculated	Pomona 10/24/72 Measured	Riverside 9/20/72 Calculated	Riverside 9/20/72 Measured
Na (b)	0.716	0.716 ±0.014	2.13	2.06 ±0.20	1.13	1.13 ±0.019
Al (b)	1.66	1.03 ±0.33	1.32	1.30 ±0.42	2.35	2.35 ±0.07
Ca (b)	0.94	0.94 ±0.10	1.83	0.8 ±0.28	1.49	1.49 ±0.07
V (b)	4.8×10^{-3}	$4.8\times10^{-3}\pm2.6\times10^{-4}$	0.014	0.014 $\pm5.2\times10^{-4}$	8.8×10^{-3}	$8.8\times10^{-3}\pm0.000$
Pb (b)	2.03	2.03 ±0.077	2.89	2.89 ±0.12	1.55	1.55 ±0.006
Mg (b)	0.34	< 0.4	0.50	< 0.4	0.50	0.97 ±0.38
K (b)	0.31	0.36 ±0.036	0.31	0.44 ±0.044	0.45	0.68 ±0.068
Mn	0.022	0.023 ±0.002	0.017	0.037 ±0.001	0.031	0.040 ±0.001
Cu	1.7×10^{-3}	0.043 ±0.002	1.6×10^{-3}	0.025 ±0.002	2.4×10^{-3}	0.29 ±0.01
Cl	0.73	0.44 ±0.22	3.6	0.93 ±0.035	1.0	0.76 ±0.026
Br	0.40	0.50 ±0.011	0.58	0.81 ±0.018	0.31	0.39 ±0.009
Cr	5.2×10^{-5}	0.006 ±0.002	1.9×10^{-4}	0.025 ±0.004	1.0×10^{-4}	0.013 ±0.002
Ni	1.8×10^{-3}	0.006 ±0.001	4.4×10^{-3}	0.024 ±0.002	3.2×10^{-3}	0.014 ±0.001
I	9.7×10^{-7}	0.0023 ±0.0005	7.9×10^{-6}	$0.0042\pm7.4\times10^{-4}$	1.9×10^{-6}	$6.4\times10^{-3}\pm7\times10^{-4}$
Fe	0.67	1.15 ±0.044	0.56	1.55 ±0.06	0.94	2.31 ±0.09
Zn	0.009	0.097 ±0.004	0.012	0.23 ±0.009	0.008	0.13 ±0.005

(a) Values in $\mu gm/m^3$; errors represent analytical errors. Calculated values are from estimates of soil dust, sea salt, auto exhaust, cement dust and fly ash from the chemical element balances.
(b) Used in making the chemical element balance; hence, close agreement is expected.
U = unknown

TABLE 8-9B

MEASURED AND CALCULATED ELEMENT CONCENTRATION (a)

Element	Fresno 9/1/72 Calculated	Fresno 9/1/72 Measured	San Jose 10/20/72 Calculated	San Jose 10/20/72 Measured
Na (b)	0.84	0.838±0.084	6.70	6.71 ±0.15
Al (b)	4.20	4.97 ±0.75	2.54	2.56 ±0.082
Ca (b)	0.98	0.98 ±0.049	2.75	2.72 ±0.58
V (b)	0.005	< 0.02	0.011	$0.011 \pm 7 \times 10^{-4}$
Pb (b)	0.87	0.87 ±0.04	3.34	3.34 ±0.13
Mg (b)	0.67	0.68 ±0.035	1.24	3.5 ±0.91
K (b)	0.75	0.70 ±0.070	0.68	0.62 ±0.062
Mn	0.056	0.051±0.003	0.033	0.047±0.003
Cu	4.1×10^{-3}	0.012±0.001	2.6×10^{-3}	1.5 ±0.006
Cl	0.15	0.38 ±0.06	11.2	7.9 ±0.20
Br	0.17	0.204±0.008	0.69	1.19 ±0.027
Cr	2.8×10^{-5}	0.012±0.003	1.4×10^{-4}	0.032±0.005
Ni	2.6×10^{-3}	0.011±0.001	3.9×10^{-3}	0.025±0.004
I	0	U	2.7×10^{-5}	0.011±0.002
Fe	1.65	2.13 ±0.08	1.0	1.95 ±0.08
Zn	0.003	0.115±0.005	0.015	0.16 ±0.006

(a) Values in $\mu gm/m^3$; errors represent analytical errors. Calculated values are from estimates of soil dust, sea salt, auto exhaust, cement dust and fly ash from the chemical element balances.

(b) Used in making the chemical element balance; hence, close agreement is expected.

U = unknown

TABLE 8-10A

ESTIMATED SOURCE CONTRIBUTIONS - 2 HR FILTERS (a)

Source	West Covina 7/24/73 1200 - 1400	Pomona 8/17/74 1200 - 1400	Rubidoux 9/6/73 1200 - 1400	Dominguez Hills 10/5/73 1000 - 1200
Sea Salt (b)	8.15 ± 0.7 (4.48 ± 0.38)	2.78 ± 6.7 (1.53 ± 0.37)	0.0 (0.0)	11.5 ± 0.69 (6.32 ± 0.38)
Soil Dust	31.5 ± 1.2	43.9 ± 1.7	40.4 ± 1.6	18.0 ± 0.8
Auto Exhaust	10.0 ± 0.4	7.80 ± 0.28	3.93 ± 0.16	3.29 ± 0.13
Diesel Exhaust	2.70 ± 0.10	2.10 ± 0.08	0.947 ± 0.035	0.891 ± 0.035
Tire Dust	1.00 ± 0.04	0.780 ± 0.028	0.393 ± 0.016	0.329
Aircraft	2.51 ± 0.10	1.95 ± 0.07	7.10 ± 0.28	0.821 ± 0.013
Industrial	9.19 ± 0.42	7.17 ± 0.28	16.9 ± 0.7	3.03 ± 0.12
Fuel Oil	0.647 ± 0.028	0.910 ± 0.038	0.190 ± 0.014	0.831 ± 0.026
Cement Dust	3.39 ± 0.18	3.09 ± 0.18	5.82 ± 0.29	0.737 ± 0.085
Agricultural	0	0	3.74 ± 0.15	0
Total Primary	69.1 ± 1.4	70.5 ± 1.9	79.4 ± 2.1	39.4 ± 1.1
Organics	56.4 ± 3.6	48.3 ± 3.0	6.39 ± 2.55	24.6 ± 2.1
$SO_4^=$ (c, e)	36.0 ± 4.3	33.4 ± 3.6	13.1 ± 1.3	42.2 ± 5.0
NO_3^- (e)	12.0 ± 1.2	14.6 ± 1.5	70.0 ± 7.0	5.1 ± 0.5
NH_4^+ (d)	13.2 ± 1.3	10.5 ± 0.8	12.4 ± 1.3	6.07 ± 0.66
Total Secondary	118 ± 7	107 ± 6	102 ± 7	78.0 ± 5.4
Water	31.4 ± 2.3	16.3 ± 2.2	22.8 ± 2.3	38.0 ± 2.1
Total Mass	219 ± 8	194 ± 7	204 ± 8	155 ± 6
Measured	268 ± 2	249 ± 2	260 ± 2	134 ± 2

(a) Contributions in $\mu gm/m^3$. Errors reflect analytical errors in chemical analyses only.

(b) First number is with Cl^- replaced by HSO_4^-. Second number is without replacement.

(c) Does not include HSO_4^- used in Cl^- replacement in sea salt.

(d) Mass fraction assumed equal to 24 hr filter.

(e) Measured.

TABLE 8-10B

ESTIMATED SOURCE CONTRIBUTIONS - 24 HR FILTERS (a)

Source	West Covina 7/24/73	Pomona 8/17/73	Rubidoux 9/6/73	Dominguez Hills 10/5/73
Sea Salt (b)	20.0 ± 0.7 (11.0 ± 0.4)	11.1 ± 0.5 (6.09 ± 0.26)	13.7 ± 0.5 (7.5 ± 0.30)	22.4 ± 0.7 (12.3 ± 0.4)
Soil Dust	30.8 ± 0.2	33.0 ± 0.2	31.3 ± 0.2	20.5 ± 0.2
Auto Exhaust	9.68 ± 0.42	5.19 ± 0.2	3.81 ± 0.16	2.80 ± 0.10
Diesel Exhaust	2.60 ± 0.10	1.40 ± 0.06	0.912 ± 0.035	0.758 ± 0.028
Tire Dust	1.31 ± 0.06	0.519 ± 0.021	0.381 ± 0.016	0.280 ± 0.010
Aircraft	2.42 ± 0.10	1.29 ± 0.06	7.24 ± 0.28	0.703 ± 0.028
Industrial	8.91 ± 0.35	4.77 ± 0.19	16.4 ± 0.7	2.58 ± 0.10
Fuel Oil	0.453 ± 0.009	0.543 ± 0.009	0.302 ± 0.008	0.952 ± 0.010
Cement Dust	3.19 ± 0.22	2.87 ± 0.22	7.01 ± 0.42	1.78 ± 0.13
Agricultural	0	0	3.62 ± 0.15	0
Total Primary	79.0 ± 1.2	60.7 ± 0.81	84.7 ± 1.4	52.8 ± 0.8
Organics	22.5 ± 2.0	17.6 ± 1.2	1.65 ± 1.50	12.1 ± 0.8
$SO_4^=$ (c,e)	18.0 ± 3.3	10.2 ± 1.8	0	15.7 ± 3.2
NO_3^- (e)	6.79 ± 0.68	4.81 ± 0.48	42.4 ± 4.2	0.936 ± 0.094
NH_4^+ (e)	10.4 ± 1.0	7.32 ± 0.73	12.3 ± 1.2	6.70 ± 0.67
Total Secondary	57.7 ± 4.0	39.9 ± 2.4	56.4 ± 4.6	35.4 ± 3.4
Water	65.1 ± 2.2	36.6 ± 1.5	64.7 ± 2.9	69.2 ± 2.3
Total Mass	203 ± 5	137 ± 3	206 ± 6	157 ± 4
Measured	211 ± 2	180 ± 2	262 ± 2	148 ± 2

(a) Contributions in $\mu gm/m^3$. Errors reflect analytical errors in chemical analyses only.

(b) First number is with Cl^- replaced by HSO_4^-. Second number is without replacement.

(c) Does not include HSO_4^- used in Cl^- replacement in sea salt.

(e) Measured.

TABLE 8-11

MEASURED AND CALCULATED ELEMENT CONCENTRATIONS (a)

Element	West Covina 7/24/73 1200 - 1400		Pomona 8/17/73 1200 - 1400	
	Calculated	Measured	Calculated	Measured
Na (N) (b)	2.20	2.12 ± 0.11	1.62	1.61 ± 0.11
Al (N)	2.67	2.39 ± 0.10	3.68	3.58 ± 0.14
Ca (x)	2.09	2.09 ± 0.08	2.11	2.11 ± 0.08
U (x)	0.0472	0.0472 ± 0.0020	0.0663	0.0663 ± 0.0027
Pb (x)	3.89	3.89 ± 0.15	3.02	3.02 ± 0.12
Mg (N)	0.689	1.71 ± 0.86	0.746	1.13 ± 1.13 (c)
K (x)	0.542	1.69 ± 0.08	0.693	1.15 ± 0.12
Mn (x)	0.0350	0.093 ± 0.007	0.0488	0.084 ± 0.007
Cu (x)	0.00381	0.061 ± 0.004	0.00533	0.028 ± 0.004
Cl (N)	2.46	0.537 ± 0.063	0.841	0.444 ± 0.061
Br (N)	1.85	0.670 ± 0.019	1.85	0.456 ± 0.013
Cr (x)	0.000647	0.035 ± 0.008	0.00091	0.012 ± 0.012 (c)
Ni (x)	0.0142	0.053 ± 0.004	0.0200	0.067 ± 0.004
I (N)	6.27×10^{-6}	0.0105 ± 0.0011	2.14×10^{-6}	0.00880 ± 0.00117
Fe (x)	1.09	3.58 ± 0.14	1.49	3.42 ± 0.14
Zn (x)	0.0275	0.456 ± 0.018	0.0213	0.193 ± 0.008

(a) Concentrations in $\mu gm/m^3$. Errors in measured values reflect uncertainties in chemical analysis. Elements above line (Na-K) used in chemical element balance.

(b) Method of analysis: N-neutron activation analysis; α-x-ray fluorescence analysis.

(c) Not detected. Assumed equal to one-half of lower limit of detection with 100% uncertainty.

TABLE 8-11

MEASURED AND CALCULATED ELEMENT CONCENTRATIONS (Continued)

Element	West Covina 7/24/73 - 24 hour		Pomona 8/17/73 - 24 hour	
	Calculated	Measured	Calculated	Measured
Na (N) (b)	4.16	4.13 ± 0.12	2.73	2.72 ± 0.08
Al (N)	2.61	2.60 ± 0.02	2.78	2.77 ± 0.02
Ca (x)	2.06	2.06 ± 0.10	1.89	1.89 ± 0.10
V (N)	0.0336	0.0336 ± 0.0007	0.0400	0.0400 ± 0.0006
Pb (x)	3.75	3.75 ± 0.15	2.01	2.01 ± 0.08
Mg (N)	0.913	1.39 ± 0.59	0.756	0.839 ± 0.466
K (x)	0.600	0.957 0.096	0.578	0.933 ± 0.093
Mn (x)	0.0341	0.076 ± 0.005	0.0366	0.071 ± 0.004
Cu (x)	0.00337	0.041 ± 0.002	0.00373	0.026 ± 0.002
Cl (N)	6.05	0.425 ± 0.024	3.35	0.343 ± 0.018
Br (N)	1.80	0.555 ± 0.016	0.965	0.433 ± 0.016
Cr (x)	0.000453	0.015 ± 0.005	0.000543	0.018 ± 0.004
Ni (x)	0.0103	0.050 ± 0.002	0.0122	0.042 ± 0.002
I (N)	1.54×10^{-5}	0.0116 ± 0.0012	8.53×10^{-6}	0.00767± 0.00073
Fe (x)	1.05	2.92 ± 0.12	1.12	2.77 ± 0.11
Zn (x)	0.0265	0.462 ± 0.018	0.0144	0.169 ± 0.007

TABLE 8-11

MEASURED AND CALCULATED ELEMENT CONCENTRATIONS (Continued)

Element	Rubidoux 9/6/73 1200-1400		Dominguez Hills 10/5/73 1000-1200	
	Calculated	Measured	Calculated	Measured
Na(N) (b)	0.983	0.969 ± 0.094	2.43	2.43 ± 0.11
Al (N)	3.45	3.34 ± 0.13	1.50	1.50 ± 0.06
Ca (x)	3.28	3.28 ± 0.13	0.693	0.693 ± 0.004
V (N)	0.0157	0.0157 ± 0.0010	0.0592	0.0592 ± 0.0018
Pb (x)	1.50	1.50 ± 0.06	1.28	1.28 ± 0.05
Mg (N)	0.698	2.35 ± 0.92	0.504	0.552 ± 0.622
K (x)	0.635	1.37 ± 0.14	0.345	0.355 ± 0.063
Mn (x)	0.0446	0.069 ± 0.006	0.0203	0.033 ± 0.006
Cu (x)	0.00361	0.042 ± 0.003	0.00310	0.021 ± 0.003
Cl (N)	0.0	0.560 ± 0.061	3.45	0.156 ± 0.53
Br (N)	0.708	0.266 ± 0.008	0.618	0.154 ± 0.004
Cr (x)	0.00019	0.011 ± 0.011 (c)	0.000831	0.0105 ± 0.015 (c)
Ni (x)	0.00545	0.010 ± 0.003	0.0173	0.047 ± 0.003
I (N)	0	0.00629 ± 0.00091	8.85×10^{-6}	0.0142 ± 0.0010
Fe (x)	1.37	3.15 ± 0.13	0.634	1.01 ± 0.4
Zn (x)	0.0106	0.142 ± 0.006	0.00918	0.142 ± 0.006

TABLE 8-11

MEASURED AND CALCULATED ELEMENT CONCENTRATIONS (Continued)

Element	Rubidoux 9/6/73 - 24 hour		Dominguez Hills 10/5/73 - 24 hour	
	Calculated	Measured	Calculated	Measured
Na (N)	3.13	3.12 ± 0.09	4.34	4.31 ± 0.12
Al (N)	2.74	2.74 ± 0.02	1.73	1.73 ± 0.12
Ca (x)	3.79	3.78 ± 0.02	1.28	1.28 ± 0.06
V (N)	0.0230	0.0230 ± 0.0005	0.0678	0.0678 ± 0.0007
Pb (x)	1.45	1.45 ± 0.06	1.09	1.09 ± 0.04
Mg (N)	0.886	1.49 ± 0.50	0.786	1.57 ± 0.46
K (x)	0.591	1.28 ± 0.13	0.454	0.568 ± 0.57
Mn (x)	0.0346	0.092 ± 0.004	0.0231	0.042 ± 0.003
Cu (x)	0.00311	0.027 ± 0.002	0.00355	0.020 ± 0.001
Cl (N)	4.14	0.844 ± 0.034	6.77	0.245 ± 0.017
Br (N)	0.700	0.217 ± 0.006	0.539	0.203 ± 0.006
Cr (x)	0.000302	0.024 ± 0.004	0.000952	0.020 ± 0.003
Ni (x)	0.00732	0.034 ± 0.002	0.0199	0.065 ± 0.003
I (N)	1.05×10^{-5}	0.00576± 0.0089	1.72×10^{-5}	0.0104 ± 0.0008
Fe (x)	1.10	3.52 ± 0.14	0.733	1.54 ± 0.06
Zn (x)	0.0103	0.172 ± 0.007	0.00785	0.353 ± 0.014

were considerably higher than those found in 1972, for which Gartrell and Friedlander[85] obtained good agreement between measured and calculated values. Elements for which the measured concentrations are higher than the calculated may come from industrial sources for which a chemical element balance was not made. Elements for which the concentrations are lower, such as bromine and chlorine, may be lost from the aerosol as a result of atmospheric chemical reactions.

Table 8-12 shows the results of the assignment of the non-organic secondary sources along with associated water based on assumption of saturated salt solutions. The calculated water concentrations ranged from 8.4 to 14.3 percent for the midday samples at West Covina, Pomona, and Rubidoux while the two hour concentration for Dominguez Hills was 24.5 percent. The twenty-four hour concentrations were on the order of 30 percent except at Dominguez Hills where it was 44 percent. The values measured in 1972 were 10 to 20 percent, indicating that the present estimates are reasonable. The assignment of the non-organic secondary components to chemical compounds was generally successful, the exceptions being the two hour samples at Rubidoux and Dominguez Hills, where exceptionally large nitrate and sulfate loadings were measured.

5. CARBON BALANCE

The 1972 carbon data were obtained by collecting with a silver membrane filter and analyzing for CO_2. The carbon balance was based on the method of Friedlander[83]. All of the diesel exhaust, aircraft and agricultural aerosols were assumed to be carbon. Frey and Corn[89] found that 85 to 93% of diesel exhaust aerosol was comprised of inorganic and organic carbon. For automobile exhaust, carbon was assumed to comprise 90% of the tar in the particulates. In the absence of other information, we have again assumed that the fraction of carbon in industrial emissions was the same as the fraction measured in the total particulate, about 25% for the daily average during these experiments. As shown below, the carbon balance is not sensitive to this assumption. In this way, estimates were made of the amounts of carbon from primary sources in the aerosol. The difference between the measured carbon and the primary carbon is assigned to organic compounds resulting from

TABLE 8-12

ASSIGNMENT OF NON-ORGANIC SECONDARY SPECIES
TO CHEMICAL COMPOUNDS AND ASSOCIATED WATER (a)

	Total (c)	$SO_4^=$	NO_3^-	NH_4^+	H_2O
West Covina - 7/24/73 1200-1400					
$NaHSO_4$	7.15 ± 0.63	5.72 ± 0.50	0	0	25.0 ± 2.2
NH_4NO_3	15.5 ± 1.5	0	12.0 ± 1.2	3.48 ± 0.30	6.41± 0.62
NH_4HSO_4	44.0 ± 5.2	36.78 ± 4.33	0	6.89 ± 0.81	0
Excess		0	0	2.84 ± 1.58	
Total (d)		42.5 ± 4.3	12.0 ± 1.2	13.2 ± 1.33(b)	
Pomona - 8/17/73 1200-1400					
$NaHSO_4$	2.44 ± 0.59	1.95 ± 0.47	0	0	8.54± 2.07
NH_4NO_3	18.8 ± 1.9	0	14.6 ± 1.5	4.24 ± 0.42	7.80± 0.78
NH_4HSO_4	40.0 ± 4.2	33.4 ± 3.6	0	6.25 ± 0.67	
Excess		0	0	0	
Total (d)		35.3 ± 3.5	14.6 ± 1.5	10.5 ± 0.8(b)	
Rubidoux - 9/6/73 1200-1400					
$NaHSO_4$	0	0	0	0	0
NH_4NO_3	55.1 ± 5.5	0	42.7 ± 4.3	12.4 ± 1.3	22.8 ± 2.3
NH_4HSO_4	0	0	0	0	0
Excess		13.1 ± 1.3	27.3 ± 8.2	0	
Total (d)		13.1 ± 1.3	70.0 ± 7.0	12.4 ± 1.3(b)	

(a) $\mu gm/m^3$

(b) Mass fraction assumed equal to 24-hr sample

(c) Excludes water

(d) Measured

TABLE 8-12

ASSIGNMENT OF NON-ORGANIC SECONDARY SPECIES
TO CHEMICAL COMPOUNDS AND ASSOCIATED WATER (Continued)

	Total (c)	$SO_4^=$	NO_3^-	NH_4^+	H_2O
Dominguez Hills - 10/5/73 1000-1200					
$NaHSO_4$	10.1 ± 0.6	8.07 ± 4.8	0	0	35.3 ± 2.1
NH_4SO_3	6.6 ± 0.7	0	5.1 ± 0.51	1.48 ± 0.15	2.72 ± 0.27
NH_4HSO_4	29.3 ± 4.1	24.5 ± 3.4	0	4.59 ± 0.64	
Excess		17.7 6.1	0	0	
Total (d)		50.3 ± 5.0	5.1 ± 0.51	6.07 ± 0.66(b)	
West Covina - 7/24/73 - 24 hr					
$NaHSO_4$	17.6 ± 0.6	14.1 ± 0.5	0	0	61.5 ± 2.2
NH_4NO_3	8.76± 0.88	0	6.79 ± 0.68	1.97 ± 0.20	3.63 ± 0.36
$(NH_4)_2SO_4$	24.8 ± 3.5	18.0 ± 3.3	0	6.76 ± 1.22	
Excess		0	0	1.67 ± 1.24	
Total (d)		32.1 ± 3.2	6.79 ± 0.68	10.4 ± 1.0	
Pomona - 8/17/73 - 24 hr					
$NaHSO_4$	9.71± 0.41	7.77 ± 0.33	0	0	34.0 ± 1.4
NH_4NO_3	6.21± 0.62	0	4.81 ± 0.48	1.40 ± 0.14	2.57 ± 0.26
$(NH_4)_2SO_4$	14.1 ± 2.5	10.2 ± 1.8	0	3.83 ± 0.69	
Excess		0	0	2.09 ± 1.01	
Total (d)		18.0 ± 1.8	4.81 ± 0.48	7.32 ± 0.73	

TABLE 8-12

ASSIGNMENT OF NON-ORGANIC SECONDARY SPECIES
TO CHEMICAL COMPOUNDS AND ASSOCIATED WATER (Continued)

	Total (c)	$SO_4^=$	NO_3^-	NH_4^+	H_2O
Rubidoux - 9/6/73 - 24 hr					
$NaHSO_4$	12.0 ± 0.3	9.61 ± 0.38	0	0	42.0 ± 1.7
NH_4NO_3	54.7 ± 5.5	0	42.4 ± 4.2	12.3 ± 1.2	22.7 ± 2.3
NH_4HSO_4	0	0	0	0	
Excess		0	0	0	
Total (d)		9.61 ± 0.38	42.4 ± 4.2	12.3 ± 1.2	
Dominguez Hills - 10/5/73 - 24 hr					
$NaHSO_4$	19.6 ± 0.7	15.7 ± 0.5	0	0	
NH_4NO_3	1.21 ± 0.12	0	0.936 ± 0.094	0.272 ± 0.027	68.7 ± 2.3
$(NH_4)_2SO_4$	21.6 ± 4.4	15.7 ± 3.2	0	5.88 ± 1.19	.501 ± 0.050
Excess		0	0	0.548 ± 1.4	
Total (d)		31.4 ± 3.3	0.936 ± 0.094	6.70 ± 0.67	

gases converted by atmospheric reactions. As shown in Table 8-13, most of the aerosol carbon came from secondary conversion with only small contributions from the individual primary sources.

Recent measurements[90] indicate that about two-thirds of the organic fraction of the Pasadena aerosol is carbon on those smoggy days when the aerosol carbon is dominated by atmospheric conversion. This is in good agreement with the results reported by Mader, et al.[91] Thus, the organic fraction of the aerosol which results from gas-to-particle transformation was assumed to be 3/2 of the excess carbon found from the carbon balance.

The results of the carbon balance for the 1973 period are shown in Table 8-14. The carbon concentration in the motor vehicle sources (auto exhaust, diesel exhaust, and tire dust) was assumed to be that in Table 8-6. Aircraft and agricultural sources were assumed to be 100 percent carbon. The fraction in industrial emissions was assumed equal to the total filter measured fraction and ranged from 6 to 18 percent. The large primary carbon contributions at Rubidoux were due primarily to the large scaling for estimating aircraft from automobile contributions in Riverside County and the large carbon content assumed for aircraft emissions.

C. SIZE DISTRIBUTIONS OF PRIMARY SOURCES

The method of estimating source contributions can be checked in part by comparing predicted and measured size distribution after accounting for particle growth. For the primary sources, Heisler et al.[84] used size distributions of auto exhaust, sea salt and soil dust reported by Whitby et al.,[92] Woodcock[93] and Blifford[94], respectively. More recent data have now become available for the size distributions of these sources.

Woodcock[93] made measurements of sea salt over the Pacific Ocean near Hawaii for a range of particle diameters from approximately 1.25 μm to 10 μm. More recently, Junge[95] has reported the size distribution of marine aerosol collected over the Atlantic Ocean for periods with and without contributions of particles from the Sahara. His measurements include particles smaller than 1 μm in diameter. Junge's data for particles with diameters ranging from 0.25 μm to 12. μm (without the contribution of dust from the Sahara desert)

TABLE 8-13

CARBON BALANCE BASED ON 1972 DATA (a)

Carbon Source	Pasadena 9/20 24-hr	Pomona 10/24 24-hr	Riverside 9/20 24-hr	Pasadena 9/20 1200-1400	Pomona 10/24 1200-1400
Auto Exhaust (b)	2.1	2.9	1.6	2.4	2.6
Diesel Exhaust (c)	1.4	1.9	0.9	1.6	1.3
Industrial Emissions (d)	1.2	1.7	4.2	1.4	1.6
Aircraft Exhaust (c)	1.3	1.8	7.4	1.5	1.7
Tire Dust (e)	0.4	0.6	0.3	0.5	0.6
Agriculture (c)	-	-	3.7	-	-
Organic Conversion as C (by difference)	19.7	19.5	16.5	22.3	28.0

(a) Values in $\mu gm/m^3$ are taken to 0.1 $\mu gm/m^3$ for bookkeeping purposes only. Since diesel, industrial, aircraft and agriculture emissions are scaled to auto exhaust using Table 8.12, it is not possible to give error values for these estimates.

(b) Carbon assumed to comprise 90% of tar in particulates.

(c) Assumed 100% carbon.

(d) Assumed equal to fraction of carbon found in aerosol, ~25%.

(e) 87.3% carbon, after Friedlander (1973).

TABLE 8-14

CARBON BALANCE (a)

Source	West Covina 7/24/73 1200 - 1400	Pomona 8/17/73 1200 - 1400	Rubidoux 9/6/73 1200 - 1400	Dominguez Hills 10/5/73 1200 - 1400
Auto Exhaust + Tire Dust + Diesel Exhaust	5.83 ± 0.24	4.54 ± 0.17	2.24 ± 0.09	1.92 ± 0.087
Aircraft (b)	2.51 ± 0.10	1.95 ± 0.07	7.45 ± 0.28	0.82 ± 0.03
Industrial (c)	1.64 ± 0.07	1.15 ± 0.06	1.34 ± 0.12	0.44 ± 0.02
Agricultural (b)	0	0	5.37 ± 0.22	0
Sum of Primary Carbon	9.99 ± 0.41	7.64 ± 0.30	16.4 ± 0.7	3.18 ± 0.13
Total Carbon	47.6 ± 2.4(d)	39.8 ± 2.0(d)	20.66 ± 1.52(e)	19.58 ± 1.35(e)
Secondary Carbon	37.6 ± 2.4	32.2 ± 2.0	4.26 ± 1.7	16.4 ± 1.4
Organics-Secondary	56.4 ± 3.6	48.3 ± 3.0	6.39 ± 2.55	24.6 ± 2.1

(a) Values in $\mu gm/m^3$

(b) Assumed 100% carbon

(c) Assumed 19% carbon

(d) Total carbon by conversion to CO_2

(e) Scaled from FID analysis using $y = 1.75 + 1.26x$ where y is value shown and x is measurement by FID. Equation is least squares best fit from data where both types of measurements were available.

TABLE 8-14

CARBON BALANCE (Continued)

Source	West Covina 7/24/73 24 Hr	Pomona 8/17/73 24 Hr	Rubidoux 9/6/73 24 Hr	Dominguez Hills 10/5/73 24 Hr
Auto Exhaust + Tire Dust + Diesel Exhaust	5.62 ± 0.23	3.02 ± 0.12	2.17 ± 0.09	1.63 ± 0.06
Aircraft (b)	2.42 ± 0.10	1.29 ± 0.06	7.23 ± 0.31	0.703 ± 0.28
Industrial (c)	1.02 ± 0.04	0.434 ± 0.03	0.947 ± 0.042	0.185 ± 0.008
Agricultural (b)	0	0	3.62 ± 0.15	0
Sum of Primary Carbon	9.06 ± 0.37	4.74 ± 0.21	14.0 ± 0.6	2.52 ± 0.10
Total Carbon	24.1 ± 1.2(f)	16.4 ± 0.8(f)	15.1 ± 0.8(f)	10.6 ± 0.5(f)
Secondary Carbon	15.0 ± 1.3	11.7 ± 0.8	1.10 ± 1.00	8.08 ± 0.51
Secondary-Organics	22.5 ± 2.0	17.6 ± 1.2	1.65 ± 1.50	12.1 ± 0.8

(f) In particles smaller than 3.5 μm diameter. Measured by conversion to CO_2.

were used as the characteristic sea salt size distribution in the calculations. The sea salt size distribution used is shown in Figure 8-4.

The size distributions for soil dust are based on recent measurements by the Air Resources Board mobile van in Goldstone, California, a desert region well away from other sources. The volume distributions for several time periods (normalized to the total volume measured in the sampling period) are shown in Figure 8-5. These volume distributions are bimodal, but as discussed below, the lower mode is probably only in part soil dust. Included in Figure 8-5 is a volume distribution of aerosol that was sampled over several hours during which the wind had been blowing across a dry lake. The solid line in Figure 8-5 represents the volume distribution used for soil dust in the calculations; the number distribution appears in Figure 8-4.

Size distributions of aerosol from the Harbor Freeway in Los Angeles were obtained by the Air Resources Board's mobile van in September 1972. During two sampling periods on September 20, the wind came directly from the freeway to the mobile van. During the first of these two periods (0500-0700), the ambient lead concentration measured at the sampling site was 23 $\mu g/m^3$, while during the second period (1700 - 1900), the lead concentration was 11.5 $\mu gm/m^3$. The measured volume distributions of aerosol for these two two-hour periods were averaged and normalized to their respective lead concentrations. The resulting normalized distributions are shown in Figure 8-6*. For particles with a diameter in the range of 0.1 μm to 1.0 μm, the normalized distributions are quite similar. Below 0.1 μm, it is believed that small particles from other local sources cause the deviation between the two distributions. Contributions from sea salt and soil dust probably result in the deviations above 1.0 μm. Since Figure 8-6 is normalized to the measured lead concentration, particles not associated with lead (i.e., particles from sources other than freeway emissions) would not be expected to have similar size distributions on this type of graph.

*It should be noted that the approach of Whitby et al.[81] gives a somewhat different aerosol distribution for motor vehicle exhaust than the Gartrell and Friedlander[85] method described here. This difference has not been resolved as yet.

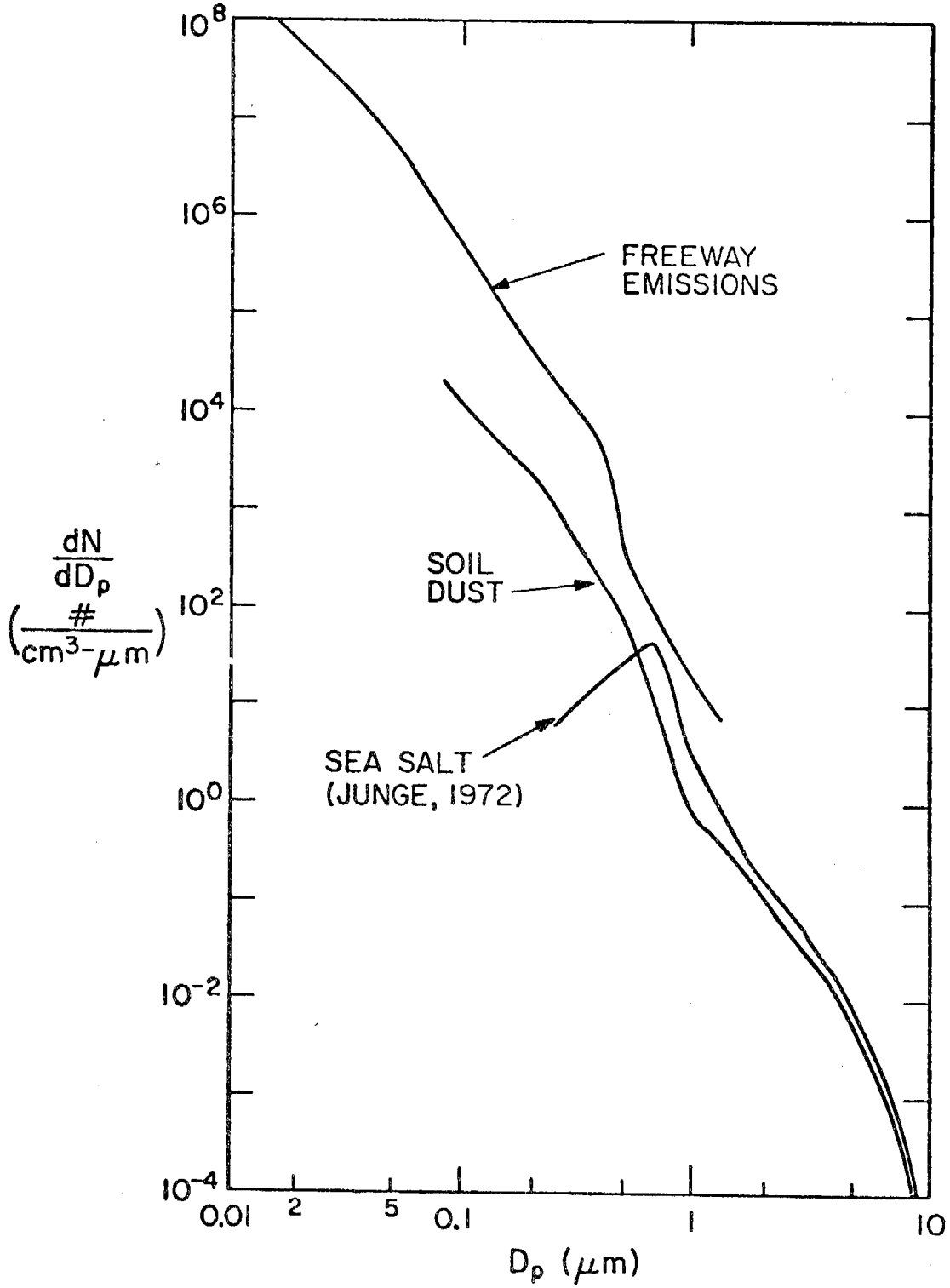

Figure 8-4. Size Distributions of Sea Salt, Soil Dust and Freeway Aerosols. Total Volume are 7.5, 6.7 and 80.6 $\mu m^3/cm^3$, respectively. Data of Whitby et al. From ACHEX.

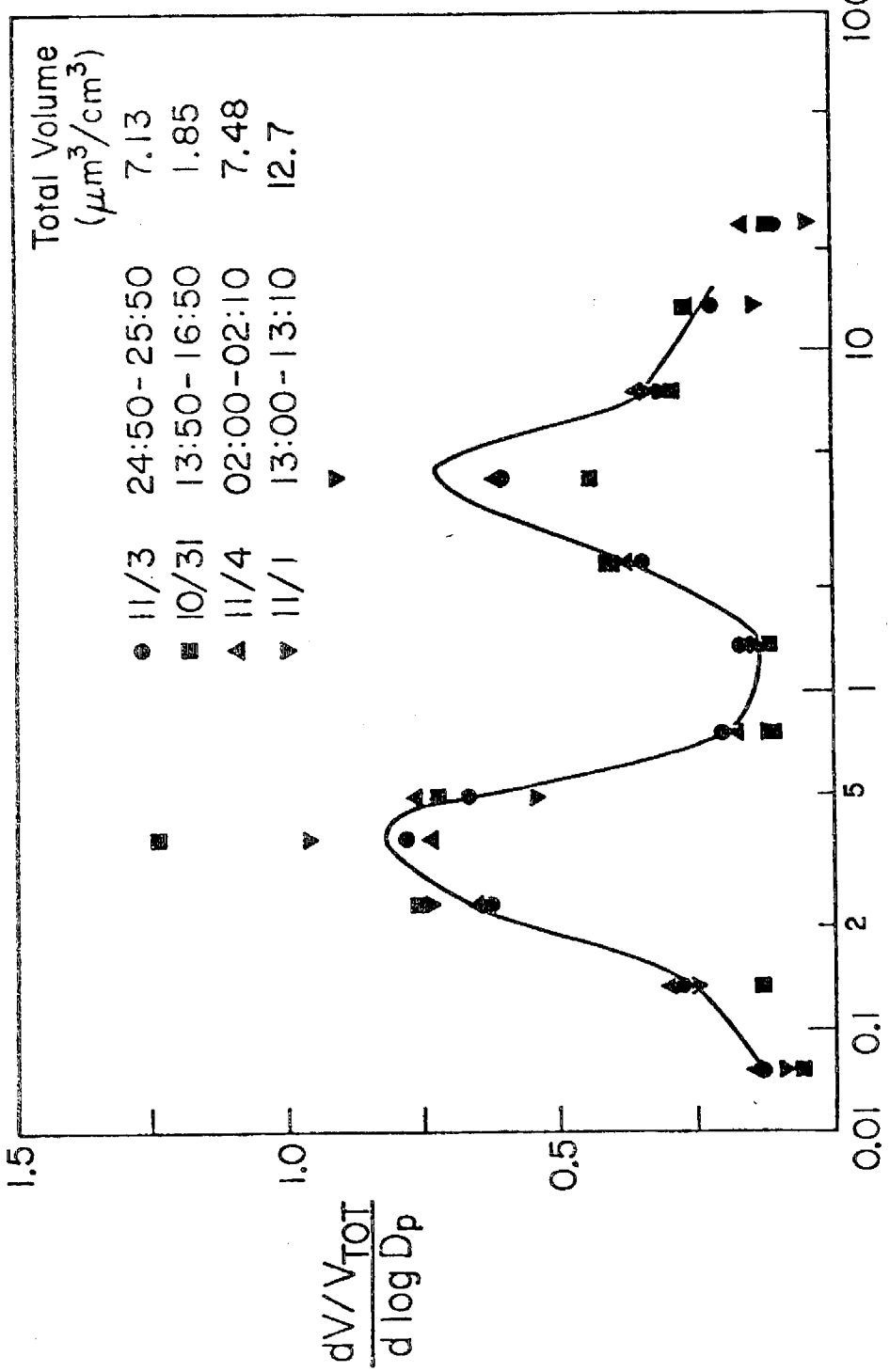

Figure 8-5. Volume Distribution of Goldstone Aerosol, Primarily Soil Dust in Origin, Normalized to Total Volume. Curve Indicates Distribution Used for Soil Dust in Calculations. Data of Whitby et al. from ACHEX.

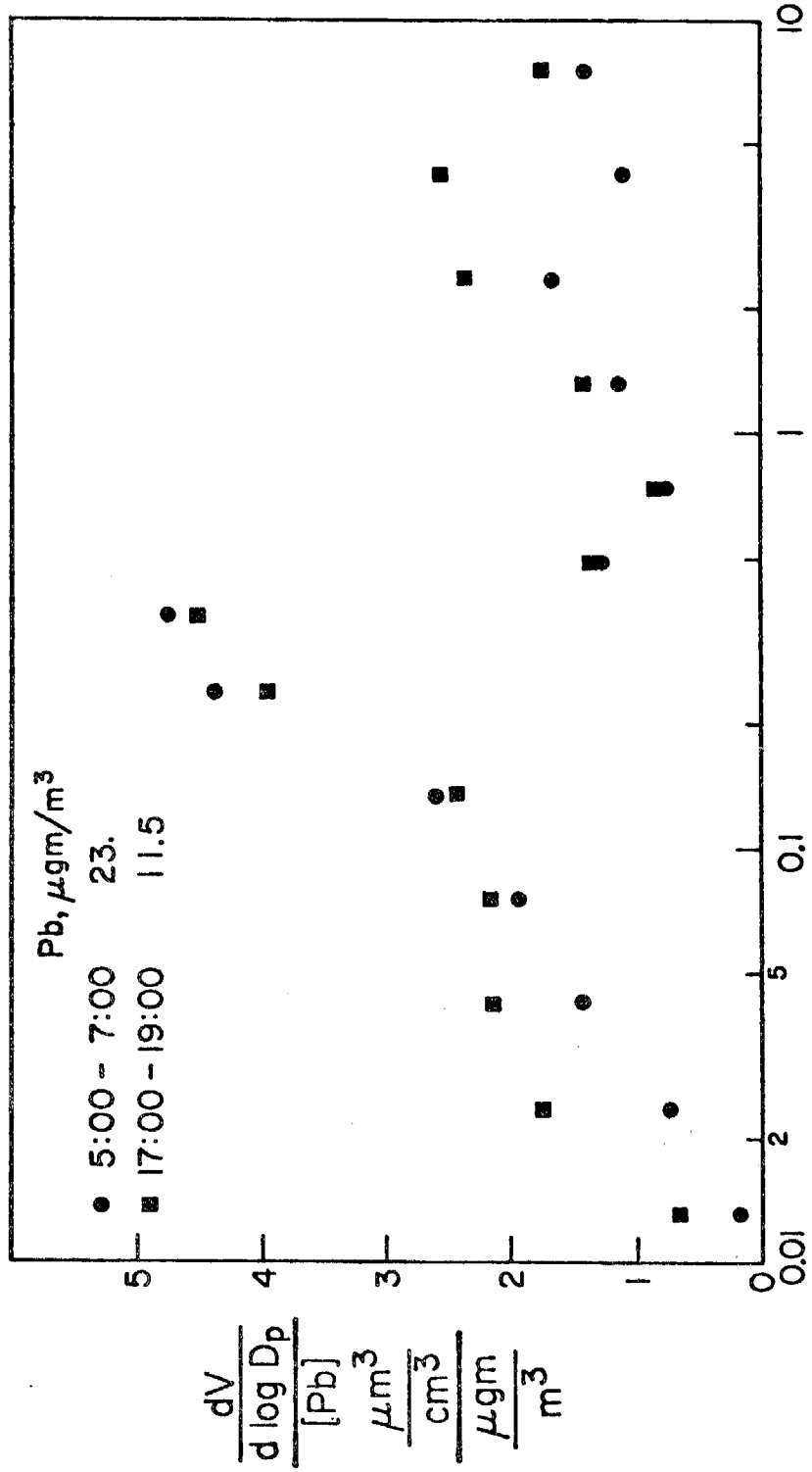

Figure 8-6. Freeway Aerosol Volume Distribution Normalized to Lead. Size Distribution for 0500-0700 was used in the Calculations. Data of Whitby et al. from ACHEX

Data from the Lundgren impactor and the associated after-filers used at the freeway indicate that most of the lead is associated with particles smaller than 0.8 μm. For this reason, and because much of the volume above 1.0 μm came from sources other than the automobile, that portion of the size distribution for particles with diameter greater than 1.0 μm was truncated. Figure 8-4 shows the size distribution used for auto exhaust in the calculations. This distribution for particles in the range 0.01 - 1 μm was averaged over the period from 0500-0700 (chosen because of the high lead concentration reported in that period).

There are few data on the size distributions of aerosols from other primary sources. The freeway size distributions include diesel exhaust as well as automobile emissions. Following the assumptions made by Heisler et al.[84] aircraft exhaust was assumed to be similar to the freeway aerosol, and cement and tire dusts to soil dust. The industrial emissions were assumed similar to the sum of all the other scaled distributions. The chemical element balances indicated a very small fuel oil fly ash contribution which was omitted in the calculations.

1. COAGULATION OF THE PRIMARY DISTRIBUTION

The automobile is the major source of atmospheric lead pollution in Los Angeles and the major source of primary particulate pollution in the submicron size range as well. Most of the lead fallout occurs near the roadways and is in the large particle size range[96]. Hence the ratio of total number concentration to lead concentration is a measure of the extent to which coagulation has occurred in the automobile emissions and is an indication of the age of the aerosol. As shown in Table 8-15, this ratio was highest at the freeway and smaller elsewhere. For this reason it was necessary to take coagulation into account in estimating the change in the freeway emissions away from their source.

In the calculation of coagulation rates, a "Monte Carlo" method was employed. The technique, as well as the computer program used, are described in detail by Husar[97]. The technique amounts to determining the probability

TABLE 8-15

RATIO OF NUMBER CONCENTRATION TO Pb CONCENTRATION

Pasadena	9/20	1200-1400 PST (a)	5.8×10^4	$\frac{\#}{cc}\frac{m^3}{\mu gm}$
Pomona	10/24	1200-1400 PST (b)	2.2×10^4	
Harbor Freeway	9/20	0500-0700 PST (b)	8.4×10^4	

(a) Based on condensation nuclei counter

(b) Based on Whitby analyzer

b_{ij} that two particles of size D_{pi} and D_{pj} will collide. A number between zero and one is chosen at random and this number is used to determine the particles involved in the collision. After each collision, the b_{ij}'s are re-evaluated (since the number distribution has changed), and the next random number is chosen.

The probability b_{ij} that a particle of size D_{pi} collides with a particle of size D_{pj} is given by:

$$b_{ij} = c_{ij}N_iN_j / \sum_{i=1}^{i} \sum_{j=i}^{j} c_{ij}N_iN_j \qquad (8\text{-}4)$$

where c_{ij} is a rate constant of coagulation and is a function of particle size, and N_i is the number of particles with a diameter of D_{pi}. For particles in the transition regime, (i.e. with a diameter such that 0.01 μm $< D_p <$ 0.1 μm for air) c_{ij} is given by Fuchs[98] as:

$$c_{ij} = 2\pi\beta_{ij}(D_i+D_j)(D_{pi}+D_{pj}) \qquad (8\text{-}5)$$

where D_i is the diffusion coefficient and β_{ij} is a number depending on particle size and r.m.s. velocity. For the calculations, the particles were grouped into size ranges of equal-log intervals of D_p, with the log mean diameter of the interval used for D_{pi}.

Because the number of particles with $D_p >$ 0.1 μm is small compared to the total number, the coagulation process was carried out only for particles with $D_p <$ 0.1 μm. To reduce the total computation time, a unit volume was chosen for which the total number of particles was about 50,000. If the number of particles in a given size range became too small, random fluctuations in the process caused excessive errors for the range. Therefore, the size distributions resulting from the coagulation process were cut off above the smallest size range for which the final number of particles was less than 200. Points between the cut off size and the original size distribution (which was used for particles greater than 0.1 μm in diameter) were interpolated as shown in Figure 8-7. The two size distributions which resulted from the coagulation calculation were used as the freeway size distributions in calculations for the two-hour periods at Pomona and Pasadena.

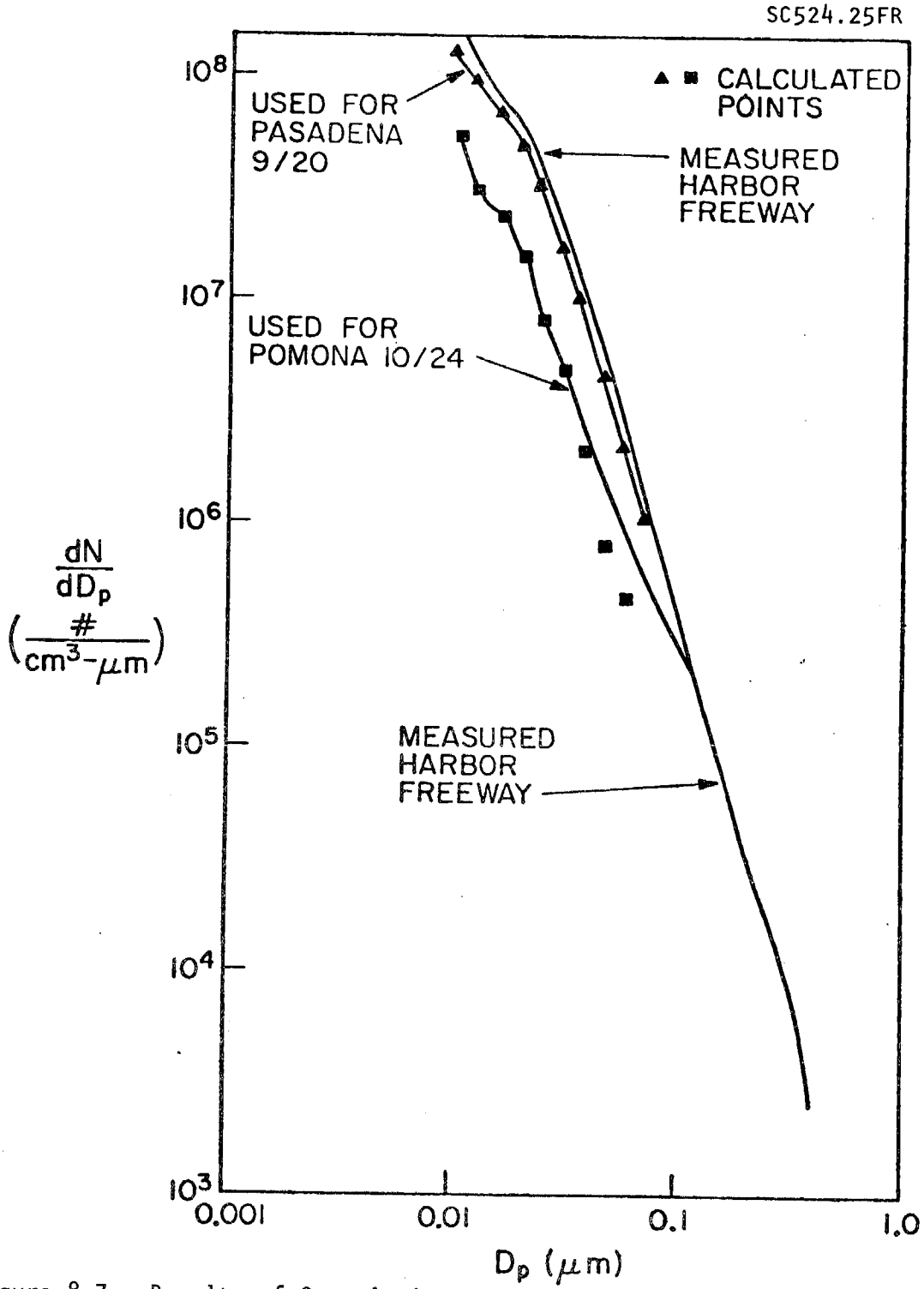

Figure 8-7. Results of Coagulation Calculations. Measured Freeway Distribution is Shown. Points Indicate Calculated Values; Lines Connecting points are Interpolated Values Used in Growth Calculations.

The average time between collision of two particles is given by:

$$\Delta T = \left(\sum_{i=1}^{\infty} \sum_{j=i}^{\infty} c_{ij} N_i N_j\right)^{-1} \tag{8-6}$$

Calculations were made to determine the average time for the coagulation process using Eq. (8-6). The interval ΔT is a function of the particle concentration, and must be re-evaluated after each collision. The total time for the coagulation is:

$$T = \sum_{k=1}^{N_t - N_f} \Delta T_k \tag{8-7}$$

where ΔT_k is the average time between the $(k-1)^{th}$ and the k^{th} collision. The results of this calculation showed that for $N_t/N_f = 4$, that is, total number of particles reduced to 1/4 the initial number, the time scale of the process was about 400 seconds. This time is of the same order as the time found by Husar (1971) in experiments on the coagulation of particles of similar concentration and size range. In the atmosphere, the time would actually be greater because of the mixing processes.

2. GROWTH CALCULATIONS

Heisler et al.[84] considered three processes for the conversion of organic gases and sulfur dioxide to the particulate phase and found that a diffusion controlled growth law which included the Kelvin effect agreed best with the experimental data. One difficulty with this approach is that it requires a somewhat arbitrary cutoff diameter, below which no condensation of organic material was allowed. Other growth processes considered by Heisler et al. were a diffusion controlled process without a Kelvin effect, which showed poor agreement with the experimental data, and a homogeneous, irreversible chemical reaction in the particulate phase, which follows the volume growth law:

$$\frac{dv}{dt} = K(t) D_p^{\gamma} \tag{8-8}$$

where v is the particle volume, K(t) is a rate coefficient, and $\gamma=3$. In this paper, the power law growth relation, Eq. (8-8), has been adopted with values

of γ adjusted to fit the experimental results.

To evaluate the number and volume distributions resulting from the growth calculations, the following method was used: Integrating Eq. (8-8) with $v=\pi D_p^3/6$, one finds that for $\gamma \neq 3$.

$$\frac{1}{(3-\gamma)} (D_p^{3-\gamma} - D_{po}^{3-\gamma}) = \int_o^t \frac{2K(t)}{\pi} dt \qquad (8\text{-}9)$$

and for $\gamma=3$

$$\frac{D_p}{D_{po}} = \exp \left\{ \int_o^t \frac{2K(t)}{\pi} dt \right\} \qquad (8\text{-}10)$$

The right-hand sides of these equations are functions of time only, and are chosen such that the total volume after the growth is equal to the sum of the total volume before growth and the volume of the material added to the aerosol.

For the new number distributions, the result is:

$$\frac{dN}{dD_p} = \frac{dN}{dD_{po}} \frac{dD_{po}}{dD_p} = \frac{dN}{dD_{po}} \left(\frac{D_p}{D_{po}} \right)^{2-\gamma} \qquad (8\text{-}11)$$

and for the new volume distributions:

$$\frac{dV}{d\log D_p} = \frac{dV_o}{d\log D_{po}} \left(\frac{D_p}{D_{po}} \right)^4 \frac{dD_{po}}{dD_p} = \frac{dV_o}{d\log D_{po}} \left(\frac{D_p}{D_{po}} \right)^{6-\gamma} \qquad (8\text{-}12)$$

These equations hold for $\gamma=3$ as well as $\gamma<3$.

The composition of the aerosol from chemical element balances and from the experimental data is given in $\mu gm/m^3$. Since the conversion processes are concerned with aerosol volumes and not masses, densities were required for the various constituents of the aerosol. The densities used in the calculations were those estimated by Heisler et al.[84]. The value for nitrate was assumed to be 1.3. For the growth calculations, it was assumed that nitrate was present in the aerosol as saturated ammonium nitrate. In this way, some,

if not all, of the reported ammonium found in the aerosol could be accounted for in the growth calculations.

3. RESULTS OF THE COAGULATION AND GROWTH CALCULATIONS

Coagulation and secondary conversion calculations were carried out for the two-hour periods at Pomona and Pasadena. Based on the chemical element balance for Pomona on October 24 and Pasadena on September 20 (both covering the period 1200-1400 PST), the sea salt, soil dust and coagulated freeway distributions were scaled such that the total volume of a given source was equal to the mass of the source divided by the appropriate density. The sea salt component was assumed to be saturated, and water (3.7 $\mu gm/m^3$ for Pasadena and 6.0 $\mu gm/m^3$ for Pomona) was included in the sea salt contribution before scaling. The primary size and volume distributions calculated in this way are shown in Figures 8-8 through 8-11. Following Heisler et al.[84], it was assumed that the sulfate and nitrate conversion process followed a cubic growth law ($\gamma = 3$).

Several values of γ were used for the organic conversion process, and it was found that as γ decreased, growth occurred increasingly in the smaller sized particles. Best agreement with the data for Pomona was found with $\gamma = 2.7$ for the organic conversion. Figures 8-8 and 8-9 show the results of the secondary conversion calculations for Pomona along with the experimental data. Agreement is best in the size range 1.0 $\mu m < D_p < 1.0$ μm. There is a deviation between the calculated and measured distributions in the upper and lower portion of the size spectrum. The spike in the volume distribution at about 1.1 μm is caused by a discontinuity in the primary size distribution. This discontinuity is caused by the sea salt distribution, and presumably would be smoothed out by coagulation for a well aged aerosol. No attempt was made, however, to "age" the primary aerosol with the Monte Carlo method of coagulation, except in the lower end of the freeway spectrum.

For the Pasadena data, shown in Figures 8-10 and 8-11, a value of $\gamma = 2.3$ for the organic conversion gave the best agreement between the calculated and experimental distributions. However, no measurements were made for

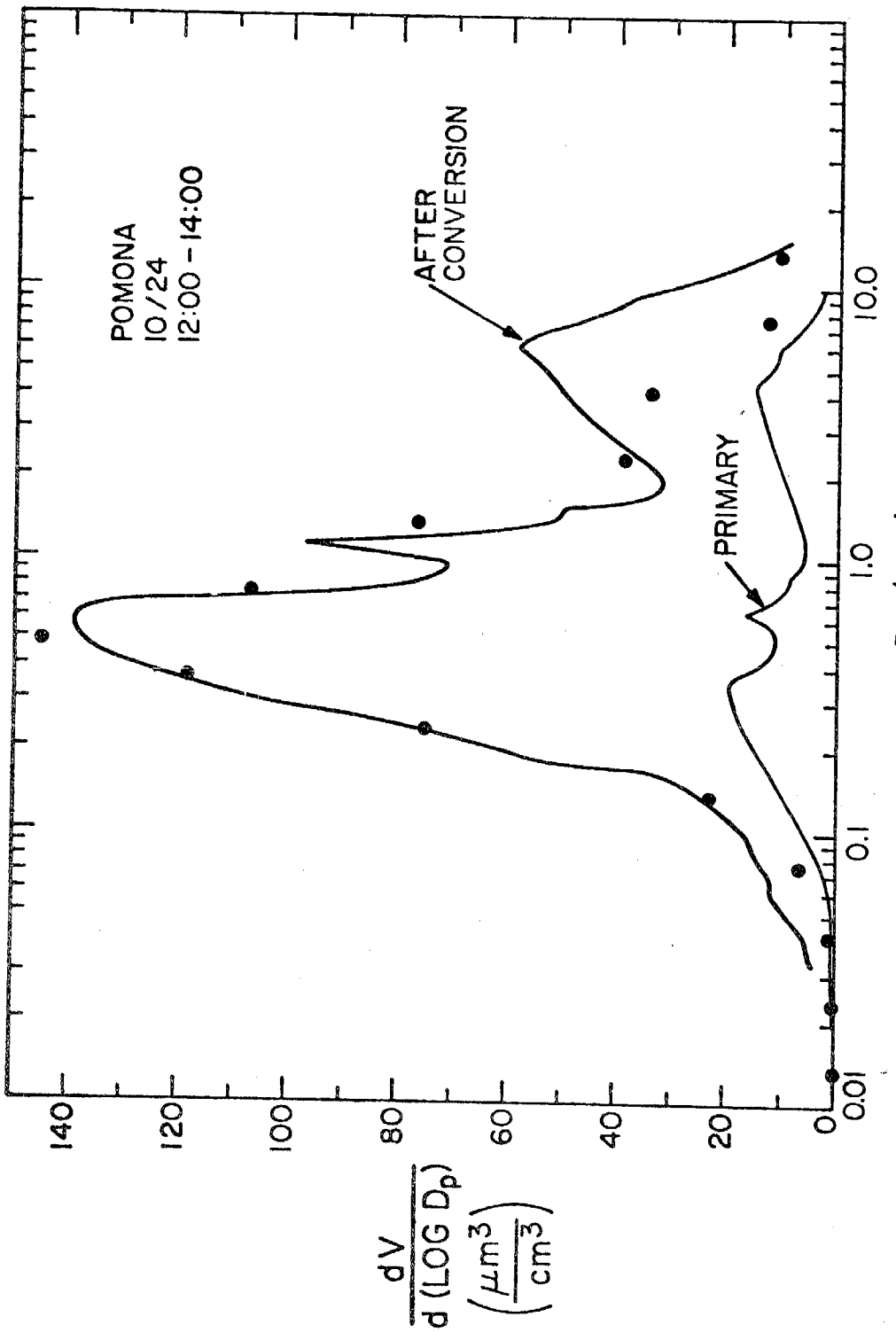

Figure 8-8. Primary Volume Distribution Based on Chemical Element Balance, and Final Volume Distribution After Secondary Conversion Calculations for Pomona. Points are Experimental data.

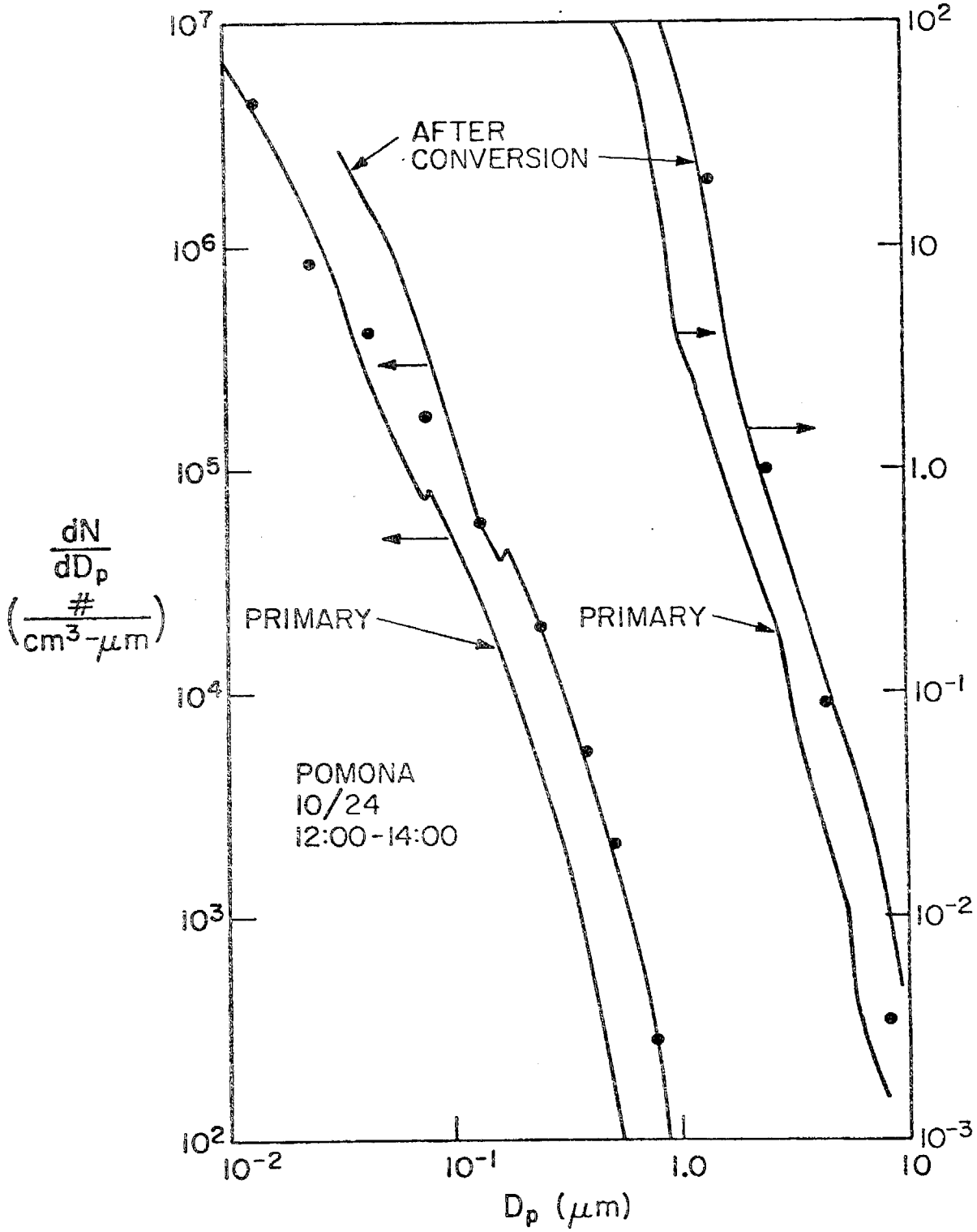

Figure 8-9. Primary Number Distribution Based on Chemical Element Balance, and Final Number Distribution after Secondary Conversion Calculations for Pomona. Points are Experimental Data.

particles with a diameter less than 0.3 μm; thus it is not known if the lower end of the size distribution is correct. It is possible that for the smaller particles, the Kelvin effect plays a role in the distribution of organics according to size, and that the chemical composition of the particles is an important factor in the growth processes.

4. SIZE DISTRIBUTION OF CHEMICAL ELEMENTS

Chemical elements in the atmospheric aerosol are distributed with respect to size in a way which depends on the sources of particulates and on atmospheric conversion processes. Air quality standards may eventually take this into account by considering particulates above and below one or two micrometers separately.

Calculations of the distributions of elements with respect to size and comparison with experiment permit a more severe test of the source breakdown calculations made in the previous sections. We have carried out such calculations assuming that the mass fraction of an element in each primary source is independent of particle size. Table 8-16 shows the calculated fraction of certain chemical species in particles smaller than 1.5 μm, together with measured values when available. Measured values are based on Lundgren impactor data calibrated for unit density spherical particles; the data have not been corrected for density effects.

Calculated values for sodium and lead are in good agreement, while agreement for aluminum is poor. If the volume distribution measured at Goldstone (Figure 8-5) is all soil dust, the calculations predict more aluminum in the smaller sizes than actually found. If, on the other hand, only particles larger than 1 μm are soil dust, the calculations predict too little aluminum in the smaller sizes. Most of the particles greater than 1 μm found at Goldstone are probably of soil dust origin, while only a fraction of the smaller smaller particles are from soil dust.

Table 8-16 also includes calculated values for secondary conversion products; the calculations indicate that most of these species exist on particles smaller than 1.5 μm. This is true also for lead and the calculations are confirmed by the experiments. Sodium, on the other hand, comes primarily from soil dust and sea salt and is associated with the larger particles.

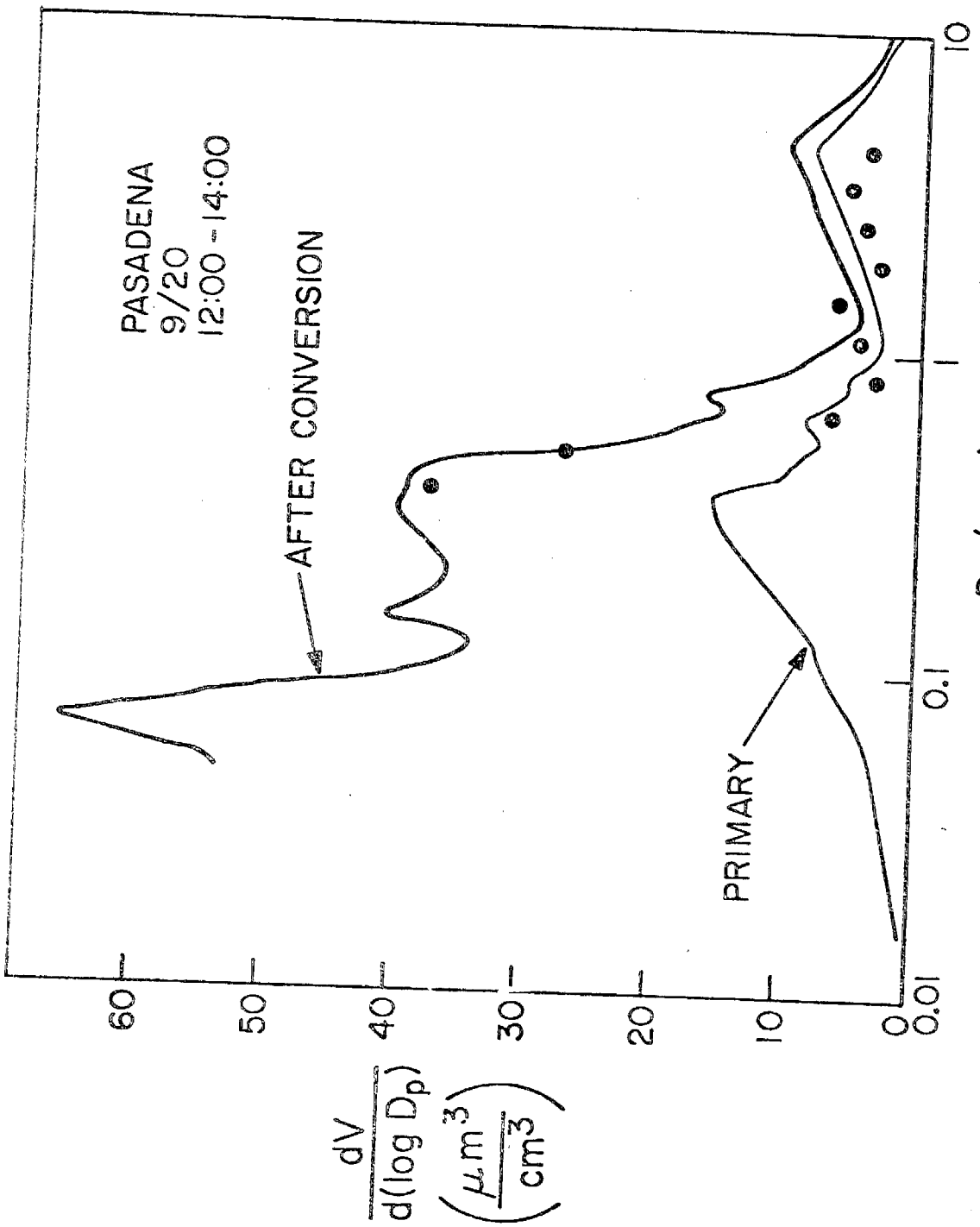

Figure 8-10. Primary Volume Distribution Based on Chemical Element Balance, and Final Volume Distribution After Secondary Conversion Calculations for Pasadena. Points are Experimental Data.

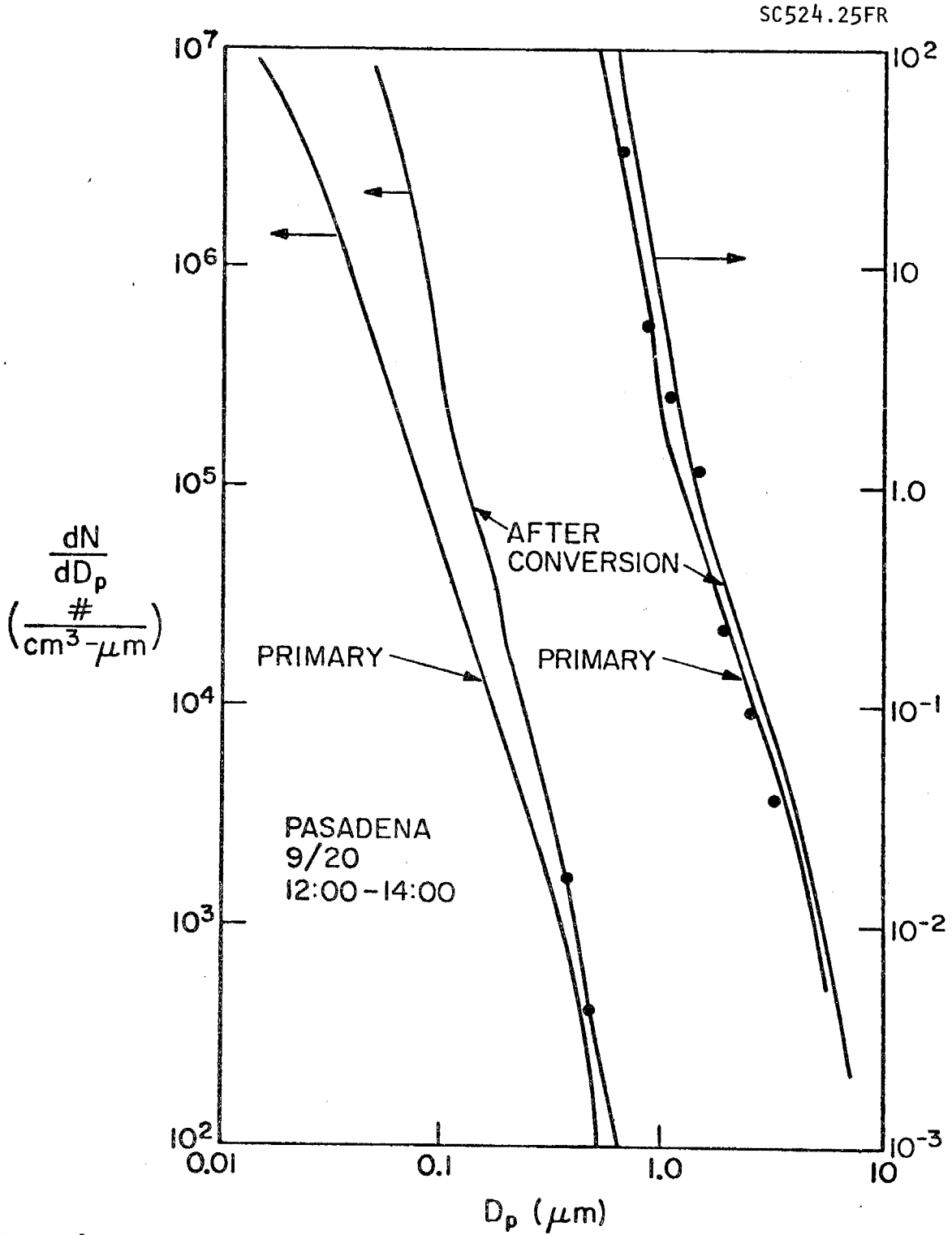

Figure 8-11. Primary Number Distribution Based on Chemical Element Balance, and Final Number Distribution After Secondary Conversion Calculations for Pasadena. Points are Experimental Data.

TABLE 8-16

FRACTION OF CHEMICAL SPECIES ON PARTICLES SMALLER THAN 1.5 μm

	Pasadena 9/20/72 1200-1400		Pomona 10/24/72 1200-1400	
	Calculated	Measured	Calculated	Measured
Na	.41	.36 ± .07	.29	.20 ± .03
Al	.56, .06 (a)	.38 ± .02	.52, .01 (a)	.10 ± .01
Pb	.99	U	.99	.95 ± .01
$SO_4^=$	.89	U	.72	U
$NO_3^=$	.89	U	.72	U
Organics	.98	U	.80	U

(a) Higher value assumes Figure 8.5 is all soil dust, lower value assumes only particles greater than 1 μm in Figure 8.5 are soil dust.

U = unknown

Calculations of the detailed distributions with respect to size, not shown, are in only fair agreement with experiment. One source of inaccuracy in the experiments is the bouncing of large particles which are carried to lower stages of the impactor. Needed, also, are better data for the distribution of chemical elements with respect to size for the primary sources, as well as more information on atmospheric growth laws.

Light Scattering and Secondary Conversion

Measurements of the light scattering coefficient, b_s, were made with an integrating nephelometer while filter samples of aerosol were being collected during the intensive sampling periods. At Pasadena, on September 20, 1972, from 1200 - 1400 PST, the average value for b_s was $2.3 \times 10^{-4} m^{-1}$ while the relative humidity was approximately 20% over the period. At Pomona, on October 24, from 1200 - 1400, the average value for b_s was $8.3 \times 10^{-4} m^{-1}$ with a relative humidity near 50%.

The extinction coefficient can be calculated from the size distribution using the following equation:

$$b_s = \int_{\lambda_1}^{\lambda_2} \int_{D_{P_1}}^{D_{P_2}} g(\lambda) K \left(\frac{\pi D_p}{2}, m \right) \frac{\pi D_p^2}{4} \frac{dN}{dD_p} dD_p \, d\lambda \qquad (8.13)$$

$$\text{where} \quad \int_{\lambda_1}^{\lambda_2} g(\lambda) d\lambda = 1$$

where λ is the wavelength of the incident light, $g(\lambda)$ is the spectral distribution of sunlight at the surface of the earth, and K, the light scattering efficiency factor, is a function of the index of refraction of the particle, m. The index of refraction for smog aerosol was assumed to be 1.5, a value which Ensor et al.[62] found to give good agreement between measured and calculated values for b_s using the 1969 data for the Pasadena aerosol. Values for K were calculated using an IBM subroutine, DAMIE. The double integral was evaluated numerically, using the size distributions obtained from the results of the coagulation and growth calculations. The limits of

the integration were .390 μm to .700 μm for the wavelengths of light and .05 μm to 4.0 μm for the particle diameters. These calculations yield values for b_s of $1.6\times10^{-4}m^{-1}$ for Pasadena and $6.5\times10^{-4}m^{-1}$ for Pomona. For the primary size distributions (Figure 8-8) before growth, b_s was calculated to be $0.6\times10^{-4}m^{-1}$ and $0.8\times10^{-4}m^{-1}$ for Pasadena and Pomona, respectively. One can easily see the effects of the formation of secondary particulate matter.

There are several possible reasons why calculated scattering coefficients are low compared with measured values. In the secondary conversion process, water other than that associated with the sea salt and the ammonium nitrate conversion was not added to the aerosol. The water content for Pomona was not known. Better agreement would have been obtained for Pasadena if the additional 8 $\mu gm/m^3$ water had been included but a suitable growth law is not yet available. In addition, the flashtube used in the nephelometer has a wavelength distribution function which does not correspond exactly to that of sunlight at the earth's surface.

Calculations were made to determine the functional relationship between b_s and the total volume of the secondary conversion products. A growth law of $\gamma = 2.8$ was applied with the calculated primary particle size distribution for the September 20 time period in Pasadena. The value of 2.8 was chosen as a rough average between the lower values found in experiments on organic conversion, and the value assumed for sulfate and nitrate conversion. As shown in Figure 8.12, the calculated values for b_s are nearly a linear function of the volume of secondary material. The function is given approximately by the expression:

$$\text{Converted Volume } \left(\frac{\mu m^3}{cm^3}\right) = 21.2\ (b_s(10^{-4}m^{-1})-0.6) \qquad (8.14)$$

Assuming a density of 1.4 for the aerosol, and including the primary mass, the result is:

$$\text{Total Mass } \left(\frac{\mu gm}{m^3}\right) \approx 33(b_s(10^{-4}m^{-1})+0.4) \qquad (8.15)$$

which compares well with the relation given by Charlson et al. (1969):

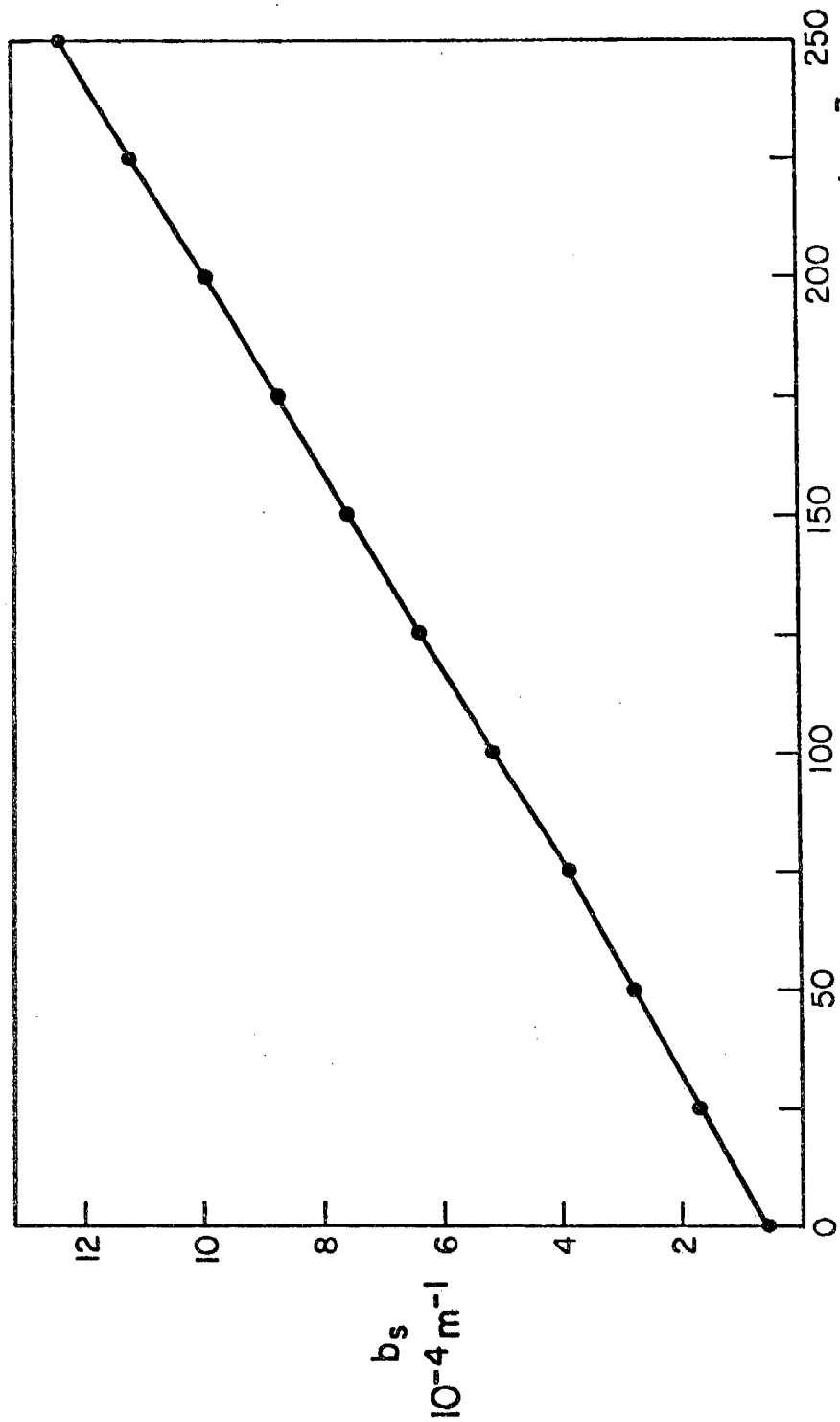

Figure 8-12. Calculated Values of b_s as a Function of Volume of Converted Material: Power Law Growth Equation with γ=2.8. Points Represent Calculations and the Straight Line an Approximate Best Fit.

$$\text{mass } (\mu gm/m^3) = 38 b_s (10^{-4} m^{-1}).$$

While b_s may often correlate well with total aerosol mass, this may not always be the case. Measurements at the Harbor Freeway showed that while the total mass may be quite high, b_s may be rather small because the aerosol is made up of very small particles which do not scatter light efficiently. In addition, relative humidity plays an important role in the light scattering properties of an aerosol, and since water that has been associated with the aerosol may be lost between the time the aerosol was sampled and the time it is weighed, further discrepancies may occur in relating mass to the light scattering coefficient.

Conclusions

The results of the analysis of the 1972 data support, in a general way, the method developed in previous publications for relating the characteristics of the pollution aerosol to its sources. The calculation of the relative contributions of the various sources is based on a chemical element balance and is independent of the wind field. Hence, it is particularly useful in dealing with long term average data such as those given in the air quality data summaries[99]. Both coagulation and growth processes as well as sedimentation depend on the time history of the aerosol. The growth calculations are empirically based and can be improved by taking into account the geographical distribution of sources and the wind field[100]. Such calculations should be verified as shown in this paper by comparing predicted size and chemical element distributions with measured values.

The visibility depends approximately on the total volume of material condensed from the gas phase. This includes sulfates, nitrates, organics, ammonia together with associated water. Only two two-hour sampling periods were analyzed in detail but the results indicate that all of these species contributed significantly. Improving visibility on days when pollution (and not sea fogs) plays the major role will require a major reduction in aerosol precursor gases.

The results of the calculations on the 1973 observations tend to support the general method. The results are not very different from those found by Gartrell and Friedlander[85] for the 1972 aerosol data. The estimated chemical composition of the primary freeway aerosol is similar to the composition estimated previously based on data from various sources for exhaust from individual automobiles.

D. STATISTICAL INTERPRETATION

1. INTRODUCTION

This section deals with the third approach to the investigation of sources and ambient aerosols and uses a method developed by White et al.[101]. The conclusions are based on statistical interpretation of the large volume of data obtained in 1973 from ACHEX II, according to our present understanding of the physical and chemical processes involved. This discussion makes use of the formulation in Section III-A-4 of the State standard for atmospheric visibility in terms of the light-scattering coefficient of the ambient aerosol, which was measured systematically throughout the study. A summary of the theory relating the light-scattering coefficient of an aerosol to its composition is also given in this earlier section. Conclusions are based primarily on measurements made with the ACHEX mobile van during the 61 "two hour" sampling intervals shown in Table 8-17. The notation, units, and analytical techniques are summarized in Table 8-18.

2. STATISTICAL METHODS

The interpretation of the data is based largely on the results of stepwise multiple linear regression analyses performed with a standard computer routine. In general, regression of a variable Y on variables $X_1, \ldots, X_n$ determines coefficients $c_1, \ldots, c_n$ which minimize the variance ε^2 of the quantity $Y - \Sigma c_i X_i$. Coefficients are set to zero if the corresponding variables are not statistically significant in reducing ε^2. In the regressions reported here, an F-level of 4.0, corresponding to about the 95% confidence level, was required to enter or remove a variable.

The notation $(n,\bar{y},r)$ at the end of a regression relationship means that regression was performed on n observations for which the mean value of the dependent variable was $\bar{y}$, and produced a multiple correlation coefficient of r. The number of observations can fluctuate slightly with changes in the set of variables, due to missing data. The square of the correlation coefficient is the proportion of the variance of the dependent variable which is explained by the regression relationship:

$$r^2 = \frac{\sigma^2 - \varepsilon^2}{\sigma^2} \qquad (8\text{-}16)$$

TABLE 8-17

"TWO-HOUR" SAMPLES USED IN REGRESSION ANALYSIS AND MOBILE VAN AVERAGES.
ALL SAMPLES WERE WEIGHTED EQUALLY, REGARDLESS OF LENGTH.
PARTICULATES WERE MEASURED ON TOTAL FILTER EXCEPT WHERE NOTED IN TEXT.
SO_2 WAS NOT MEASURED AT RUBIDOUX.

Mobile Van Site	Date	Pacific Standard Time 3	4	5	6	7	8	9	10	11	12	13	14	15	16	17	18	19	20	21	22	23
West Covina	(07-24-73)				—	—	—	—	—	—	—	—	—	—	—	—	—	—	—	—		
West Covina	(07-25-73)			—	—	—	—	—	—	—	—	—	—	—								
West Covina	(07-26-73)				—	—	—	—	—	—	—	—	—	—	—	—						
West Covina	(08-09-73)				—	—	—	—	—	—	—	—	—	—	—	—						
Pomona	(08-17-73)				—	—	—	—	—	—	—	—	—	—	—	—	—	—	—	—		
Rubidoux	(09-06-73)	—	—	—	—	—	—	—	—	—	—	—	—	—	—	—	—	—	—	—	—	—
Rubidoux	(09-19-73)	—	—	—	—	—	—	—	—	—	—	—	—	—	—	—	—	—	—	—	—	—
Dominguez Hills	(10-05-73)				—	—	—	—	—	—	—	—	—	—	—	—	—	—	—	—		
Dominguez Hills	(10-11-73)				—	—	—	—	—	—	—	—	—	—	—	—	—	—	—	—		

TABLE 8-18
NOTATION, UNITS, AND ANALYTICAL TECHNIQUES

b_{scat} ($10^{-4} m^{-1}$) aerosol light scattering coefficient, nephelometer

MASS ($\mu g/m^3$) aerosol mass concentration, gravimetric

NO_3^- ($\mu g/m^3$) particulate nitrate concentration, wet chemistry[a]

$SO_4^=$ ($\mu g/m^3$) particulate sulfate concentration, wet chemistry

TNPV ($\mu g/m^3$) particulate carbon concentration, flame ionization detector

CEL ($\mu g/m^3$) particulate carbon concentration, ashing

C ($\mu g/m^3$) estimated CEL, C = 1.26 TNPV[b]

NITRATES ($\mu g/m^3$) estimated concentration of particulate nitrate compounds as ammonium salts, NITRATES = 1.3 $NO_3^=$

SULFATES ($\mu g/m^3$) estimated concentration of particulate sulfate compounds as ammonium salts, SULFATES = 1.3 $SO_4^=$

ORGANICS ($\mu g/m^3$) estimated concentration of particulate organic compounds as oxygenated hydrocarbon compounds, ORGANICS = 1.4 C

NH_4^+ ($\mu g/m^3$) particulate ammonium ion concentration, wet chemistry

Na ($\mu g/m^3$) particulate sodium concentration, neutron activation

Al ($\mu g/m^3$) particulate aluminum concentration, neutron activation

$Na_{sea\ salt}$ ($\mu g/m^3$) estimated concentration of particulate sodium due to sea salt, $Na_{sea\ salt}$ = Na - (.025/.082) Al

SOIL DUST ($\mu g/m^3$) estimated concentration of soil dust, SOIL DUST = (1/.082) Al

Pb ($\mu g/m^3$) particulate lead concentration, x-ray fluorescence

Ni ($\mu g/m^3$) particulate nickel concentration, x-ray fluorescence

V ($\mu g/m^3$) particulate vanadium concentration, neutron activation

CO (ppm) carbon monoxide concentration, gas chromatography, followed by flame ionization detector

NO_x (ppm) nitrogen oxides concentration, chemiluminescence detector

TABLE 8-18 (continued)

SO_2 (ppm) sulfur dioxide concentration, gas chromatography, followed by flame photometric detector

N_T ($\mu g/m^3$) nitrogen concentration, $N_T = 573 \times NO_x + (14/46) \times NO_3$

S_T ($\mu g/m^3$) sulfur concentration, $S_T = 1309 \times SO_2 + (32/96) \times SO_4$

(a) The values of NO_3^- obtained on 3/22/74 for four total filters which had passed through the neutron activation procedure were anomalously low. In our calculations we use interpolated values for these four samples: interpolated NO_3^- = MASS (BNO_3^- /BMASS + ANO_3^- /AMASS)/2, where the prefixes B and A denote the values for the samples taken immediately before and after the sample in question.

(b) Both types of carbon analyses, TNPV and CEL, were made on a total of 47 after, total, and two-stage hi-vol filters. On the evidence of these data, TNPV and CEL appear to be related by the following formula:

$$CEL = 1.26\ TNPV + 1.7 \pm 2.6 \quad .$$

Here σ^2 is the original variance of the dependent variable and ε^2 is the variance remaining after regression.

We will be interested only secondarily in the amount of scatter in a regression relationship; our primary interest will be the determination of the coefficients of the relationship. The physical or chemical significance of these coefficients of course ultimately depends on the validity of the underlying linear model tested. For this reason, the models used in regression analyses are restricted to those which have some basis in our understanding of the physical and chemical processes involved. Assuming that the model used in the regression is correct, the accuracy with which the coefficients in the model are determined depends not only on the scatter in the relationship, but also on the degree of intercorrelation among the variables. In the regressions which follow, coefficients whose standard error, calculated from the covariance matrix of the variables, exceeds 20% will be marked with an asterisk (*).

a. Mass Concentrations of Nitrates, Sulfates, and Organics.

In terms of mass concentration, the three most important elemental and ionic species found in the aerosols sampled were NO_3^-, $SO_4^=$, and C. In this section we discuss the probable nature of the nitrate, sulfate, and carbonaceous compounds these represented in the aerosol, and describe their distribution with respect to particle size.

Likely nitrate and sulfate compounds in the aerosol include ammonium salts formed by absorption of ammonia from the gas phase, and sodium salts formed by replacement of chloride in sea salt. A mole balance on the 24-hour hi-vol samples from the mobile van indicates that most of the nitrate and sulfate ion can be accounted for in this way:

$$\frac{NH_4^+}{18} = .06 + .90\frac{NO_3^-}{62} + 1.55\frac{(SO_4^= - (96/46)\,Na_{\text{sea salt}})}{96} \pm .04 \quad (8\text{-}17)$$

$$(n = 11,\ \bar{y} = .43,\ r = .988)$$

This result indicates that nearly all of the nitrate is ammonium nitrate, and at least three-fourths of the sulfate not associated with sea salt is ammonium sulfate or bisulfate.

Expression (8-17) was obtained by regression of NH_4^+ on NO_3^- and $(SO_4^= - (96/46)\, Na_{sea\ salt})$, where $Na_{sea\ salt}$ is calculated from sodium and aluminum concentrations as in Miller et al.[16]. In this model, it is assumed that marine sodium chloride is converted to sodium sulfate. Other possible models for regression, in which sodium chloride is converted to sodium bisulfate or sodium nitrate, produce slightly poorer fits. The consensus of these is that the average mass ratio of compounds to ion for both nitrates and sulfates should be about 1.3:

$$NITRATES/NO_3^- = SULFATES/SO_4^= = 1.3 \quad .$$

In analyses of one and two-hour hi-vol filter samples taken at Pasadena during the period of ACHEX II, Grosjean and Friedlander[53] found that most of the carbon was contained in organic compounds, whose carbon content ranged from 67 percent for the polar fractions to 85 percent for the non-polar fractions. Based on the predominance of polar material they found in their samples, we estimate the average ratio of organic compounds to elemental carbon in the aerosol to be about 1.4 (100%/71%):

$$ORGANICS/C = 1.4 \quad .$$

Table 8-19 gives the average mass concentration of nitrates, sulfates, and organics in the two-hour samples from the mobile van, based on the scaling factors estimated above. These three components account for over half of the average aerosol mass. Judging from the eleven two-hour samples analyzed for aluminum, soil dust accounts for 35-40 percent of the remainder, leaving an average of about 60 $\mu g/m^3$ to be attributed to water and primary anthropogenic aerosols.

The light scattering effectiveness of an aerosol depends not only on its chemical composition, but on the distribution of particle sizes as well.

TABLE 8-19

ESTIMATED BREAKDOWN OF AEROSOL MASS CONCENTRATION FOR TWO-HOUR AEROSOL SAMPLES AT MOBILE VAN

	AVERAGE MASS CONCENTRATION ($\mu g/m^3$)		
	Total of 199 $\mu g/m^3$ Derived From:		
	All Sources	Gasoline	Fuel & Crude Oil
Nitrate Compounds	41	32	9
Sulfate Compounds	33	5	28
Organic Compounds	30	30	0
Sum	104	67	37

Table 8-20 shows the average mass fraction of each aerosol component which was found in particles less than one-half micron in diameter.

It is evident from Table 8-20 that the chemical composition of the aerosol varies with particle size. The smaller particles were found to be enriched with carbon, while nitrate and aluminum were concentrated in the larger particles. Although its effect cannot be determined with high accuracy from our data, ambient relative humidity appears as an important determinant of particle size. Nitrate and sulfate size distributions are particularly affected by relative humidity; this is consistent with the known hydroscopicity of the probable nitrate and sulfate compounds in the aerosol, but may also reflect humidity-dependent formation mechanisms for these compounds.

3. LIGHT SCATTERING BY AEROSOLS OF SULFATE, NITRATE & ORGANIC MIXTURES

It is our objective in this section to quantify the contributions of nitrates, sulfates, and organics to aerosol light scattering. This is a difficult problem, because of the complex dependence of the light scattering coefficient on aerosol composition. Our approach will be to establish a simple approximate relationship, of the form relating b_{scat} and the constituents to sulfate, nitrate and other materials, dominated by organics.

Ambient aerosols are distributed with respect to particle size, and b_{scat}/MASS for such an aerosol is obtained by averaging:

$$b_{scat}/MASS = \int G(D_p)\,mass(D_p)\,dD_p \quad , \qquad (8\text{-}18)$$

where $G(D_p)$ is the ratio for a monodisperse aerosol, given in Equation (3-8), and mass (D_p) is the normalized aerosol mass distribution. It is found empirically that this ratio has a fairly narrow distribution for ambient Los Angeles aerosols. The approximate proportionality between b_{scat} and MASS for 60 two-hour samples taken at the mobile van was illustrated in Figure 3-10. The average b_{scat}/MASS for these samples was .032, with a standard deviation of .009:

$$b_{scat}/MASS = .032 \pm .009 \qquad (3\text{-}10)$$

TABLE 8-20

RATIO OF MASS ON AFTER FILTER (PARTICLE DIAMETERS LESS THAN 0.5μ) TO MASS ON TOTAL FILTER (PARTICLE DIAMETER LESS THAN 15μ) FOR INDIVIDUAL AEROSOL COMPONENTS. (AVERAGE AND STANDARD DEVIATION OF TWO-HOUR AEROSOL SAMPLES AT MOBILE VAN. CARBON CALCULATED FROM 18 TWO-HOUR SAMPLES FOR WHICH CEL WAS MEASURED. ALUMINUM CALCULATED FROM 11 TWO-HOUR SAMPLES ANALYZED BY NEUTRON ACTIVATION.)

AF/TF Average

Aerosol Component	Overall	RH<60%	RH>60%
Total Aerosol	.37 ± .10	.43 ± .06	.30 ± .09
Nitrate	.33 ± .16	.39 ± .10	.28 ± .19
Sulfate	.49 ± .20	.64 ± .12	.34 ± .14
Carbon	.72 ± .13		
Aluminum	.08 ± .09		

Some variability in the ratio b_{scat}/MASS is to be expected, since chemical compositions and particle size distributions differ from sample to sample. It was found that some of the deviation in (3-10) was in fact associated with variations in aerosol composition:

$$b_{scat}/MASS = .020 + .056\ SO_4^{=}/MASS + .064\ \mu^2\ NO_3^{-}/MASS \pm .006 \quad . \qquad (8\text{-}19)$$

$$(n = 58,\ \bar{y} = .032,\ r = .724)$$

Here, μ denotes the ambient relative humidity: μ = %RH/100. As shown in Figure 8-13, the ratio b_{scat}/MASS tended to be higher than average for aerosols rich in sulfates and nitrates, and lower than average for aerosols poor in these compounds.

We can rewrite (8-19) in a suggestive form if we use the conclusion of the last section that NITRATES/NO_3^- = SULFATES/SO_4^- = 1.3. Simple algebraic manipulation of (8-19) then gives

$$b_{scat}/MASS = .020\ (MASS - SULFATES - NITRATES)/MASS + (.020 + .056/1.3)\ SULFATES/MASS + (.020 + .064\ \mu^2/1.3)\ NITRATES/MASS \pm .006,$$

or:

$$b_{scat}/MASS = .020\ (MASS - SULFATES - NITRATES)/MASS + 0.62\ SULFATES/MASS + (.020 + .049\ \mu^2)\ NITRATES/MASS \pm .006 \quad . \qquad (8\text{-}20)$$

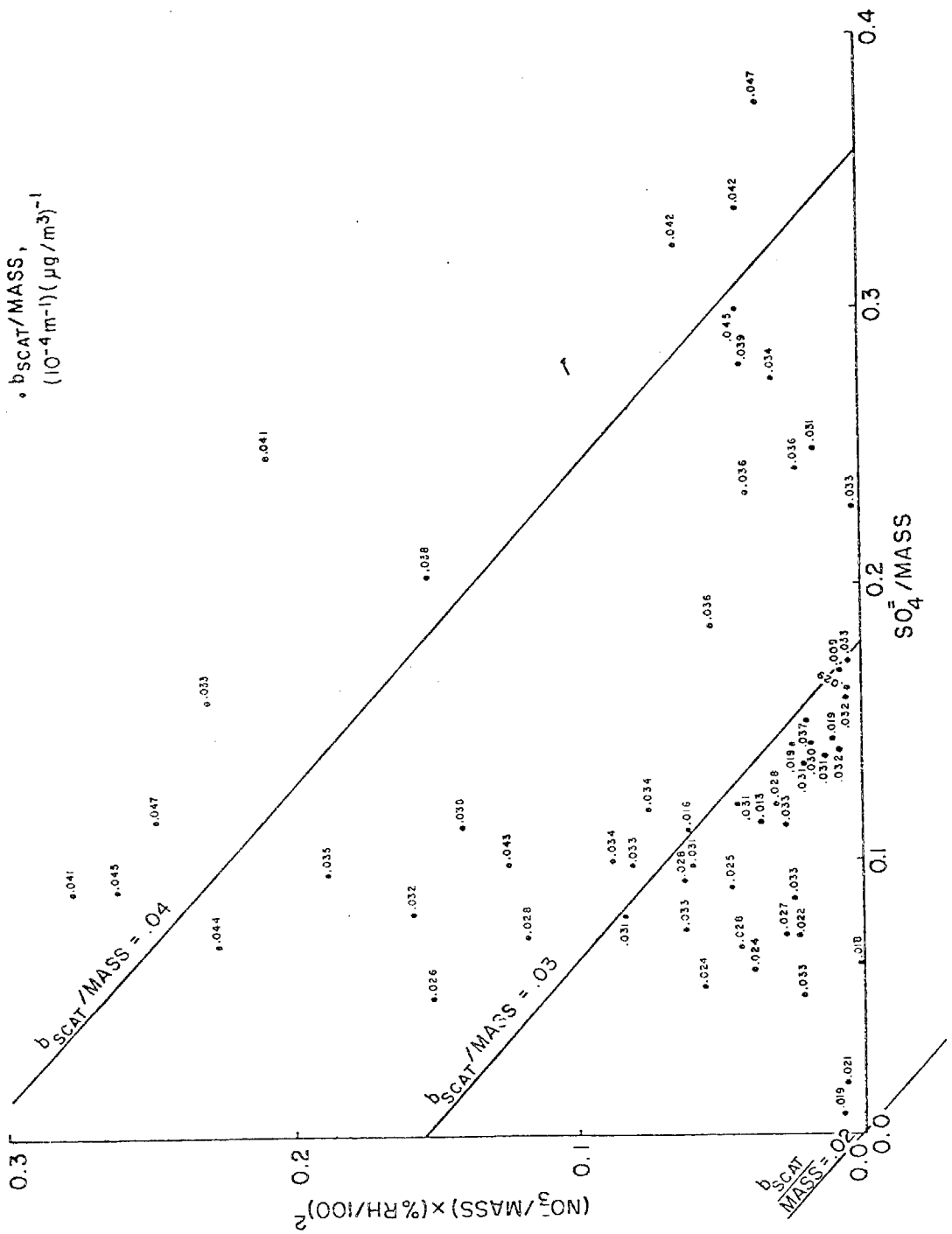

Figure 8-13. Ratios b_{scat}/MASS from Two-Hour Samples at Mobile Van, Plotted as a Function of $SO_4^=$/MASS, NO_3^-/MASS, and Relative Humidity. Values Indicated at Each Point are the Observed b_{scat}/MASS Ratios. Sloping Lines Indicate the b_{scat}/MASS Ratio Predicted by the Regression Relationship.

In (8-20), $b_{scat}/MASS$ is presented as the average of three different values, weighted according to the composition of the aerosol. The variable estimate for $b_{scat}/MASS$ obtained in this way is a significant improvement over the constant estimate of (3-10).

What we have done in (8-20) is to break the overall ratio $b_{scat}/MASS$ into terms corresponding to individual aerosol components as follows,

$$b_{scat}/MASS = \Sigma C_i(\mu)\ MASS_i/MASS \quad , \tag{8-21}$$

where $MASS_i$ is the mass concentration of the i^{th} component. The factor $C_i(\mu)$ in (8-21) is calculated as in (8-18):

$$C_i(\mu) = \int G_i(\mu,D_p)\ mass_i\ (\mu,D_p)\ dD_p \quad , \tag{8-22}$$

where $mass_i\ (\mu,D_p)$ is the normalized component mass distribution. If each component of the aerosol possessed a characteristic normalized mass distribution which depended only on the relative humidity, then the factors $C_i(\mu)$ would be uniquely determined, and all of the variability in the ratio $b_{scat}/MASS$ would be associated with changes in the mass fractions $MASS_i/MASS$ of the aerosol components. The success of regression (8-20) indicates that this is to some extent the case.

It is natural, then, to identify $C_i(\mu)\ MASS_i$ as the contribution of the i^{th} aerosol component to the light scattering coefficient. This contribution can be estimated from the coefficients of regression (8-20) and the measured component mass concentrations. On this basis, sulfates and nitrates together account for more than half of the light scattering observed in the two-hour samples at the mobile van, as shown in Table 8-21.

The scattering power of a particle does not increase or decrease in proportion when a mass of material is added or removed, because the resulting change in particle size produces a change in the particle's scattering to mass ratio. Caution is thus called for when extrapolating (8-20) to conditions greatly changed from those for which it was derived, and it may be safer to interpret the numbers in Table 8-21 as the marginal, rather than the absolute,

TABLE 8-21

ESTIMATED BREAKDOWN OF LIGHT SCATTERING COEFFICIENT FOR TWO-HOUR AEROSOL SAMPLES AT MOBILE VAN

	AVERAGE CONTRIBUTION TO b_{scat} (10^{-4} m^{-1}) Total of 6.4 x 10^{-4} m^{-1} Derived From:		
	All Sources	Gasoline	Fuel & Crude Oil
Nitrate Compounds	1.7	1.4	0.3
Sulfate Compounds	2.0	0.3	1.7
Organic Compounds	0.6	0.6	0.0
Sum	4.3	2.3	2.0

scattering contributions of the aerosol components. Notwithstanding these caveats, examination of Figure 8-13 shows that the relationship in (8-20) describes the ACHEX II light scattering data rather well over a considerable range of variations in aerosol composition.

The coefficients of (8-20) are chosen to minimize the scatter relative to aerosol mass concentration; the coefficients which minimize the absolute scatter are slightly different:

$$b_{scat} = -1.1 + .025\ (\text{MASS} - \text{SULFATES} - \text{NITRATES}) + .074\ \text{SULFATES} + (.025 + .049\ \mu^2)\ \text{NITRATES} \pm .9 \qquad (8\text{-}23)$$

$$(n = 58,\ \bar{y} = 6.4,\ r = .970)$$

Analogues of (8-20) and (8-23) are illustrated in Figure 3-10, where the line through the origin with slope equal to average b_{scat}/MASS minimizes scatter relative to aerosol mass concentration and the steeper line with negative b_{scat} intercept minimizes absolute scatter. Because the strong correlation of b_{scat} with MASS has not been factored out of (8-23), the correlation coefficient for this regression is much more impressive than the correlation coefficient for (8-20). On the other hand, precisely because the correlation of b_{scat} with MASS has been factored out of (8-20), the evidence from this regression for the optical importance of sulfates and nitrates is the more convincing.

The functional relationships in (8-20) and (8-23) are but two of scores which were tested in regressions. In this report we will simply summarize the results.

Of all the significant statistical relationships found in our regression of the light scattering data, those of (8-20) and (8-23) minimize the residual scatter in the data. All regressions selected $SO_4^=$, followed by NO_3^-, as the parameters with the highest F - levels and the lowest standard errors in their coefficients. Although carbon was a major constituent of the aerosol, in its

light scattering effectiveness it could not be distinguished statistically from the rest of the non-sulfate, non-nitrate fraction. The inclusion of nickel and lead as tracers for primary aerosols did not significantly improve the relationships. No significant non-linear relationships were found between light scattering and any of the aerosol components. Regression of MASS on aerosol composition indicated that the sulfate and nitrate terms in (8-20) and (8-23) do represent sulfate and nitrate compounds, and do not include significant contributions from unrelated material statistically associated with $SO_4^=$ and NO_3^-.

The importance of sulfate compounds for visibility appears to be due in part to their distribution with respect to particle size. Comparison of Table 8-20 with Figure 3-9 shows that the mass median particle diameter of sulfates averaged a little over 0.5 μ, right in the middle of the particle size range producing the most scattering for a given mass concentration. For comparison, the mass median diameter of carbon was well below 0.5 μ; many of the carbonaceous particles were too small to scatter effectively. Another probable factor contributing to the superior scattering effectiveness of sulfates and nitrates is the affinity of these compounds for water. Much of the scattering statistically associated with sulfate and nitrate may have been due to unbound water which was not measured gravimetrically due to losses in sampling and equilibration.

a. Role of Water Vapor

A possible physical explanation for the superior scattering effectiveness of sulfates and nitrates lies in the known hydroscopicity of some of these compounds, for the addition of water increases scattering without increasing measured mass. We looked for this effect by segregating the two-hour sample periods into two groups by relative humidity, and repeating the above regressions on each group separately.

Of the functional forms tested in regressions for the RH-dependent coefficients $C_i(\mu)$, quadratics generally gave the best fit to the data, as in (8-20) and (8-23). As Figure 8-14 shows, the effects of relative humidity on light scattering determined statistically are similar to those measured directly

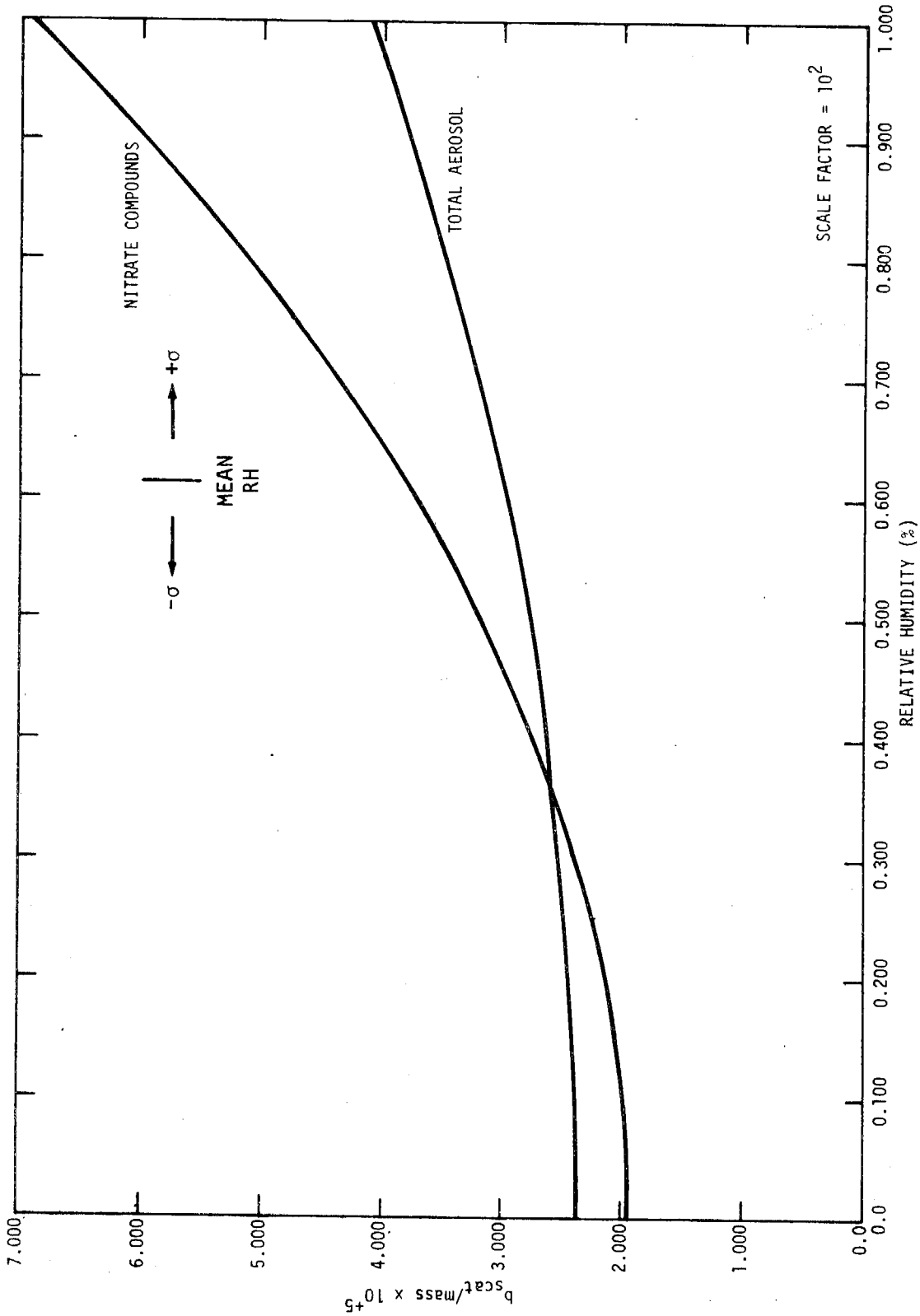

Figure 8-14. Influence of Relative Humidity on b_{scat}/mass Based on Statistical Analysis of Nitrate Behavior and Total Aerosol. Deviations From the Mean Relative Humidity, RH, are Given by ± σ.

with the humidified nephelometer (Covert et al.[61]). The statistical "humidograms" may, of course, be influenced by RH-dependences in the aerosol formation mechanisms, and are not equivalent to true humidograms, which measure specifically the hygroscopicity or deliquescence of the aerosol as sampled. The inclusion of relative humidity effects narrowing the range of estimated scattering effectiveness somewhat. The dependence of aerosol light scattering on relative humidity appears to be due principally to the nitrate compounds, although the size distribution of sulfate compounds shows a statistical dependence on relative humidity.

4. SOURCE CONTRIBUTIONS TO THE AEROSOL

a. Sources of Aerosol Precursors

Mass balances based on known emissions of primary aerosol account for only a small fraction of the nitrates, sulfates, and organics found in the Los Angeles smog aerosol, and the bulk of each of these species is thought to result from gas-to-particle conversion in the atmosphere[84,85]. The mechanisms involved are poorly understood, but the presumed precursors of these species in the gas phase are the nitrogen and sulfur oxides and certain hydrocarbons, particularly the C_6 and larger olefins and some aromatics. Table 8-22 presents an abbreviated inventory of the sources of these gases.

Table 8-22 shows that two broadly defined groups of sources, with mutually distinct geographical distributions and characteristic emissions, are responsible for nearly all of the production of reactive gases in Los Angeles. The gasoline sources are distributed fairly uniformly over a large area of the basin, and produce nearly all of the reactive hydrocarbons. The fuel and crude oil sources are clustered along the coast, and produce most of the sulfur oxides. In this section we identify, and statistically validate, chemical tracers for the emissions of these two source groups.

Lead aerosol and carbon monoxide are important constituents of the exhaust from gasoline powered motor vehicles. This single source is estimated to account for 97-98% of all emissions of these species in the Los Angeles air basin, about 9 tons/day of airborne lead (estimated from Huntzicker et al.[96] and 10,000 tons/day of carbon monoxide (from APCD figures). The reliability of

TABLE 8-22

INVENTORY OF ESTIMATED REACTIVE GAS EMISSIONS IN THE LOS ANGELES BASIN COMPILED FROM MOST RECENT INVENTORIES BY LOCAL AIR POLLUTION CONTROL DISTRICTS: LOS ANGELES (1973), ORANGE COUNTY (1972), SAN BERNARDINO (1972), AND RIVERSIDE (1970).

SOURCE TYPE	Emissions (metric tons/day) NO_x	SO_2	RHC[a]
1. Gasoline	1040	40	1070
Motor vehicle exhaust and blowby[b]	1040	40	770
Evaporation	0	0	300
2. Fuel oil and crude oil	430	345	10
Power plants	150	190	
Industry and commerce	160	20	
Ships, railroads, jets, diesel vehicles	90	20	5
Petroleum refining and sulfur recovery	30	115	5
3. Other	10	55	70

(a) Reactive hydrocarbons as defined by the APCD's include some species, such as the light olefins, which are not converted to aerosol in significant amounts.

(b) Based on the seven-mode cycle.

lead and carbon monoxide as tracers can be judged from their correlation in the two-hour samples taken at the mobile van:

$$CO(ppm) = .8 + .83\ Pb \pm .5 \quad (n = 53,\ \bar{y} = 3.3,\ r = .964) \quad . \qquad (8\text{-}24)$$

The non-dimensional value of the lead coefficient in (8-24) is 954, which is close to the estimated mass ratio of carbon monoxide emissions to lead emissions, 10,000/9 = 1,111.

Nickel and vanadium are, like sulfur, trace constituents of the heavier fractions of petroleum, and are exhausted to the atmosphere in aerosols during the regeneration of refinery catalyst and the combustion of fuel oil. It is estimated that, nationwide, more vanadium is released to the atmosphere in this manner than is consumed in all metallurgical applications combined[103]. Nickel correlates with vanadium in the eleven two-hour samples analyzed for vanadium and in the 24-hour hi-vol samples:

$$V = 0.11 + .72*Ni \pm 0.14 \quad (n = 11,\ \bar{y} = .051,\ r = .829) \qquad (8\text{-}25a)$$
(2-hour)

$$V = .006 + .91\ Ni \pm .008 \quad (n = 11,\ \bar{y} = .030,\ r = .907) \qquad (8\text{-}25b)$$
(24-hour)

The ratio of Ni to V in fuel and crude oils fluctuates greatly from batch to batch, and we are unable to estimate the ratio of the emissions of these elements for comparison with the Ni coefficients of (8-25).

Of the four source tracers discussed above, only lead and nickel were monitored for all two-hour samples taken at the mobile van and satellite stations. Figure 8-15 shows the geographical distribution of the nickel to lead ratio calculated from the average values of lead and nickel during the sea breeze regime. The limited data suggest a nickel-rich plume originating in the area between El Segundo and Alamitos Bay and following wind streamlines to the north and east.

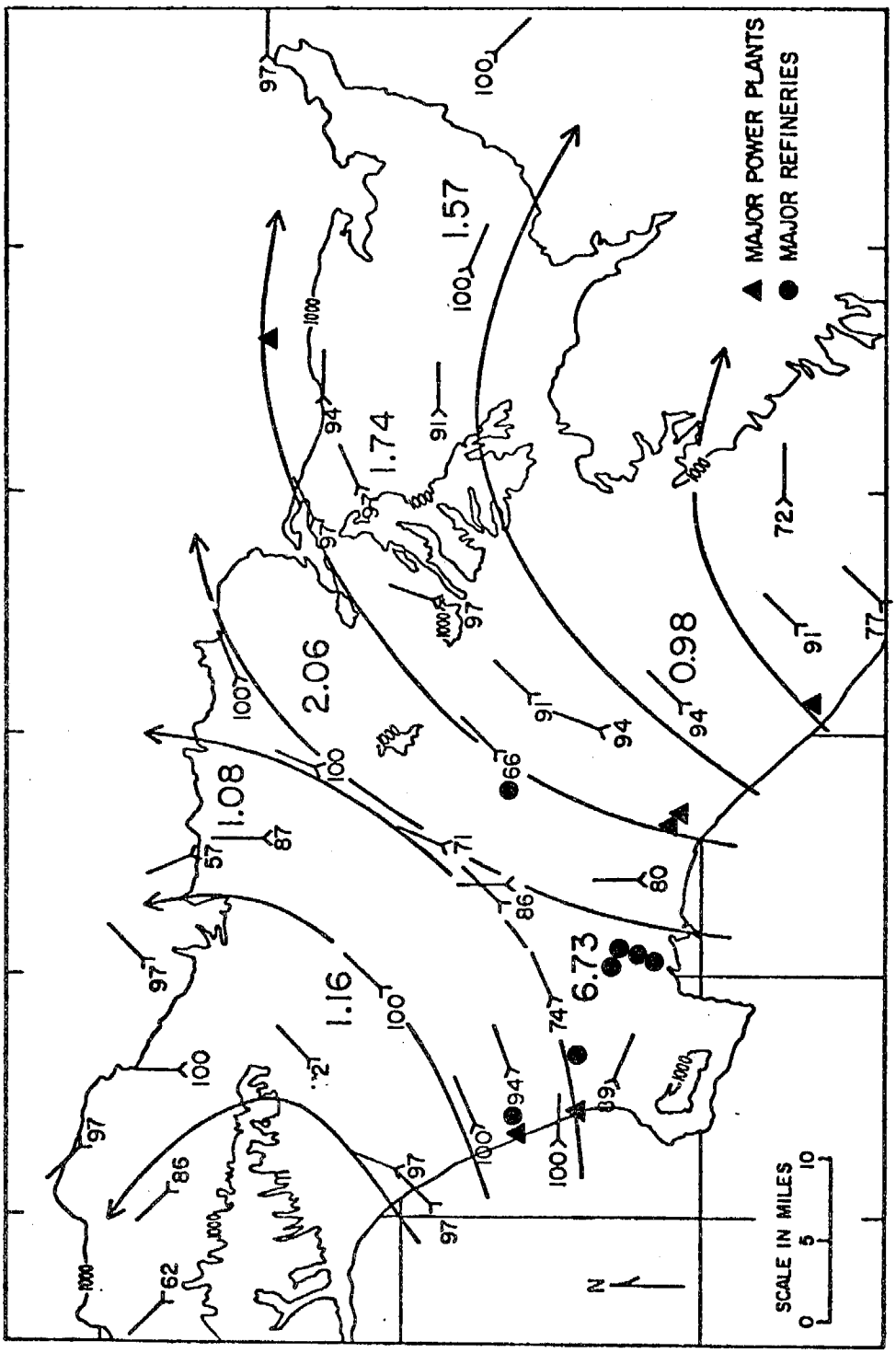

Figure 8-15: Patterns of Pollutant Transport in Afternoon. Arrows Show Most Frequent Surface Wind Directions on 16-Point Compass, With Percent Frequency of Three Adjacent Directions Given by Numbers at Tails. (One-Hour Readings 12:00-18:00 on 7/25, 8/9, 8/17, 9/6 and 10/5, Collected From APCD's and National Weather Service by Meteorology Research, Inc.) Bold Numbers Give Ratios Ni/Pb. (From Average Ni and Pb in Two-Hour Aerosol Samples Taken 12:00-18:00 at Mobile Van and Satellite Stations.)

Oxides of nitrogen and sulfur were measured during the two-hour sampling periods at the mobile van. If we set $N_T = N_{NO_x} + N_{NO_3^-}$ and $S_T = S_{SO_2} + S_{SO_4^=}$, and regress N_T and S_T on Pb and Ni, we find:

$$\begin{aligned} &\text{(a)}\quad N_T = -11 + 34Pb \pm 32 \quad (n = 17,\ \bar{y} = 145,\ r = .954) \\ &\qquad\qquad\qquad\qquad \text{before 10:00 PST} \\ &\text{(b)}\quad N_T = 7 + 17Pb + 199{*}Ni = 10 \quad (n = 43,\ \bar{y} = 57,\ r = .884) \\ &\qquad\qquad\qquad\qquad \text{after 10:00 PST} \end{aligned} \tag{8-26}$$

$$\begin{aligned} &\text{(a)}\quad S_T = 4 + 746Ni \pm 11 \quad (n = 14,\ \bar{y} = 45,\ r = .949) \\ &\qquad\qquad\qquad\qquad \text{before 10:00 PST} \\ &\text{(b)}\quad S_T = 25 + 430{*}Ni \pm 16 \quad (n = 30,\ \bar{y} = 49,\ r = .559) \\ &\qquad\qquad\qquad\qquad \text{after 10:00 PST} \end{aligned} \tag{8-27}$$

These relationships are in qualitative agreement with the inventory, linking nitrogen primarily to gasoline sources and sulfur to fuel and crude oil sources. The scatter in both morning relationships is small, and we can use the coefficient of (8-27a), together with known sulfur emissions, to estimate emissions of nickel in the Los Angeles air basin: [(32/64) 385 tons/day]/ $746 \cong \frac{1}{4}$ ton/day. The coefficient of lead in (8-26a) is close to the estimated ratio of nitrogen emissions to lead emissions for motor vehicles, [(14/46) 1040]/9 = 35.

In view of the lack of any correlation between nitrogen and nickel in the morning, the sulfur present at this time probably came principally from refinery operations, which produce only small amounts of nitrogen oxides, and not from power plants, which produce comparable quantities of nitrogen and sulfur oxides. The much higher effective stack heights of power plants apparently enabled their emissions to penetrate the low morning inversions.

There is a good deal of scatter in the afternoon relationships, and the coefficients of Pb and Ni are lower than they are in the morning. These lower coefficients may reflect the loss of nitrogen and sulfur oxides to atmospheric and surface sinks.

b. Calculation of Source Contributions

In this section we develop estimates for the contributions of the two source groups identified in the preceding section to ambient levels of particulate nitrates, sulfates, and organics. To simplify notation, let X_1, X_2, and X_3 represent secondary nitrates, sulfates, and organics, and let $[X_j]_i$ be the concentration, in a given air parcel, of X_j produced from the emissions of source group i. If source group i is considered as a single emitter, then $[X_j]_i$ is given formally by:

$$[X_j]_i = f_{ij} \frac{\phi_i}{V} e_{ij} \quad ,$$

where e_{ij} (tons/day) is the emission rate of X_j precursor by source group i, ϕ_i (days) is the fraction of source group i's daily emissions which is exhausted into the air parcel, $V(m^3)$ is the volume of the air parcel, and f_{ij} (ug/ton) is the mass of X_j produced from a ton of precursor emitted by source group i.

We have no way of measuring f_{ij}, and will assume for simplicity that $f_{1j} = f_{2j}$; for each species, the fraction of the gas-phase precursor converted to particulate is independent of the precursor source. If we assume also that the two source groups of Table 8-22 account for all emissions of X_j precursor, then the fraction of X_j attributable to each source group is:

$$[X_j]_1/[X_j] = e_{1j}/(e_{1j} + we_{2j}), \tag{8-28}$$

$$[X_j]_2/[X_j] = we_{2j}/(e_{1j} + we_{2j}) \quad ,$$

where $w = \phi_2/\phi_1$. The quantities e_{ij} are given in Table 8-22, and w can be determined from the source tracers identified in the preceding section:

$$w = (Ni/e_{2,Ni})/(Pb/e_{1,Pb}) = (Ni/\tfrac{1}{4})/(Pb/9) = 36Ni/Pb \tag{8-29}$$

The quantity $[X_j]$ is just the measured concentration of particulate nitrates, sulfates, or organics, if we neglect the contributions of primary aerosols.

Table 8-19 gives average values for $[X_j]_i$, calculated from (8-28) and (8-29) using concentrations of compounds and tracers samples during ACHEX II. Table 8-21 presents corresponding breakdowns of the aerosol light scattering coefficient. The calculations are not very sensitive to the crude assumptions on which they are based, because most nitrogen oxides and reactive hydrocarbons come from gasoline sources, while most sulfur oxides come from fuel and crude oil sources. Indeed, the estimated total contributions of the two source groups are not very different if we simply attribute all nitrates and organics to gasoline sources and all sulfates to fuel and crude oil sources.

It should be noted that, while the sources itemized in Table 8-22 are involved in producing a large fraction of the ambient aerosol, they are not the sole agents of this production. For example, sulfur oxides are essential to the formation of sulfate aerosol, but the process is facilitated by the presence of ammonia and reactive hydrocarbons. The major sources of sulfur oxides are not major sources of ammonia and reactive hydrocarbons, so that it is somewhat misleading to attribute all effects of sulfates to the sources of sulfur oxides.

c. Geographical Variations in Aerosol Composition

ACHEX II revealed substantial geographical variations in aerosol concentration and composition. The relative contributions of individual aerosol components and precursor source groups depended strongly on location, as shown in Figures 8-16 to 8-19. These figures are based on data from the satellite stations. Since relative humidity was not monitored at these stations, the breakdown of b_{scat} if Figures 8-17 and 8-19 is based on the following regression, rather than regression (8-20):

$$b_{scat}/\text{MASS} = .015\ (\text{MASS} - \text{SULFATES} - \text{NITRATES})/\text{MASS} \qquad (8\text{-}30)$$

$$+ .071\ \text{SULFATES/MASS} + .050\ \text{NITRATES/MASS} \pm .007$$

$$(n = 58,\ \bar{y} = .032,\ r = .600) \quad .$$

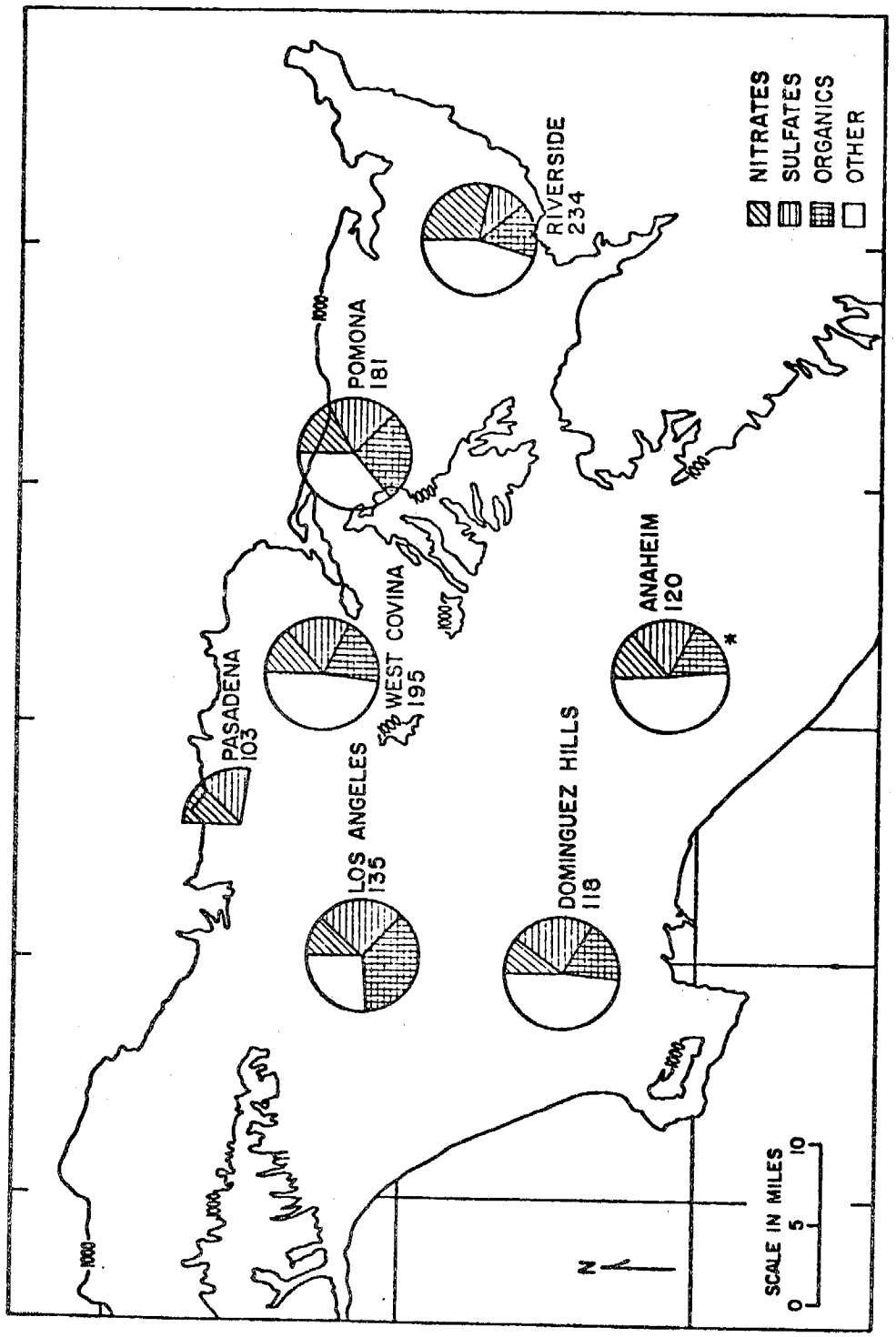

Figure 8-16. Geographical Distribution of Aerosol Mass Concentration Given as # ($\mu g/m^3$) and Estimated Breakdown by Component. (Average of Two-hour Aerosol Samples at Mobile Van and Satellite Stations.) Asterisk Indicates Carbon Measured for Less Than 2/3 of Samples at that Location.

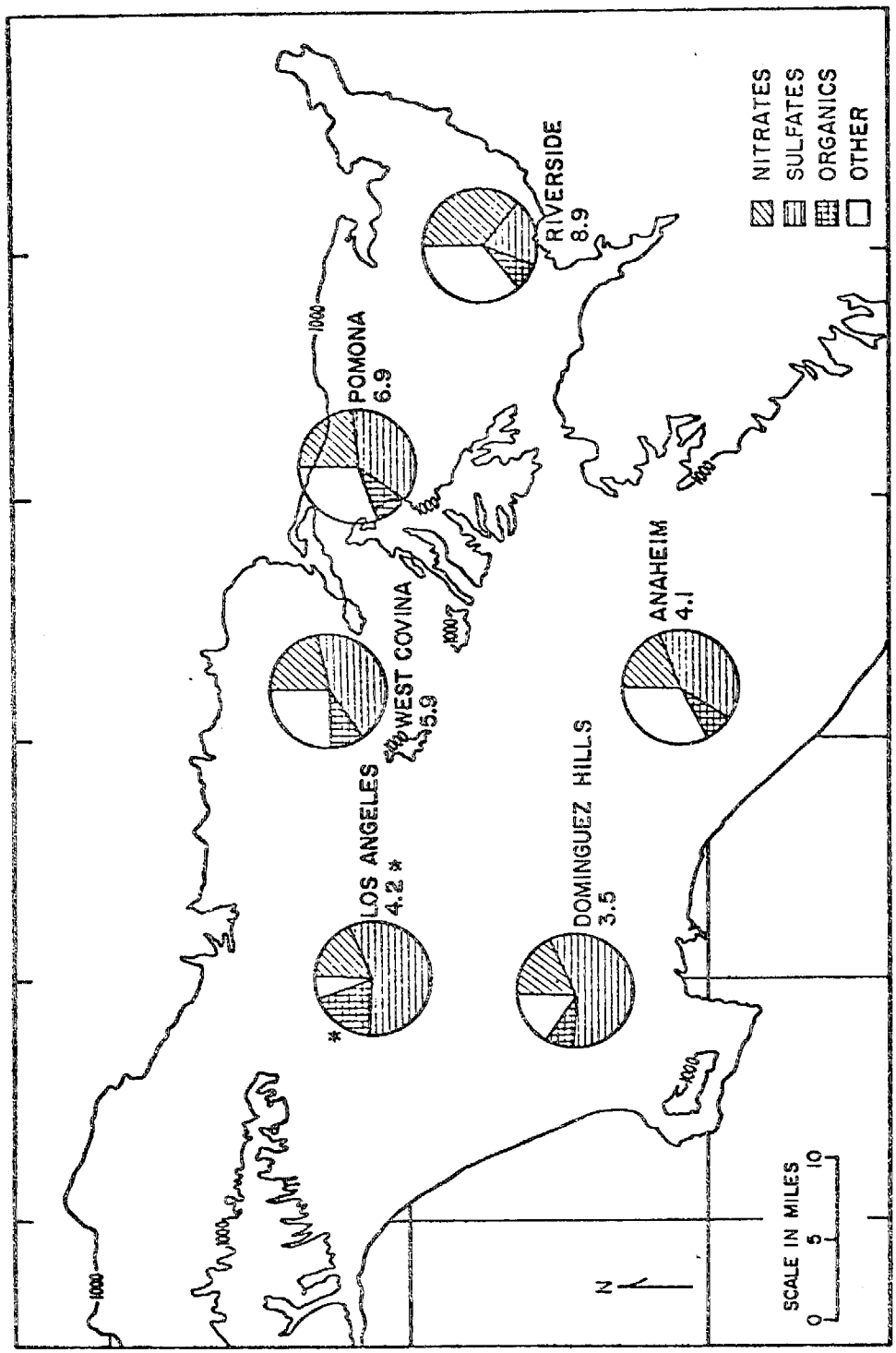

Figure 8-17. Geographical Distribution of Aerosol Light Scattering Coefficient (10^{-4} m^{-1}) and Estimated Breakdown by Component. (Average of Two-Hour Aerosol Samples at Mobile Van and Satellite Stations.) Asterisk Indicates Carbon or b_{scat} Measured for Less Than 2/3 of Samples at That Location.

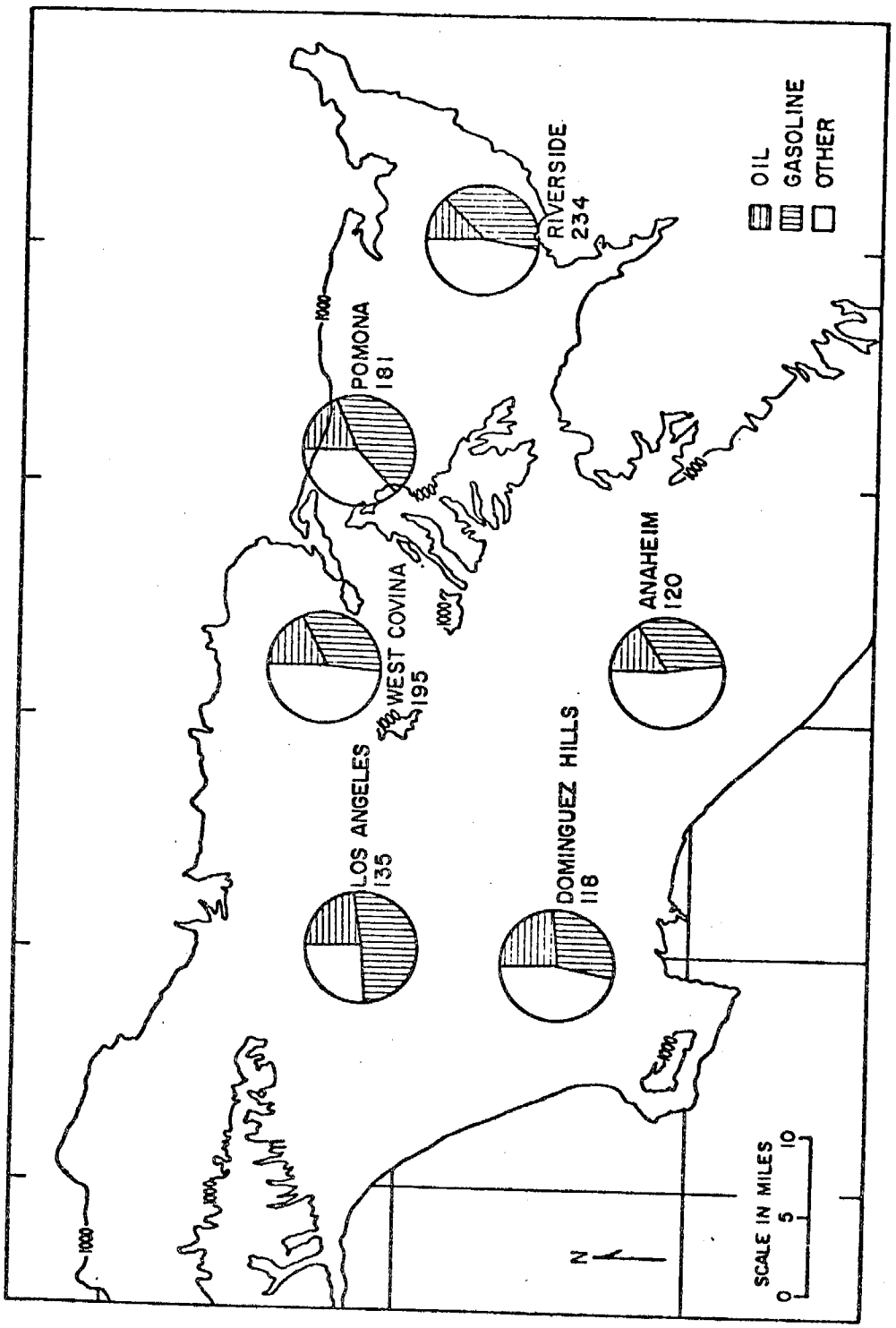

Figure 8-18. Geographical Distribution of Aerosol Mass Concentration ($\mu g/m^3$) and Estimated Breakdown by Source Type. (Average of Two-Hour Aerosol Samples at Mobile Van and Satellite Stations.)

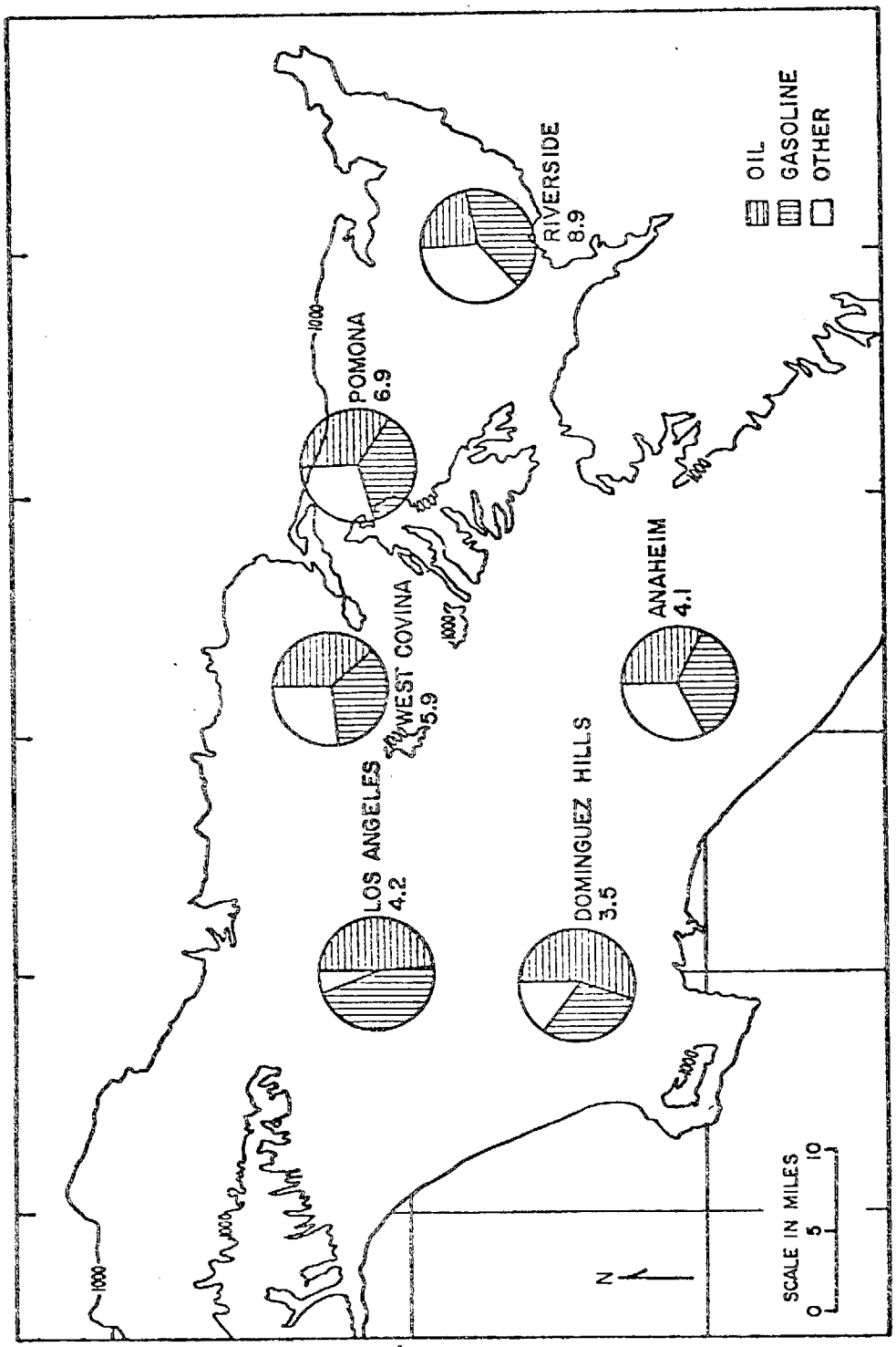

Figure 8-19. Geographical Distribution of Aerosol Light Scattering Concentration (m^{-1}) and Estimated Breakdown by Source Type. (Average of Two-Hour Aerosol Samples at Mobile Van and Satellite Stations.)

This regression, based on mobile van data, gives a relationship which is "averaged" over the distribution of relative humidities experienced at the van.

Generally, sulfates and oil based sources were determined to be more important on the western portion of the basin, and nitrates and mobile sources were more important on the central and eastern side of the basin. The calculated contributions to the total mass concentration of suspended particles suggest that the major secondary contributions, nitrate, sulfate and organics, account for half or more of the aerosol. Organics are a particularly large fraction of the material in Downtown Los Angeles, and sulfate is more or less uniformly distributed across the Basin. In contrast, the secondary constituents account for a significantly larger fraction of the light scattering than the total mass concentration. From 60% to 80% of b_{scat} is ascribed to sulfate, nitrate and organics. Over most of the basin, sulfate accounts for a large fraction of b_{scat}; on the eastern side of the basin, nitrate becomes an increasingly important factor (Figure 8-17).

The calculation of the contribution of all gasoline based sources to the total mass concentration, shown in Figure 8-18, indicates that the southwest corner is influenced heavily by oil and "other" sources, whereas much of the remaining part of the basin has a stronger contribution from gasoline related sources. The "other" source category accounts for a significant fraction of the total mass concentration. The source contributions to the light scattering on the other hand, are heavily dominated by the combustion of oil and gasoline related sources. On the western side, oil related (stationary) sources are key factors, while on the central and eastern parts of the basin, the gasoline (transportation) related sources become equally important and perhaps dominant in the Riverside area. In any case, the role of "other" sources cannot be neglected in consideration of a particulate and visibility control strategy for the South Coast Air Basin.

5. SUMMARY AND CONCLUSIONS

Atmospheric visibility is related to the light scattering coefficient, b_{scat}, of the ambient aerosol. As part of the 1973 Aerosol Characterization Study (ACHEX II) for the California Air Resources Board, the light scattering coefficients and chemical compositions of ambient aerosols were measured at

IX. RECOMMENDED CONTROL STRATEGY FOR AEROSOLS

The ACHEX data and the analysis of this information provide a framework for the development of a control strategy for aerosols in California. The results, of course, apply principally to the South Coast Air Basin, but they can be extrapolated using similar methods to other areas including the San Francisco Bay area and the San Joaquin Valley.

The objective of this section is to review the ACHEX conclusions in the light of a possible control strategy for the South Coast Basin, and provide several recommendations to the Air Resources Board.

As a result of the episodal nature of the ACHEX, questions may arise about the representativeness of the ACHEX data compared with monitoring data taken on an annual basis. Qualitative comparison indicates a satisfactory correspondence between these two data sources. Furthermore, the ACHEX was designed to investigate worst case conditions, which are of principal interest for control policy. Thus, the ACHEX program serves as a basis for the strategic recommendations listed below:

1) To achieve the primary ambient air quality standards for total suspended particulates, effort must be continued to control SO_x, NO_x, and reactive hydrocarbon emissions from all sources because of their importance to atmospheric particle formation.
2) Since the organic fraction is a large portion of the ambient aerosol mass concentration, control of organics is crucial, particularly for reductions in the vapor of compounds with a carbon number six and higher.
3) A reduction in aerosol should occur in the South Coast Basin with implementation of projected controls on NO_x and hydrocarbon vapors. Reduction of these precursors not only will directly influence airborne particles but will be of indirect assistance in reducing the intensity of photochemical reactions.
4) To improve visibility, highest priority should be given to reductions in sulfate from stationary sources and NO_x emissions from motor vehicle sources.

5) Top priority should be given to the South Coast Basin for use of natural gas and low sulfur fuels to minimize emissions of the aerosol precursors NO_x and SO_x.

6) Consideration should be given to priority control of SO_x and NO_x emissions at ground level; in the former case, improvement should occur in haze levels if substantial reductions are made in SO_x emissions from chemical plants in the west and southwest part of the Los Angeles Basin.

7) Continued efforts should be made to improve the control of primary emissions, particularly those derived from transportation sources. Lead and carbonaceous particles represent particularly important contributors. The use of non-leaded fuels may aid in such reductions, but this conclusion requires verification by new studies on vehicle emissions.

8) Consideration of control effort for primary sources must be given to reduction in the emissions of particles 1 μm or less in diameter, so that the sub-micron fraction is preferentially treated.

9) The necessity for the control of the emission of ammonia should be examined in greater detail, as the influence of the gas is to stabilize visibility degrading aerosol.

A. APPROACH TO ACHIEVEMENT OF STANDARDS

The standards that apply to California air are twofold; they include both the federal and state requirements, which are:

1) Suspended Particulate Matter

California: 60 $\mu g/m^3$ annual geometric mean.
100 $\mu g/m^3$ maximum 24 hour average sample

Federal:

(Primary) 75 $\mu g/m^3$ annual geometric mean.
260 $\mu g/m^3$ 24 hour average not to be exceeded more than once per year.

(Secondary) 60 $\mu g/m^3$ annual geometric mean.
150 $\mu g/m^3$ 24 hour average not to be exceeded more than once per year.

2) Visibility

California:

Not to be reduced under ten miles for conditions of less than 70% relative humidity.

The California standards are the more rigid requirements for control of aerosols.

The control strategy for airborne particles requires consideration of two separate standards for ambient air quality. The two criteria are not necessarily compatible, as exemplified by the fact that the super-micron fraction influences the total mass concentration more than the visibility, which depends primarily on the particle range between 0.1 μm and 1.0 μm diameter. Furthermore, the statistical (regression) analysis of the 1973 data indicates empirically a different dependence of mass concentration and light scattering coefficient on key chemical constituents. Therefore, any strategy contemplated may require some compromise to meet both standards. The principal differences lie in dealing with the organic constituent, which influences the mass concentration more strongly than the light scattering coefficient.

Since the ACHEX data apply to extreme conditions on a 24 hour basis, further consideration of control strategy is confined principally to the realization of the short term standards.

B. TOTAL MASS CONCENTRATION

1. SIGNIFICANCE OF SECONDARY CONTRIBUTIONS

Examination of the analysis using trace constituents discussed in Chapter VIII indicates the importance of secondary aerosol production as compared to primary constituents and the natural background. This can be illustrated readily by the diagrams in Figure 9-1. Here two cases are shown for different sites and different times of 1972 in the north central and northeast part of the Los Angeles Basin. From such results it is clear that the achievement of the primary air quality standards will depend on the continued efforts to control SO_x, NO_x and reactive hydrocarbon emissions from all sources.

A. PASADENA 9/20/72
1200 - 1400 PST
LOW OXIDANT, TOTAL MASS
CONCENTRATION, 79 $\mu g/m^3$

B. POMONA 10/24/72
1200 - 1400 PST
MODERATE OXIDANT, TOTAL
MASS CONCENTRATION, 178 $\mu g/m^3$

Figure 9-1. Distribution by Source of Aerosol Mass Concentration for Filter Samples Collected Over Two Hour Periods, and Equilibrated to Air at Less Than 50% Relative Humidity

Organic Precursors

The hydrocarbon precursors to aerosol formation are particularly important from the standpoint of control. These constituents of smog have not been identified, but the arguments given in Chapter VI provide compelling evidence that high molecular weight vapors corresponding to materials of carbon number six and higher should be of primary concern. The sources of such vapors, particularly non-aromatic materials, are not well known, but studies of diesel exhaust, for example, have shown that hydrocarbons up to C_{12} are present. Although no reports are available of hydrocarbon vapor emissions with molecular weights greater than approximately C_8 compounds from light duty motor vehicles, there is no reason why compounds of higher carbon number might not be present.

The importance to aerosol formation of aromatic vapors with a carbon number greater than ten has not been determined. However, these materials should not be ruled out as possible precursors without further investigation.

Inorganic Gases

The evidence from ACHEX shows clearly that the achievement of ambient air quality standards requires heavy emphasis on the reduction of sulfur oxide emissions and nitrogen oxide emissions in the Basin. Reasons for identification of SO_x mainly with stationary sources and burning of fuel oil have been presented on the basis of the Los Angeles Basin emission inventories. On the other hand, the emission data suggest that NO_x is limited more to transportation sources. The results of the analysis in Section VIII, shown in Figure 9-2, suggest that transportation sources, identified as gasoline users, contribute heavily to aerosol loading over the Basin through NO_x and hydrocarbon emissions. However, stationary sources, through SO_x, are significant over the northern part of the Basin.

In such simplified discussions of contributions to aerosol loading, differences in source-mass concentration relationships have been recognized. However, there is a major uncertainty in the significance of the vertical distribution of precursors. Previously, arguments have been given suggesting that the sulfur oxide emissions having greatest impact on the Basin are those

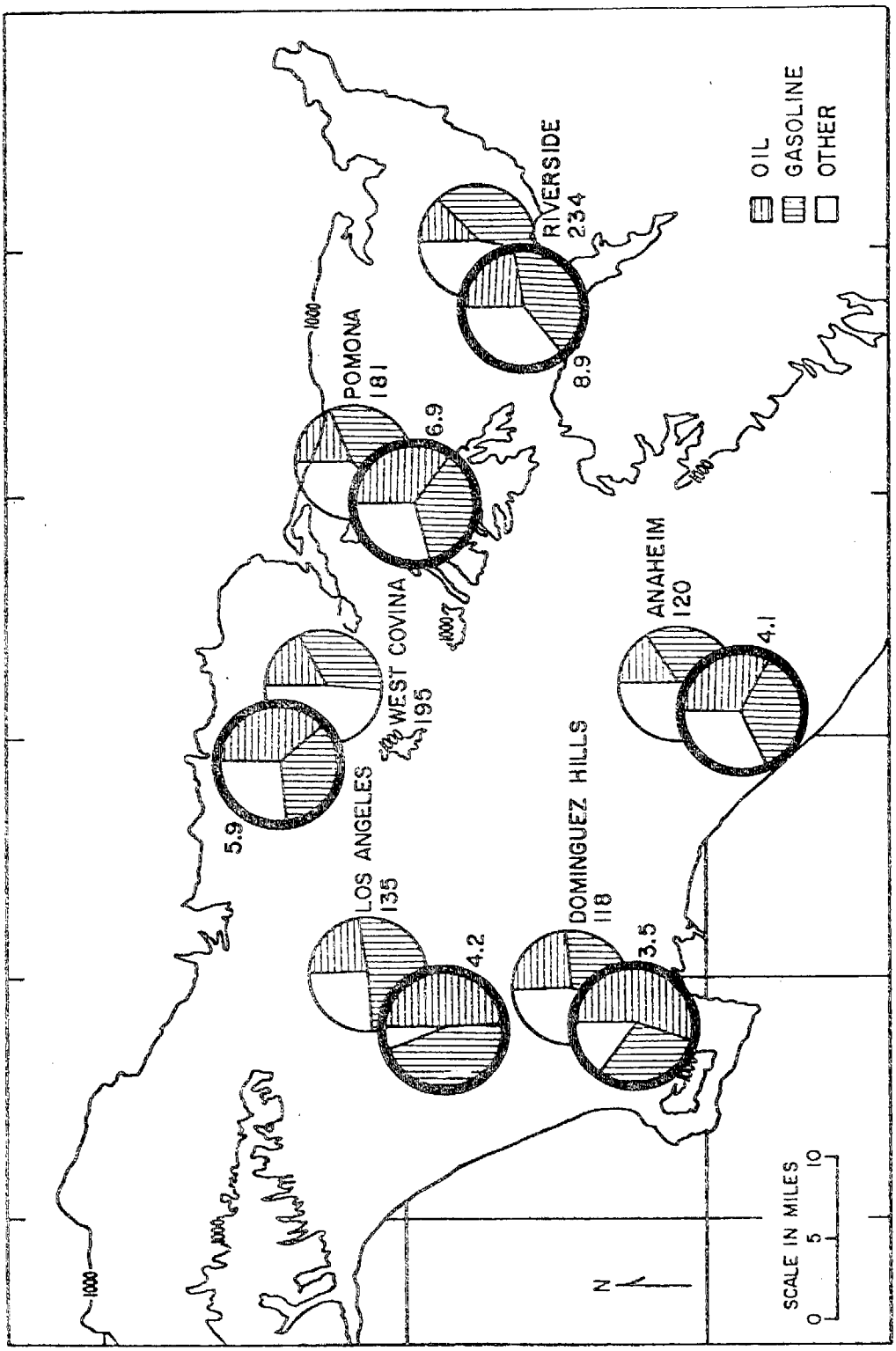

Figure 9-2. Comparison of the Distribution of Sources for Aerosol Mass Concentrations and Light Scattering in the South Coast Air Basin. Numbers by These Outlined Discs are Averaged Mass Concentrations of 2 hr 1973 Samples. Numbers by the Thick Discs are Averaged Light Scattering Coefficient in 10^{-4} m^{-1}. The Contour is the 1,000 ft. Height Level.

emitted from non-fuel burning sources, or the refineries and chemical plants in the west and northwest parts of the Los Angeles area. This raises the question of the importance of elevated sources in the evolution of smog aerosol over the city. In particular, there is considerable uncertainty in the identification of sulfur oxides solely with the chemical industry in the eastern part of the Basin, especially in Riverside, where material from elevated sources to the west may reach the ground. At the same time, a significant contribution to nitrate from the oxidation of NO_x from elevated stationary sources cannot be ruled out in the eastern part of the Los Angeles Basin. Thus, the strategy for controlling the inorganic fraction of the aerosols must take into account the spatial distribution and the vertical structure of the reactive gas concentrations. Such an analysis was beyond the scope of the ACHEX. However, an attempt could be made to improve our conclusions by further study of the ACHEX results in the light of the MRI/Navy aircraft program, and the Metronics tracer studies.

Another important question that remains unresolved is the role of ammonia in stabilizing the nitrate aerosol. In view of the strong differences in nitrate between the western and eastern parts of the Los Angeles Basin, and the evidence for differences in ambient ammonia levels, we recommend that further investigation of the ammonia question be undertaken. In particular, an ammonia emissions inventory and more extensive observations of ambient ammonia concentrations would provide a better basis for development of a knowledgeable aerosol control strategy.

Photochemical Enhancement

The evidence of ACHEX indicates a strong interaction between gas reactions and haze formation in smog. Because of the physico-chemical synergism between aerosols and the oxidant precursors, hydrocarbons and NO_x, the control strategy for oxidant should improve directly the aerosol situation. Although the details of these interactions are not known at this time, it is clear that substantial reductions in NO_x during the next several years should improve the nitrate levels in the South Coast Basin. The relation between non-methane or reactive hydrocarbons and aerosols is more tenuous, but qualitatively, less organic aerosol should be expected with reduction

in the intensity of photochemical oxidant production.

Use of Low Sulfur Fuels

Whatever the details of the interactions leading to oxidation of SO_x and NO_x in the atmosphere, it is clear from the discussions in Chapter VIII and this section that improvement in ambient air quality with respect to aerosols requires a strategy of low sulfur fuel usage at highest priority in the South Coast Basin. Increases in sulfur content of fuels will surely lead to increases in sulfate production if the conversion ratio remains roughly constant. Furthermore, switching from natural gas usage to fuel oil will increase the sulfur oxides substantially, even with low sulfur fuel, and will increase the NO_x production in major stationary sources. Therefore, efforts should be made on a statewide and nationwide basis to place the South Coast Basin high on the regional priority list for low sulfur fuels.

Influence of Auto Exhaust Control

An additional factor that must be accounted for in control strategy is the influence of the auto emission catalyst control system on sulfates. The addition of catalysts to automobiles in 1975 and later models is expected to create conditions for increasing sulfate emissions from motor vehicles. These emissions are believed to be small at present. Based on the results of this study, a maximum influence on ambient sulfate can be estimated. We take the average conversion ratio for sulfur in the Los Angeles area to be 0.25. Using the 1971 emissions inventory of the Los Angeles County APCD, the following distribution is assumed:

Source	SO_2 Emissions (tons/day)
Motor Vehicle	35
Other (including aircraft and stationary sources)	215
Total	250

Evidence from motor vehicle emission tests suggests that approximately 40% of the sulfur in gasoline will be converted to sulfate in catalyst equipped cars. With these assumptions, a comparison between the case for completely equipped catalyst cars and no catalyst cars is shown in Table 9-1. Based on these calculations, one can expect that a maximum increase in sulfate of 10%-20%

TABLE 9-1

ESTIMATED INFLUENCE OF AUTO EXHAUST CONTROL ON AMBIENT SULFATE LEVELS
(ALL VALUES GIVEN IN $\mu g/m^3$ SO_2 EQUIVALENTS)

A. Without Catalyst

	Particulate	Gas
Motor Vehicle (Primary)	0	8.4
(Secondary)	2.1	-
Stationary Source	12.9	51.6
Total	15	60

B. With Catalyst

	Particulate	Gas
Motor Vehicle (Primary)	3.4	5.0
(Secondary)	1.3	-
Stationary Source	12.9	51.6
Total	17.6	56.6

can be expected with use of present catalyst emission control systems on a basinwide average. This change is likely to be overshadowed strongly by increases expected from more widespread use of fuel oil for stationary sources in the Los Angeles area.

The arguments used for basinwide changes in sulfate, of course, do not preclude the possibility of a major sulfate exposure hazard developing on or near the freeways. However, this is a different question from the ones under consideration here.

2. PRIMARY EMISSIONS AND NATURAL BACKGROUND

Although the secondary contribution to the aerosol concentration is the major factor, based on ACHEX data, the role of primary emissions and uncontrollable factors such as the natural background and liquid water also must be taken into account. In the examples in Figure 9-1, the sea salt and soil dust contributions to the aerosol amount to an appreciable fraction of the ambient air quality standard. Combined with water and sulfate and nitrate, the uncontrollable portion of the ambient aerosol will amount to approximately one third or more of the standard level of 100 $\mu g/m^3$ over a 24 hour period. On the other hand, the (controllable) primary emissions from stationary sources and from transportation sources contribute about 10%-20% to the total loading.

The statistical analysis of White *et al.*[101] discussed in Chapter VIII shows that the aerosol mass concentration is influenced significantly by material from sources other than those related to $SO_4^=$, NO_3^- and organic carbon. In Figure 9-2, essentially half of the material in West Covina, Anaheim, Dominguez Hills and Riverside are in the "other" category. It is likely that a significant portion of this fraction is the natural or quasi-natural background, and the remainder may be accounted for by a number of poorly defined primary sources that cannot be linked with combustion or processing of fossil fuels. Thus, it is important that continued efforts be made to identify such sources and reduce their emissions.

A potentially important controllable emission for which a California regulation exists is lead from automobile exhaust. The lead emissions are

accompanied by roughly an equal amount of particulate carbon. The use of non-leaded fuel, required by catalyst-equipped cars, will improve the lead halide emissions. However, the evidence that non-leaded fuels also will decrease other auto emissions, such as a carbon, is ambiguous. Further examination of this question with new automobiles and older models with substantial mileage should clarify this issue.

C. THE VISIBILITY STANDARD

The work of the ACHEX amply demonstrates that a distinction must be made between the visibility reducing fraction of the aerosol and the total mass concentration. A simple interpretation of the aerosol data depends on the uniqueness of the link between particle concentration, the light scattering coefficient, b_{scat}, and visibility. Accepting the existence of such a practical relationship, the difference between optical effects and total mass concentration appears to be dominated for a given air basin by the particle size distribution. Thus, the central strategy for particulate matter in California must take into account the differences in aerosol behavior with particle size. Our analysis indicates that the bulk of the secondary aerosol accumulates in the light scattering range between 0.1 μm and 1.0 μm. In addition, the production of aerosols from primary anthropogenic sources tends to be confined to the range < 1.0 μm diameter through aging processing and the influence of modern combustion methods. Thus, the development of controls for primary emissions should take into account the heavy influence on the submicron aerosol fraction. New, more efficient methods now are required to improve the control of aerosol emissions from primary sources. Heaviest emphasis should be placed on the development of such new equipment because of the projected needs to use "dirtier" (more particle producing) fuels in the future.

Qualitatively, the light scattering coefficient has been shown to be correlated well with sulfate, nitrate and carbon content of the aerosol in the Los Angeles Basin. However, the statistical analysis by major source in Chapter VIII indicated that major distinctions existed between the contributions to aerosol loading by total mass concentration vs. the light scattering coefficient. This is shown graphically in Figure 9-2, where the emission

distributions by major source for the two parameters are superimposed. As expected from considerations of the differences in behavior of the sub-microns and super-micron particle size ranges, the secondary dominated contributions related to $SO_4^=$ and NO_3^- dominate to a much greater extent the light scattering than the total mass concentration. In addition, the analysis suggests a shift in dominance of the light scattering by stationary sources in the western and central parts of the Basin to transportation sources in the eastern side of the Basin.

From a comparison of the empirical results in Equations (8-20) and (8-23), the scattering coefficient depends most strongly on the sulfur oxide and nitrogen oxide contributions (per unit mass), rather than other material, including carbon, which tends to dominate the mass concentration. Thus, the control strategy for improvement of visibility in the Los Angeles area must place highest priority on reduction of sulfur dioxide and nitrogen oxide emissions, particularly on the western and northwest-central areas of the Basin. Such a conclusion comes from the combined analysis of b_{scat} and mass concentration, and could not be derived from evaluation of one or the other of these simple measurable parameters alone.

D. ESTIMATION OF EMISSION REDUCTIONS

The discussion so far has centered on a qualitative assessment of the ACHEX results which suggest control measures for achievement of the ambient air quality standards for aerosols. The conclusions can be made somewhat more quantitative by applying the traditional rollback model for relating emissions to air quality. The calculations using data for the chemical nature of the aerosols in Los Angeles air indicate that stringent requirements will be necessary for reduction of the secondary contributions. The statistical analysis given in Section VIII-D, is most straightforward for application to a control strategy. However, the following assumptions must be borne in mind:

1) The empirical relations for relating total mass concentration and light scattering coefficient are applicable despite the limited data base used for their derivation.

2) The emissions inventory for the South Coast Basin is an accurate assessment of the contributions of individual sources to various pollutants, and the inventory is applicable over time periods corresponding to daily behavior.

3) A direct proportionality exists between sulfate and SO_2 related emissions, NO_3 and NO_x related emissions, and organic material and non-methane related hydrocarbons (NMHC) emissions.

4) The behavior of total mass concentration and b_{scat} are dominated by NO_3^-, SO_4 and organics even though other particulate materials may correlate closely with one or more of these components.

5) No "value added" reduction resulting from reduction in photochemical smog activity is taken into account.

6) The time period from 1972 through 1980 is adopted for changes. To make the calculations, the following model aerosol is taken as typical of an aerosol condition experienced in the Basin during smog conditions with oxidant in excess of 0.2 ppm on the central and eastern parts of the Basin:

	$\mu g/m^3$
Total Mass	200
*Sulfate	15
*Nitrate	20
*Non-Carbonate Carbon	50
Relative Humidity (μ)	0.60
Base Year: 1972	

To illustrate the impact of a control strategy, the following empirical relations derived from the analysis in Chapter VIII are employed:

Total Mass Concentration

$$\text{mass } (\mu g/m^3) = 26 + 1.56\ (NO_3^-) + (1.28 - 0.58\ \mu^2)\ (SO_4^=) + 2.55\ (\text{Organics}) \pm 21 \qquad (9\text{-}1)$$

*Includes related substances (see Section VIII).

Light Scattering Coefficient

$$b_{scat} \times 10^4 (m^{-1}) = -1.1 + 0.074(SO_4^{=}) + (0.025 + 0.049\,\mu^2)\,(NO_3^{-}) + 0.025\,(\text{Organic C}) + 0.025\,(\text{Mass} - SO_4^{=} - NO_3^{-} - \text{Organics}) \pm 0.9 \qquad (8\text{-}23A)$$

The constituent concentrations are given in $\mu g/m^3$.

Reduction in Nitrate and Non-Methane Hydrocarbons (NMHC)

During the next few years, the present control strategy for the South Coast Basin calls for a substantial reduction in NO_x and NMHC emissions. The impact of these expected reductions can be estimated from the above equations. To make such an estimate, the fractional reductions projected for NO_x and NMHc from the Los Angeles County Air Pollution Control District[24] are adopted. For oxides of nitrogen, a reduction of approximately two by current control procedures is estimated between 1972 and 1980. At the same time, a reduction of a factor of four is estimated for NMHC.

Using the 1972 model aerosol, the projected reductions in NO_x and NMHC should result in a model concentration of 99 $\mu g/m^3$ by 1980, without reduction of the SO_x contributions. Therefore, this agreement suggests that the ambient aerosol standard will be approached in 1980 if the proportional relationships to NO_x and NMHC are borne out. However, there is a large uncertainty in such an estimate.

Accompanying the decrease in aerosol mass concentration from 1972 to 1980 would be a change in b_{scat} from 6.1×10^{-4} m^{-1} in 1972 to 2.0×10^{-4} m^{-1} by 1980. This corresponds to an improvement in visual range from 8.7 km(5 mi) to 23 km (~ 14 mi), using the relation that the visual range is $4.7/b_{scat}$ for visible light[77].

This result suggests that the reduction in mass concentration by the existing NO_x and NMHC control strategy should yield an improvement in aerosol levels and in visibility over the South Coast Basin that will provide conditions approaching the 24 hour averaged ambient air quality standards. However, these results are very uncertain and contain no safety factor for control strategy goals.

Implications of a Sulfate Standard

The projected federal ambient air quality standard for water soluble sulfates of 10 $\mu g/m^3$ for a 24 hour average maximum based on health effects, has further influence on the control of airborne particles in the South Coast Basin. On the basis of the ACHEX results, the application of rollback in the form:

$$\% \text{ Reduction} = \frac{\text{Present Ambient Concentration - Derived Concentration}}{\text{Present Concentration - Background Concentration}}$$

is useful. Taking 4 $\mu g/m^3$ $SO_4^=$ for the background, the reduction in SO_x emissions required based on the model aerosol sulfate concentration of 15 $\mu g/m^3$ is approximately 40%. Such a reduction would correspond to the following estimated (24 hour averaged) ambient levels by 1980:

Total mass concentration = 83 $\mu g/m^3$ ± 21

$b_{scat} = 1.6 \times 10^{-4} (m^{-1})$, or visual range ~ 18 miles.

These results are encouraging for predicting improvements in the ambient aerosol concentration in the South Coast Air Basin. However, the rollback estimates should be taken with great caution until the inter-relations between aerosol precursors, particularly NO_x and NMHC, are better determined.

In the meantime, the pressure to implement a sulfate standard based on health effects is mounting. It seems prudent for the State of California to consider a SO_x control strategy at high priority, which will create conditions for improvement of not only the sulfate levels but the total suspended particle levels and the atmospheric visibility.

In any case, we recommend that the results derived from the ACHEX be reviewed carefully in the light of all other available data so that our conclusions can be substantiated further. This is particularly true of the projections for nitrate and organic aerosols, which are based on arbitrary relations to the gaseous precursors, and not well-established chemical relationships emerging from this study or others in the South Coast Basin.

X. INSTRUMENTATION FOR AEROSOL MONITORING

The objective of this section is to review the results of the ACHEX data in the light of future requirements for ambient air monitoring. The present standards for ambient air quality of particulate material are shown in Table 10-1.

The present regulatory requirements state that the total mass concentration of aerosols is to be measured gravimetrically by collecting of material on acid washed glass fiber filters placed in high volume samplers. The weight difference of the filters is to be determined with the filters equilibrated at less than 50% relative humidity.

The visibility conditions are currently monitored by trained observers located at airports and other installations. Visibility measurements are ideally made during the day by distinguishing a black object against a horizon sky at a distance of ten miles. It has been suggested that the integrating nephelometer could be used as a "rational" substitute for the human observer.

The standard for lead represents the first regulation for a chemical constituent of the aerosol. The method requires analysis by the dithizone procedure using high volume filter samples.

For some time, the high volume filter has been criticized for being an inadequate measure of ambient air quality for particulate matter. The high volume sampler suffers from uncertainties in the large particle range because of poorly defined collection efficiency of particles greater than 10 μm. Furthermore, the procedure fails to recognize that there are now known to be major distinctions between the origins and behavior of the submicron and the supermicron size fractions of the aerosol.

The problems of obtaining self-consistent weight differences on filter substrates have been studied for sometime, and these appear to have been solved with stable conditions of relative humidity during weighing.

TABLE 10-1

AMBIENT AIR QUALITY STANDARDS FOR PARTICULATES

Pollutant	California Standard			National Standard		
	Averaging Time	Concentration	Method	Primary	Secondary	Method
Suspended Particulate Matter	Annual Geometric Mean	60 $\mu g/m^3$	High Volume Sampling	75 $\mu g/m^3$	60 $\mu g/m^3$	High Volume Sampling
	24 hour	100 $\mu g/m^3$		260 $\mu g/m^3$	150 $\mu g/m^3$	
Visibility Reducing Particles	1 observation	* In sufficient amount to reduce the prevailing visibility to less than 10 miles when the relative humidity is less than 70%		-	-	-
Lead	30 Day Average	1.5 $\mu g/m^3$	High Volume Sampling, Dithizone Method	-	-	-

*Prevailing visibility is defined as the greatest visibility which is attained or surpassed around at least half of the horizon circle, but not necessarily in continuous sectors.

The choice of filter substrate remains a major uncertainly in sampling and analysis of airborne particles because of interactions between particles and absorbable gases, difference in collection efficiency, and analytical requirements. It now appears clear that different substrates are required for sampling material for organic analysis vs. inorganic analysis.

A. RECOMMENDED IMPROVED STANDARDS

1. SUBMICRON FRACTION

On the basis of the evidence provided from the ACHEX study and other programs, including the 1969 Pasadena Experiment, there is a need to include at least a secondary standard for the mass concentration of fine particles. In particular, we recommend that consideration be given to a California ambient standard in the range of 50-70 $\mu g/m^3$ annual average of 24 hour samples for particles less than 3.5 microns in diamter. The results from the Noll impactor experiments and the Lundgren impactor suggest that the large particle fraction, which has been found to be largely influenced by soil dust or sea salt, amounts to 10 $\mu g/m^3$ in urban air. Thus, one can expect that any ambient standard for mass concentration of small particles should be less than 75 $\mu g/m^3$.

The 3.5 micron diameter particle size presently is being considered by the Environmental Protection Agency to define the upper limit of the respirable particle fraction, as contrasted with material that is eliminated mainly by deposition in the nasal passages. The respirable fraction definition has been a subject of controversy among physiologists for some time. The 3.5 μm diameter appears to be an acceptable one on grounds of available information on the efficiency of particle collection in the human lung. However, this limit might be rationalized as easily to be 1 μm diameter. This smaller value has certain advantages in that it would permit a new standard to be written for the fine particle fraction to be both for health considerations and for light scattering and visibility. The ACHEX data taken in 1973 show a useful correlation between b_{scat} and the particle volume less than 1 μm diameter. This type of correlation is even better if one confines the volume range of interest between 0.1 μm and 1.0 μm in diameter.

2. OTHER STANDARDS

With new atmospheric studies like ACHEX and new health effects studies (e.g., CHESS[104]), there is increasing evidence that sulfate and nitrate as well as some heavy metals in addition to lead, such as vanadium, should be covered by ambient air quality standards. If such standards are promulgated, it will be necessary to institute systematic monitoring in several areas. Some of this is currently being undertaken in the State, but the program may require expansion.

Since organic constituents make up a large fraction of the airborne particle mass concentration, consideration should be given to monitoring routinely for total non-carbonate carbon, which has been found to be a useful index for organic material.

Thus, we recommend that air quality standard be established in California for particulate sulfate, nitrate, and total non-carbonate carbon. On the basis of existing health considerations evolving from Federal data, sulfate should be examined in the range between 10 - 20 $\mu g/m^3$ on a 24-hour average. Nitrates and organics should be monitored to control the total suspended particle concentration unless new health hazard data warrant consideration of an air quality standard for such materials. To achieve the total mass concentration standard in the South Coast Basin, particulate, nitrate and non-carbonate carbon should be reduced to 24-hour average levels in the range between 10 - 20 $\mu g/m^3$.

B. APPROACH TO INSTRUMENTATION

Review of the ACHEX results and the measurement needs for the present regulations in the State of California, as well as recommended changes, indicated that a three staged program for aerosols would be most useful. The three parts are classed as: (1) a routine long term monitoring program, (2) a short term, intermittent surveillance program, and (3) a continuing research and standards program.

1. MONITORING PROGRAM

The present State and Federal regulatory structure requires that long term monitoring be done at the State and local level to determine progress

towards achieving the air quality standards. The objective of this program then would be aerosol monitoring on a long term basis to determine compliance with standards.

The present program routinely uses only gravimetric high volume filters with intermittent chemical analysis. However, this effort should be improved to provide a better basis for evaluating trends in air quality.

There is presently such a long history of high volume filter data, using glass fiber substrates, that, as a practical matter, it does not appear feasible to make a major change in direction for the monitoring effort. On that basis, we recommend that the high volume filter continue to be used with acid washed glass fiber substrates for 24-hour averaged total mass concentration and analysis for total carbon. The total carbon is a useful measure of non-carbonate carbon in urban areas because the carbonate concentration is small relative to organic and elemental carbon. Most of the organic and elemental carbon is in the submicron fraction in urban air so that no size fractionation is required. The glass fiber substrate is less susceptible to gravimetric weighing error than other substrates, particularly with variations in humidity.

The first hi-volume unit should be supplemented by a second unit employing an impactor plate designed to have a 90% cut point at 3.5 μm diameter to prevent penetration of the larger particles. Again, 24-hour samples should be taken using a Whatman 41 paper substrate. Analysis should be made for mass concentration (nominally < 3.5 μm diameter), total sulfur and lead by x-ray fluorescence, and nitrate by wet chemistry.

To complete the monitoring station array, it is recommended that the integrating nephelometer be added to provide a continuous measure of the light scattering coefficient, which in turn is a useful practical measure of the particle volume < 1 μm diameter. This instrument has been found to yield a somewhat different relationship between b_{scat} and mass concentration at different locations (e.g. Samuels et al.[105]). However with filter data, the instrument has proved to be very useful in ACHEX as a "rational" continuous monitor for visibility reducing aerosol volume. Thus, the nephelometer is recommended as continuous aerosol monitor to replace the older soil index devices.

A series of approximately thirty aerosol monitoring stations should be employed in the State. Site selection should be made on the basis of enhancing the capability of the present ARB monitoring network, with additional sites located in local district stations in particularly sensitive areas.

2. SURVEILLANCE STATIONS

The second level of aerosol measurement would have the objective of short term or intermittent characterization of aerosols in specific locations chosen for extreme conditions as source dominated or receptor sites.

Because of the complexity of the urban aerosol behavior, some studies of areas that have heavy exposure to haze will be required with a measurement sophistication greater than available or practical for the monitoring stations. The surveillance stations should contain the instrumentation specified for the monitoring station, but should include the following additions:

1) Three stage rotating drum impactor using paraffinated mylar substrates and an after filter using Whatman 41 paper. The impactor to be selected could be the design currently employed by Dr. Cahill (U. C. Davis). The impactor should be operated to obtain two hour samples, which should be analyzed by α x-ray fluorescence analysis for elements heavier than Mg. A sequential after filter unit should be employed to provide samples for the submicron range, assuming a designed impactor cut at 1 μm diameter. The after filters should be analyzed by α x-ray fluorescence analysis for elements heavier than Mg and by wet chemistry for $SO_4^=$ and NO_3^-.
2) A condensation nuclei counter such as the Environment-1 Counter should be added to measure continuously nuclei populations, for correlation with sources and with b_{scat} measurements. (See also Appendix C).
3) As an optional item, an optical counter having size discrimination over the range between 0.3 and 3 μm could be added to provide a data base in sensitive areas for changes in the size distribution of a large fraction of the submicron size range. By measurement

of such changes, the potential shifts in source contributions and secondary aerosol production processes could be kept under surveillance over long enough periods to make judgments about the significance of control factors. Addition of this instrument will require significant extra processing and data handling capability for individual stations. This should be kept in mind in the choice of priorities for instrumentation.

Based on practical considerations of cost for equipment, calibration, and data analysis, approximately ten surveillance stations should be ample for use in the State. These systems could be used effectively if they were added to existing ARB mobile laboratory units. Certain key monitoring stations also could be upgraded to include the surveillance instrumentation.

3. AEROSOL RESEARCH LABORATORY

A third level of sophistication in aerosol measurement capability undoubtedly will have a continuing usefulness. At this level the program objective would be the conduct of short term, advanced studies of special ambient aerosol problems and the evaluation of new instrumentation and analytical methods for air quality measurement.

The present ARB/ACHEX mobile laboratory has proved to be well suited for this final objective. It is recommended that the mobile laboratory be maintained in operational condition and used for new aerosol research in areas of California, as required. At the present time, there does not appear to be a need for additional units of this kind.

C. SUMMARY

The results of the ACHEX show the need for a long term, continued monitoring surveillance and research programs for aerosols, which would involve high volume filter collection with analysis for sulfate, nitrate, and organics. At the very least, such continued effort is necessary to confirm the trends expected for reductions in these secondary products as smog levels are reduced, and NO_x and hydrocarbon emissions are decreased. Although x-ray fluroescence analysis shows promise for measuring sulfate as sulfur, the

traditional wet chemical methods remain most suitable for determination of $SO_4^=$, and NO_3^-. Non-carbonate carbon can be determined usefully by a simple total carbon procedure.

A moderate program to monitor changes in aerosol behavior by continuous measurement is needed. The use in the ACHEX of the β-attenuation instrument for continuous monitoring of aerosol mass concentration showed promise, but further development of this method is required before it can be adopted. The integrating nephelometer offers a useful operational instrument to replace the soil index as a continuous measure of the aerosol volume concentration in the 0.1 μm to 1.0 μm diameter range. This device gives added information about aerosol light scattering that can be interpreted semi-quantitatively in terms of visibility degradation.

Size fractionation to establish trends in the submicron fraction is an important requirement. At the same time, the State of California has requirements for intermittent surveillance of certain classes of sources or unusual problems such as that which exist in the eastern part of the South Coast Basin. There is also a continuing need for more sophisticated aerosol research such as that requiring the capabilities of the ACHEX mobile laboratory.

On the basis of this study, we recommend that a three level aerosol program be established by the Air Resources Board that would use the instrument packages listed in Table 10-2. Such a program would provide the State with the needed range of capabilities to maintain a continuing surveillance of aerosol behavior and visibility change.

TABLE 10-2

RECOMMENDED INSTRUMENT HIERARCHY FOR MEASURING ATMOSPHERIC AEROSOLS

A. Monitoring Program (approximately 30 stations)

Objective: Aerosol monitoring on a long term basis to determine compliance with Federal and State standards.

	Instrumentation	Analysis
1.	High Volume Sampler Glass fiber filter	24 hr. Total Mass, Total Carbon
2.	High Volume Sampler for respirable fraction (< 3.5 μm) Whatmann 41 filter	24 hr. Sample, Total Mass, Total Sulfur, Pb and NO_3^-
3.	Integrating Nephelometer	Light Scattering Coefficient

B. Surveillance Stations (approximately 10)

Objective: Short term or intermittent characterization of aerosols in specific locations sited for extreme conditions as source dominated or receptor sites.

	Instrumentation	Analysis
1.	High Volume Sampler Glass fiber filter	24 hr. Total Mass, Total Carbon
2.	High Volume Sampler (< 3.5 μm) Whatmann 41 filter	24 hr. Total Mass, Total Sulfur, NO_3^-, and Pb
3.	Integrating Nephelometer	Light Scattering Coefficient
4.	Three Stage Impactor paraffinated mylar substrate Whatmann 41 after filter	2 hr. samples; α-XRFA for elements heavier than Mg on two hour sections, and on the after filter
5.	Condensation Nuclei Counter	CNC vs. b_{scat} Correlations
*6.	Optical Particle Counter	Changes in submicron-micron particle site distributions

C. Mobile Research Laboratory (1 unit)

Objective: Short term, advanced studies of special ambient aerosol problems and evaluation of new instrumentation and analytical methods for air quality measurement.

	Equipment
1.	ARB/ACHEX Laboratory

*Optional

XI. ACKNOWLEDGEMENTS

We are grateful to the Air Resources Board for sponsoring this ambitious undertaking. The wholehearted, continuing support of Messrs. Dale Hutchinson, A. Bockian, Harris Samuels, and Jack Suder has provided a firm basis for the development of the program as scheduled, despite a number of difficulties, not the least of which was the weather.

Much of the success of this program can be attributed to the careful administration of the program by the initial program manager, Dr. T. L. Loucks. His influence on the experiment and the organizations participating were crucial to the timely, well-organized operations that took place.

This project could not have achieved its effective completion without the efforts of many people who contributed their energies tirelessly to the program. These were:

Rockwell Science Center

Technical

C. A. Battle
C. S. Burton
R. S. Carpenter
J. H. Davis
D. Dockweiler
P. Friedman
J. R. Gardner
R. M. Govan
D. H. Hern
J. R. Hribar
K. Kubler
C. Landon
R. A. Meyer
R. L. Myers
E. P. Parry
H. H. Wang

Administrative

K. Bader
J. L. Balderston
C. Coffindaffer
J. F. Davis
W. Dinkin
N. R. Johnson
A. J. Lewin
M. E. Lyon
M. McGuire
R. A. Mekaelian
K. L. Nolte
P. K. Ocorr
D. E. Palermo
R. L. Seale
H. Shannon
D. B. Stephens
B. B. White

Air and Industrial Hygiene Laboratory

A. E. Alcocer
Dr. T. Belsky
C. Bunce
P. Bussard
Dr. T. Cahill (UC, Davis)
M. Fracchia
M. Hoffer
S. Hope
M. Imada
E. Jeung

AIHL (Continued)

F. Jung
R. Kaifer (Lawrence Livermore Lab)
S. Kerns
D. Levaggi (BAAPCD)
J. Medaxian
H. Moore
D. Mosley
Dr. K. Noll (U. of Tennessee)
C. Ong (BAAPCD)
L. Parton
L. Pierce
Dr. A. Ragaini (Lawrence Livermore Lab)
A. del Rosario
W. Siu (BAAPCD)
K. Smith
R. Stanley
J. Tang
S. Twiss
S. Wall
B. Wright
F. Yoon

California Institute of Technology

P. Andriola
C. Davidson
G. Gartrell
D. Grosjean
S. L. Heisler
R. Lamb
D. Landis
P. McMurry
P. Roberts
J. Seinfeld
W. H. White

Meteorology Research, Inc.

D. L. Blumenthal
D. Brown
J. Brunton
C. Chien
J. Cooper
W. Davis
R. Day
R. W. Green
T. Howland
S. Kosewski
R. Lawrence
C. Ludd
S. Marsh
P. McMurray
V. Mirabello
D. Moellenberndt
J. Moellenberndt
S. Muller
J. Munger
A. Ollivares
A. Ostrye
C. Phyakul
W. Rider
R. Sherrard
R. Sicherman
T. Sperling
J. R. Stinson
H. Wilkinson
J. Whitney
L. York

University of California, Riverside

T. Cree
G. Kats
L. M. Kienitz
M. Price
R. Tenorio
C. R. Thompson

Lawrence Berkeley Laboratory

R. Garrett
L. Goda

University of Minnesota

B. Y. H. Liu
V. A. Marple
D. Y. H. Pui
G. M. Sverdrup
G. Sem (Thermo-Systems, Inc.)
K. Willeke

University of Washington

N. Ahlquist
D. Covert
D. Cronn
P. Solem
A. Vanderpol
A. Waggoner

This project required the commitment of resources far beyond those that could be covered by the reserves of the Air Resources Board Contract. We are indebted to each of the institutions involved in this study and for their enthusiastic support and commitment of extra personnel, equipment, and facilities.

Particular thanks go to Dr. W. Wilson and to Dr. P. Hanst of the Division of Chemistry and Physics of the Environmental Protection Agency (EPA) for contributing several instruments to the study which significantly enhanced the observational capabilities. EPA also complemented the ARB program by adding several experiments, of mutual interest at the Pasadena site, under the direction of Dr. Wilson.

We appreciate the enthusiastic cooperation of the local and state Air Pollution Control Districts, especially in the early stages of the program. We are particularly grateful to the Bay Area APCD for their generous help in allowing us to use their San Jose station for our study. Dr. Milton Feldstein and his staff gave the utmost attention to this experiment, far beyond the support expected. Staff at the Fresno County APCD and the Kern County APCD aided the program extensively in suggesting useful sampling sites and providing background data for their areas.

Special thanks go to the Air Resources Board through John Kinosian for permitting us to use the Riverside monitoring station during the 1973 program. We appreciate the strong cooperation of the Los Angeles Air Pollution Control District and the Orange County Air Pollution Control District respectively for making space available at the Downtown Los Angeles and the Pomona monitoring stations, and the Anaheim Station.

We are indebted to Mr. F. Bonamassa and Dr. A. Bockian for making it possible to coordinate out 1973 field program with studies with the ARB/El Monte Laboratory summer program. Special thanks go to Dr. John Holmes for his efforts in aiding out satellite program and to Ms. Mary Hostak who participated in the 1973 mobile laboratory operations as a key member of the crew.

The timely and efficient establishment of the sites for the mobile laboratory would not have been possible, but for the close cooperation of the following:

San Pablo Water Treatment Plant

David Sullivan, Plant Superintendent
Paul Soltow, Engineer, Manager

San Francisco Airport

Emmet Smith, Assistant Deputy Director of Administration
James Carr, Director of Airports

Fresno County Fairgrounds

Ralph Hinds, Assistant Manager

Hunter-Liggett Military Reservation*

Robert Vasquez, Director of Facilities & Engineering
Leonard Morley, Colonel, Deputy Post Commander

Harbor Freeway - May Company

Richard Green, Real Estate Administrator
Andrew Briggs, General Manager

Los Angeles County Fairgrounds (Pomona)

Lyle Mills, Leasing Officer
William Shepard, Manager

* We are particularly grateful to Colonel Richard C. Chabot, Signal Corps Commanding Officer and Director, for supplying us with extensive meterological data from the Hunter-Liggett site.

Goldstone Tracking Station - JPL

Howard Olsen, Station Manager
William Bayley, Assistant Laboratory Director

U.S. Coast Guard - Point Arguello

Lt. R. E. Buzhart, Group Commander
Lt. Commander Lovern, Commander Aids to Navigation Branch
Chief Dibble, Commander Pt. Arguello

North American Rockwell Site - Bakersfield+

Hank Miller, Contr. Coordinator
John McGann, Project Engineer
Carl Kiefer, Director of Facilities and Industrial Engineering

University of California Marine Biology Lab - Bodega Bay+

Dr. Jere Lipps, Acting Director
Jerry Tinkess, Business Manager
Dr. C. Hand, Director

Del Monte Plant - San Leandro+

Dr. C. E. Geise, Director of Agricultural Research
R. S. Bowen, Superintendent
Bert Davis, Assistant Plant Superintendent

North American Rockwell Site - El Segundo+

Carl Kiefer - Director of Facilities and Industrial Engineering
Ed Fleishman, Facilities Design

A number of experimenters chose to extend the ARB experiment by undertaking complementary programs, parallel to the ARB work. Aside from other ARB project, such as the three-dimensional gradient study and the tracer study, and the EPA program, the following experiments were conducted:

1) NASA Lidar Study - Dr. M. P. McCormick, PI (NASA/Langley)
2) EPA Lidar Survey - Dr. Warren Johnson, PI, (EPA, Research Triangle Park)
3) GM Observational Program - Dr. P. Groblicki, PI (General Motors Research Labs)
4) EPA-LBL-Ford X-ray Fluorescence Experiment - Dr. F. Goulding, PI (Lawrence Berkeley Laboratory), William Pierson and R. Hammerle (Ford Research Labs, Detroit).

+Not used in 1972

XII. REFERENCES

1. P. Leighton, Photochemistry of Air Pollution, Academic Press, New York (1961).

2. K. T. Whitby (ed.), "Aerosol Measurements in Los Angeles Smog." Air Pollution Contr. Office Publ. No. APTD-0630, U.S. Environ. Protection Agency, Research Triangle Park, North Carolina.

3. G. M. Hidy (ed.), Aerosols and Atmospheric Chemistry, Academic Press, New York (1972).

4. K. T. Whitby, W. E. Clark, V. A. Marple, G. M. Sverdrup, K. Willeke, B. Y. H. Liu, and D. Y. H. Pui, "Evolution of the Freeway Aerosol," presented at the Symposium on Surface and Colloid Chemistry in Air Pollution Control, ACS National Meeting, Chicago, Ill., Aug. 26-31, 1973.

5. K. T. Whitby, R. B. Husar, and B. Y. H. Liu, "The Aerosol Size Distribution of Los Angeles Smog," J. Colloid & Interface Sci. 39, 177-204 (1972).

6. G. M. Hidy, "Removal Process of Gaseous and Particulate Pollutants," Chemistry of the Lower Atmosphere, S. I. Rasool (ed.), Plenum Press, New York, in press.

7. S. K. Friedlander, "Similarity Considerations for the Particle-Size Spectrum of a Coagulating Sedimenting Aerosol," J. Meteorol. 17, 479-483 (1960).

8. G. M. Hidy, "The Dynamics of Aerosols in the Lower Troposphere," Assessment of Airborne Particles, T. T. Mercer, P. E. Morrow, and W. Stober, Ed. (C. C. Tomas Publ., Springfield, Ill.), 81-115 (1972).

9. H. C. van de Hulst, Light Scattering by Small Particles, Wiley, New York (1957).

10. R. J. Charlson, N. C. Ahlquist, H. Selvidge, and P. B. Mac Cready, Jr., "Monitoring of atmospheric aerosol parameters with the integrating nephelometer," J. Air Pollution Contr. Assoc. 19, 937-942 (1969).

11. E. S. Greacen, G. M. Sverdrup, and K. T. Whitby, A preliminary report on correlation of b_{scat} vs. submicron volume" (June 1974).

12. D. S. Covert, "A Study of the Relationship of Chemical Composition and Humidity to Light Scattering by Aerosols," Thesis, University of Washington (January 1974).

13. G. M. Hidy, P. K. Mueller, H. H. Wang, J. Karney, S. Twiss, M. Imada, and A. Alcocer, "Observations of Aerosols over Southern California Coastal Waters," J. Appl. Meteor. 13, 96 (1974).

14. U.S. Environmental Protection Agency, "Air Quality Data from the National Air Surveillance Network, 1968," APTD (1970).

15. P. K. Mueller, R. W. Mosley, and L. B. Pierce, "Chemical Composition of Pasadena Aerosol by Particle Size and Time of Day IV. Carbonate and Noncarbonate Carbon Content," Aerosols and Atmospheric Chemistry, G. M. Hidy (ed.), Academic Press, New York, 295-299 (1972).

16. M. S. Miller, S. K. Friedlander, and G. M. Hidy, "A Chemical Element Balance for the Pasadena Aerosol," J. Colloid Interface Sci. 39, 165-176 (1972).

17. TRW, Inc., "The Development of a Particulate Implementation Plan for the Los Angeles Region," Report #3 Air Quality-Emission Level Relationship. TRW, Inc., El Segundo, CA (1974).

18. C. S. Burton, "Investigation of Gas-Aerosol Properties in California Smog," Interim Report on Contract EPA 68-02-0583, Rockwell International Science Center, Thousand Oaks, Calif. (1973).

19. F. L. Ludwig, D. M. Coulson, E. Robinson, L. A. Cavanagh, Interim SRI Report for Contract PH 86-64-54 (December 1964).

20. D. A. Lundgren, Paper 69-168 APCA Meeting, New York City (June 22-26, 1969).

21. J. F. Roesler, H. J. R. Stevenson, and J. S. Nader, J. Air Poll. Cont. Assoc. 15, 576 (1965).

22. N. L. Craig, A. B. Harker, and T. Novakov, Atmos. Env. 8, 15-21 (1964).

23. H. W. Georgii, "Contribution to the Atmospheric Sulfur Budget," J. Geophys. Res. 75, 2365-2372 (1970).

24. Los Angeles Air Pollution Control District, "Profile of Air Pollution Control," County of Los Angeles, Los Angeles, California, 84 pp.

25. W. D. Scott and P. V. Hobbs, "The Formation of Sulfate in Water Droplets," J. Atmos. Sci. 24, 54 (1967).

26. T. A. Cahill and P. J. Feeney, "Contribution of freeway traffic to airborne particulate matter," Crocker Nuclear Laboratory, University of California, Davis, California (June 15, 1973).

27. J. G. Calvert, "Modes of Formation of the Salts of Sulfur and Nitrogen in an NO_x-SO_2-Hydrocarbon-Polluted Atmosphere," presented at Conf. on Atmos. Salts & Gases of Sulfur & Nitrogen in Assoc. with Photochem. Oxidant, Univ. of California, Irvine (Jan. 7-9, 1974); see also Proc. of Conf. on Health Effects of Pollutants, Assembly of Life Sci., National Acad. Sci., U.S. Govt. Printing Office No. 93-15, 19 (1973).

28. R. B. Husar, and D. Blumenthal, unpublished report (1974).

29. P. Roberts and S. K. Friedlander, "Conversion of SO_2 to Particulate Sulfates in the Los Angeles Atmosphere," presented at Conf. Health Consequences of Environ. Controls: Impact of Mobile Emission Controls. U.S. Environ. Protection Agency, Durham, N.C. (April 17-19, 1974).

30. R. O'Brien et al., "Organic Photochemical Aerosols. II: Atmospheric Analysis," submitted to Environ. Sci. & Technol.

31. O. B. Toon, and J. B. Pollack, J. Geophys. Res. 78, 7051 (1973).

32. M. J. Bufalini, Environ. Sci. & Technol. 5, 685 (1971).

33. R. A. Cox and S. A. Penkett, J. Chem. Soc., Faraday Soc. 68, 1735 (1972).

34. D. D. Davis, W. A. Payne, and L. J. Stief, Science 179, 280 (1973).

35. H. Harrison and T. Larson, J. Geophys. Res. 79, 3095 (1974).

36. A. Harker, "The Formation of Sulfate in the Stratosphere through the Gas Phase Oxidation of Sulfur Dioxide," submitted to J. Geophys. Res.

37. E. J. Hamilton, Jr., private communication.

38. W. A. Payne, L. J. Stief, and D. D. Davis, J. Amer. Chem. Soc. 95, 7614 (1973).

39. H. F. Johnstone and D. R. Coughanowr, Ind. Eng. Chem. 50, 1169 (1968).

40. M. Matteson, S. Stober, and H. Luther, Ind. Eng. Chem. Fundamentals 8, 677 (1969).

41. J. M. Miller and R. G. dePena, Proc. 2nd IUAPPA Congr., Academic Press, New York, 375 (1971).

42. M. Corn and R. T. Cheng, J. Air Poll. Contr. Assoc. 22, 871 (1972).

43. S. A. Penkett, Nature, Phys. Sci. 240, 105 (1972).

44. E. C. Fuller and R. H. Christ, J. Amer. Chem. Soc. 63, 1644 (1941).

45. L. C. Schroeter, J. Pharm. Sci. 52, 559 (1963).

46. T. Novakov, S. G. Chang, and A. B. Harker, "Sulfates in Pollution Particulates: Catalytic Formation on Carbon (Soot) Particles," unpublished manuscript, Lawrence Berkeley Laboratory.

47. K. Yamamoto, S. Michiham, and K. Kunitaro, Nippon Kaguku Kaiski 7, 1268 (1973).

48. R. O'Brien et al., "Organic Photochemical Aerosol I: Environmental Chamber Experiments," submitted to Environ. Sci. & Technol.

49. T. Nash, J. Chem. Soc. (A) 18, 3023 (1970).

50. M. T. Borok, Zhurn. Prikladnoi Khimii 33, 1761 (1960).

51. A. V. Baranov, E. A. Liberzu, and T. I. Popova, Trudy Sibiskogo Techologicheskogo Instituta 38, 77 (1966).

52. P. C. Colodny and B. R. Appel, "Thermal Analysis of Carbonaceous Atmospheric Particulate Matter Preliminary Findings and Evaluation of the DuPont 916 Analyzer," AIHL Report No. 159 (December 1973).

53. D. Grosjean and S. K. Friedlander, "Gas-Particle Distribution Factors for Organic Pollutants in the Los Angeles Atmosphere," submitted to J. Air Poll. Contr. Assoc.

54. E. R. Stephens, E. F. Darley, and F. R. Burleson, "Sources and Reactivity of Light Hydrocarbons in Ambient Air," Proc. API Div. of Refining 47, 466 (1967).

55. D. Schuetzle, "Computer Controlled High Resolution Mass Spectrometric Analysis of Air Pollutants," Ph.D. Thesis, University of Washington (1972).

56. C. S. Burton, G. M. Hidy, and E. Franzblau, "Aerosol Formation from Ozone-Olefin Reactions," in preparation.

57. W.E.K. Middleton, Vision through the Atmosphere, University of Toronto Press, Toronto, Canada (1952).

58. F. Kasten, "The Influence of the Aerosol Size Distribution and its Change with Relative Humidity on Visibility," Contributions to Atmos. Physics 41, 33-51 (1967).

59. K. E. Noll, P. K. Mueller, M. Imada, "Visibility and Aerosol Concentration in Urban Air," Atmos. Envir. 2, 465 (1968).

60. G. Hanel, "New Results Concerning the Dependence...of Visibility on Relative Humidity and Their Significance in a Model for Visibility Forecast," Beitr. Physik der Atmos. 44, 137-167 (1971).

61. D. S. Covert, R. J. Charlson, N. C. Ahlquist, "A Study of the Relationship of Chemical Composition and Humidity to Light Scattering by Aerosols," J. Appl. Met. 11, 968-976 (1972).

62. D. S. Ensor, W. M. Porch, M. J. Pilat, R. J. Charlson, "Influence of Atmospheric Aerosol on Albedo," J. Appl. Met. 10, 1303-1306 (1971).

63. A. Goetz and R. Pueschel, "Basic Mechanisms of Photochemical Aerosol Formation," Atmos. Environ. 1, 287-306 (1967).

64. R. A. Meyer, G. M. Hidy, and J. H. Davis, "Determination of Water and Volatile Organics in Filter Collected Aerosols," Environmental Letters 4, 9-20 (1973).

65. K. B. Husar, K. T. Whitby, and B. Y. H. Liu, "Physical Mechanisms Governing Dynamics of Los Angeles Smog Aerosol," J. Colloid and Interface Sci. 39, 211 (1972).

66. Clyde Orr, Jr., F. K. Hurd, and W. J. Corbett, "Aerosol Size and Relative Humidity," J. Colloid and Interface Sci. 13, 472-482 (1958).

67. Peter Winkler, "Untersuchung über das GrößBenwachstum natürlicher Aerosolterlchen mit der relativen Feuchte nach einer Wägemethode," Annalen der Meteorologie 4, 134-137 (1969).

68. C. E. Junge, Air Chemistry and Radioactivity, Academic Press, New York (1963).

69. C. H. Keith and A. B. Arons, "The Growth of Sea-Salt Particles by Condensation of Atmospheric Water Vapor," Journal of Meteorology 11, 173 (1954).

70. B. J. Mason, The Physics of Clouds, Oxford Press, London, 1-83 (1957).

71. N. H. Fletcher, The Physics of Rainclouds, Cambridge University Press, London (1966).

72. W. H. White, R. B. Husar, D. L. Blumenthal, and D. S. Ensor, Los Angeles Smog Aerosol Dynamics Derived from Spatio-Temporal Distribution Data, Private Communication.

73. R. J. Charlson, A. H. VanderPol, D. S. Covert, A. P. Waggoner, N. C. Ahlquist, "Sulfuric Acid - Ammonium Sulfate Aerosol: Optical Detection in St. Louis Region," Science 184 156-158 (1974).

74. Samuel S. Butcher and Robert J. Charlson, An Introduction to Air Chemistry Academic Press, New York (1972).

75. Peter Winkler and C. E. Junge, "Comments on 'Anomalous Deliquescence of Sea Spray Aerosols,'" J. Appl. Meteor. 10, 159-163.

76. R. J. Charlson, "Multiwavelength Nephelometer Measurements in Los Angeles Smog Aerosol," J. Colloid and Interface Sci. 39, 240 (1972).

77. R. J. Charlson, "Atmospheric Visibility Related to Aerosol Mass Concentration: A Review," Environmental Science and Technology 3, 913 (1969).

78. D. A. Landis, "Calibration of a FH62A Dust Monitor Using Glass Fiber Filters," Science Center Technical Report No. 73-10 Rockwell International Science Center, Thousand Oaks, CA (1973).

79. P. Winkler and C. E. Junge, "The Growth of Atmospheric Aerosol Particles as a Function of Relative Humidity I," 1973 Jour. of Recherches Atmospheriques, 613 (1973).

80. G. Hänel, "Computation of the Extinction of Visible Radiation by Atmospheric Aerosol Particles as a Function of Relative Humidity," Aerosol Sci. 3, 377 (1972).

81. K. T. Whity, W. E. Clark, V. A. Marple, G. M. Sverdrup, G. J. Sem, K. Willeke, B. Y. H. Liu, and D. Y. H. Pui, "Size Distribution of Freeway Aerosol," submitted to Atmos. Environ.

82. B. Y. H. Liu, "A Portable Electrical Aerosol Analyzer for Size Distribution Measurement of Submicron Aerosols," presented at the 66th Annual Meeting of the Air Pollution Control Association, Chicago, Ill., June 24-28, 1973 (COO-1248-37).

83. S. K. Friedlander, "Chemical Element Balances and Identification of Air Pollution Sources," Environ. Sci. and Technol. 7, 235-240 (1973).

84. S. L. Heisler, S. K. Friedlander, and R. B. Husar, "The Relationship of Smog Aerosol Size and Chemical Element Distributions to Source Characteristics," Atmospheric Environment 7, 633-649 (1973).

85. G. Gartrell, Jr. and S. K. Friedlander, "Relating particulate pollution to sources: the 1972 California Aerosol Characterization Study," to appear in Atmospheric Environment.

86. Hirschler et al., Ind. Eng. Chem. 49, 1131 (1957).

87. C. D. Hodgman (ed.), Handbook of Chemistry and Physics, The Chemical Rubber Publishing Co., Cleveland, 661-1701 (1961).

88. Air Resources Board, "The State of California Implementation Plan for Achieving and Maintaining the National Ambient Air Quality Standards," (January 30, 1972).

89. J. W. Frey and M. Corn, "Physical and Chemical Characteristics of Particulates in a Diesel Exhaust," American Indust. Hygiene Assoc. Jour. 28, 468-478 (1967).

90. D. Grosjean, Private Communication (1973).

91. P. P. Mader, R. D. MacPhee, R. T. Lofberg, and C. P. Larson, "Composition of Organic Portion of Atmospheric Aerosols in the Los Angeles Area," Ind. Eng. Chem. 44, 1352-1355 (1952).

92. K. T. Whitby, R. B. Husar, A. R. McFarland, and M. Tomaides, "Generation and Decay of Small Ions," Particle Laboratory Publication #137, Department of Mechanical Engineering, University of Minnesota (1969).

93. A. H. Woodcock, "Salt Nuclei in Marine Air as a Function of Altitude and Wind Force," J. Meteor. 10, 362-371 (1953).

94. I. H. Blifford, Jr., "Tropospheric Aerosols," J. Geophys. Res. 75, 3099-3101 (1970).

95. C. E. Junge, "Our Knowledge of the Physico-Chemistry of Aerosols in the Undisturbed Marine Environment," J. Geophys. Res. 77, 5183-5200 (1972).

96. J. J. Huntzicker and S. K. Friedlander, "The Flow of Automobile Emitted Lead through the Los Angeles Basin," presented at the 166th National ACS Meeting (August 1973).

97. R. B. Husar, Coagulation of Knudsen Aerosols, Ph.D. Thesis, The University of Minnesota, Minneapolis, Minnesota (1971).

98. N. A. Fuchs, The Mechanics of Aerosols, The MacMillan Col, New York, 294 (1964).

99. Environmental Protection Agency, "Air Quality Data for 1968" APTD-0978, Research Triangle Park, North Carolina (1972).

100. W. H. White, R. B. Husar, and S. K. Friedlander, "A Study of Los Angeles Smog Aerosol Dynamics by Air Trajectory Analyses," presented at the June, 1973 Annual Meeting, APCA, Chicago, Illinois (1973).

101. W. H. White, S. K. Friedlander, and P. T. Roberts, "On the Nature and Origins of Visibility-Reducing Aerosols in the Los Angeles Basin," manuscript dated August, 1974, revised 1975.

102. J. J. Huntzicker, S. K. Friedlander, and C. I. Davidson, "A material balance for automobile emitted lead in the Los Angeles basin," submitted to Environmental Science and Technology.

103. R. P. Fischer, "Can American oil refineries yield vanadium?" presented before the Division of Petroleum Chemistry of the American Chemical Society, Chicago, Illinois (August 26-31, 1973).

104. Human Studies Laboratory, EPA, "Health Consequences of Sulfur Oxides: A Report from CHESS, 1970-1971" EPA-650/1-74-004, U.S. Environmental Protection Agency, Research Triangle Park, N.C. (May, 1974).

105. California Air Resources Board, "Visibility, Light Scattering and Mass Concentration of Particulate Matter." Report of the California Tri-City Aerosol Sampling Project, July, 1973, 28p.

106. Gillette, D. A., and Blifford, I. H., "Composition of Tropospheric Aerosols as a Function of Altitude," J. of the Atmospheric Sciences, 28:1199-1210 (1971).

107. Hoffman, G. L., and Duce, R. A., "Consideration of the Chemical Fractionation of Alkali and Alkaline Earth Metals in the Hawaiian Marine Atmosphere," J. of Geophysical Research, 77:5161-5169 (1972).

108. Abundance of Chemical Elements, Cherdyntsev, V.V., Trans. by W. Nichiporuk, University of Chicago Press, (1961).

APPENDIX A

A PRELIMINARY REPORT ON THE MISMATCH OF THE AEROSOL SIZE DISTRIBUTIONS OBTAINED DURING THE ACHEX*

INTRODUCTION

A number of investigators have noted the importance of an aerosol's liquid water content. Recent work has suggested that liquid water content has a direct influence on visibility reduction.[1] The results of the Rockwell waterometer from ACHEX I indicate that a significant fraction of the marine and urban aerosol observed is free water in the relative humidity range between 40% and 75%.[2]

Based on the aerosol size distributions measured with the continuous aerosol instrumentation during the ACHEX, it is believed that when the outside temperature (TO) was less than the temperature inside the mobile lab (TIN), and when the relative humidity (RH) was greater than about 50%, water was evaporated from the aerosol before the aerosol reached the aerosol sensors inside the mobile lab. Figure A-1 shows three volume distributions from the Harbor Freeway. The distributions have been divided into three segments corresponding to data taken with the Whitby Aerosol Analyzer (WAA), .01 μm to 0.422 μm, the Royco Model 220 Optical Particle Counter (OPC), .422 μm to 5.62 μm, and the Royco Model 245 OPC, 5.62 μm to 38 μm. For Run 56 in which TO > TIN and RH was low, the distributions obtained with the three instruments match very well. However, for Run 54 when TO < TIN and RH = 77.8%, there is a mismatch between the Royco 220 and Royco 245 data. At a higher RH (Run 52) the mismatch is greater.

The purpose of this paper is to report the preliminary work which has been done to characterize the mismatch problem.

---

*From a report by George M. Sverdrup and Kenneth T. Whitby, Particle Technology Laboratory, Mechanical Engineering Department, University of Minnesota, July 1974.

INSTRUMENTATION

Figure A-2 shows a schematic of the instrumentation in the mobile lab. The Royco 245 sensor was mounted on a stand 1.1 meters above the roof of the trailer. The outside temperature sensor was located just below the Royco 245 sensor. The Royco 245 data were unaffected by a difference between TO and TIN.

The Royco 220 sensor was located inside the mobile lab. The sample stream passed through a 0.25 in. diameter by 50 in. long aluminum tube from the aerosol manifold to the Royco 220 sensor, and at most locations through a diluter.

The effect of the diluter on the Royco 220 performance was investigated at Point Arguello. From Figure 3, it can be seen that the mismatch was not due to the presence of the diluter.

For a flow rate of 0.1 cfm, the Reynolds number based on tube diameter was 122 and the transit time was 4.3 seconds. For these conditions it is estimated that the bulk temperature of the sample stream increased from its value of TO to within about a degree of TIN by the time the air parcel reached the Royco 220 sensor.

The Royco 220 was modified with a sheath air inlet (see Figure A-4). This inlet removes about 85% of the total flow, filters this air and returns it as a clean air sheath around the sample stream. Since the temperature inside the Royco 220 box was higher than TIN and since the sheath air line passed close to the Royco 220 light bulb, the sheath air was at a higher temperature when it returned to the sample inlet than when it first entered the inlet. In order to investigate this effect, a Royco 220 OPC similar to the one used in the ACHEX was operated with a thermocouple placed in the sheath air line just before the sheath air returned to the inlet and with a thermocouple placed in the Royco 220 box near the inlet.

Table A-I shows the results of the experiment. The sheath air temperature was about 1.5 to 2°C higher than room temperature. Since the sheath air flow rate was .0873 cfm, and the sample flow rate was .0127 cfm, some heat was transferred from the sheath air stream to the sample air stream.

Based on the above considerations, it is reasonable to assume that the aerosol stream was at the temperature TIN when it passed through the viewing volume of the Royco 220 OPC.

The OPC's were calibrated with a non-volatile oil having a refractive index of 1.49. The mismatch between the Royco 220 data is complicated by the fact that the refractive index of the particles changes as the amount of liquid water changes. Since the Royco 245 uses a forward light scattering system and the Royco 220 uses a 90° system, the response of the two instruments to changes in refractive index is quite different. In order to determine the magnitude of this effect, the results of Berglund's work were utilized. Figure A-5 shows the results of a change in refractive index for Run 49 at the Harbor Freeway. The data for m = 1.40 are based on Berglund's experimental work. The data for m = 1.33 are presented as a limiting case and were calculated from Berglund's thesis using Quenzel's theory.[5] The data show that a change in refractive index alone is not enough to account for the mismatch.

The WAA was also operated inside the mobile lab. The response of the WAA with respect to this problem is difficult to analyze. The aerosol traveled through a rubber hose between the aerosol manifold and the WAA. The aerosol charger is operated with dry compressed air. The flow rates were checked at Berkeley on September 26, 1972. The compressed air flow rate was 0.18 cfm and the charged aerosol flow rate was 0.32 cfm. Therefore, in the charger section of the WAA much of the liquid water in the aerosol was probably evaporated.

In the mobility tube the aerosol is introduced as a thin annular sheath surrounding a clean air flow with the collection rod serving as the inner wall for the inner annulus (clean air flow). The ratio of clean air to aerosol flows was 14:1. Figure A-6 shows a schematic of the inlet to the mobility tube. Any particles which are collected by the rod must pass through the clean air flow. The temperature of the mobility tube was monitored (TANL), and it was usually within one degree C. of (T:N). It is believed that the temperature of the aerosol stream was at TANL degrees C. when collected by the rod. The history of evaporation and recondensation of water on the aerosol while in the WAA is unknown; however, it is believed that the humidity at which the WAA measured the aerosol was probably close to the humidity inside the mobile lab.

Referring to Figure A-1, it is seen that if there was a mismatch between the WAA and the Royco 220, it is not apparent. Since the data at 0.365 μm are at the mode of the volume curve, it is difficult to determine if this point is

depressed. Figure A-7a shows a surface distribution from Pt. Arguello. This distribution shows a mismatch between the WAA and the Royco 220. Figure A-7b shows the corresponding volume distribution. The mismatch between the WAA and the Royco 220 based on surface distributions was much less than the mismatch between the two OPC's as expected.

ANALYSIS OF MISMATCH

The preliminary work reported here was conducted in order to determine which parameters the size distribution mismatch depended upon. No attempt was made to characterize the mismatch in such a way that the distributions could be corrected.

One method of analysis would be to examine the overlap region between the aerosol instruments. Such data were recorded; however, these data were not included in the subsequent data reduction. Such an analysis will be possible in the future when time permits.

No attempt was made to analyze the WAA data. Whereas the Royco 220 data at 4.21 μm can be compared to the Royco 245 at 7.5 μm, there is no standard with which to compare the WAA data. If an accurate estimate of the flux of water from the aerosol were made at about 4.2 μm, the flux at other sizes could be estimated using a theory which relates mass transfer with Knudsen number. However, since Lundgren impactor analyses have shown that the chemical composition is a function of particle size, the assumption that the evaporation is only a function of size may not be justified. Therefore, for the present work the WAA data were not analyzed.

The fact that the mismatch appeared to have a diurinal variation (Figures A-8 and A-9) suggested that a correlation be made between the mismatch and RH and ΔT (TIN - TO). In order to do this it was necessary to define the mismatch. The method for obtaining a mismatch parameter must not vary from run to run and must apply to as many runs as possible. The present method of determining a mismatch parameter uses the volume distributions. Figure A-10 shows a typical distribution in which there is a mismatch and the method for determining the mismatch parameter MM. Since a good distribution normally has a volume mode at 4.2 μm the Royco 245 data were used to determine the

value of $\Delta V/\Delta \log Dp$ at 4.2 μm. A line was drawn from 7.5 μm to 4.21 μm (point A) with the same slope as between 7.5 μm and 13.3 μm. The mismatch parameter was then determined from the following equation:

$$MM = \frac{(\Delta V/\Delta \log D_p)A - (\Delta V/\Delta \log D_p)B}{(\Delta V/\Delta \log D_p)A}$$

Thus, the value of the mismatch is between 0 and 1. It should be emphasized that this parameter is not intended to represent the amount of water evaporated, but is merely a parameter used to characterize the mismatch. The results are shown in Figures A-11 and A-12.

For the ACHEX I, the total number of runs with TO < TIN and RH > 50% is 46. The number of runs for which MM was calculated is 35. The number of runs that show a mismatch which this method of calculation cannot adequately handle is 6. The number of runs with TO < TIN and RH > 50% which apparently show no mismatch is 5 or 11% of the total. Two of these are Runs 44 and 45 at Goldstone where the waterometer[2] and water filters[4] showed no detectable liquid water in the aerosol.

The following table illustrates the results for Goldstone Runs 44 and 45, for which essentially no liquid water was in the aerosol:

GOLDSTONE

Run	TO	TIN	ΔT	RH	MM
44	6.4	21.4	15.0	66.0	-.437
45	5.5	26.3	20.8	92.8	-.398

For the ACHEX II, 42 runs have TO < TIN and RH > 50%. MM was calculated for 13 runs with 12 runs questionable. Seventeen or 42% showed no apparent mismatch.

The fact that MM was not obtained for all the runs with the appropriate conditions is probably due not only to a difference in liquid water content at different sites and in different air parcels, but also due to the method of calculation. However, there appears to be a difference between the ACHEX I and II size distributions.

A multiple linear correlation was run between MM and RH and ΔT. The following tables of correlation matricies were obtained.

1. ACHEX I, all sites

Using the data in Figures A-9 and A-10 from all ACHEX I sites, it can be seen that the correlation of MM vs. RH and MM vs. ΔT is about the same. The multiple correlation coefficient, R^2, was 0.719.

	RH	ΔT	MM
RH	1	.718	.741
ΔT		1	.819
MM			1

$R^2 = .719$

F Ratio = 44.8

$MM = -.0253 + 3.758 \times 10^{-3} RH + .0291\ (\Delta T)$

2. ACHEX I and II, all sites

For all sites from both ACHEX I and II the correlations between MM vs. RH and MM vs. ΔT were not as good as for the ACHEX I data alone. $R^2 = .558$.

	RH	ΔT	MM
RH	1	.648	.578
ΔT		1	.735
MM			1

$R^2 = .558$

3. ACHEX I, all sites, RH > 100%

Since the relative humidity was often calculated as being greater than 100%, a correlation was run using RH > 100% when indicated. The following matrix illustrates the results.

	RH	ΔT	MM
RH	1	.542	.637
ΔT		1	.819
MM			1

$R^2 = .723$

The correlation between MM and RH was worse than for case (1) (.637 compared to .741); however, R^2 was essentially the same (.723 for case (3) and .719 for case (1)). Therefore, for the remaining correlations relative humidities of over 100% were set to 100%.

4. ACHEX I, all sites except Pt. Arguello

Since the Pt. Arguello aerosol differed from urban aerosols in many respects, a correlation was run on all ACHEX I data except those taken at Pt. Arguello. The following correlation matrix shows the results.

	RH	ΔT	MM
RH	1	.737	.724
ΔT		1	.792
MM			1

$R^2 = .670$

5. Harbor Freeway, 9-20-72

These results for the Harbor Freeway on September 20, 1972, showed the highest degree of correlation, $R^2 = .899$. The size distributions are plotted in Figures A-6 and A-7.

	RH	ΔT	MM
RH	1	.871	.893
ΔT		1	.622
MM			1

$R^2 = .899$

6. Harbor Freeway, 9-27-72

These results for the Harbor Freeway on September 27, 1972 showed a much lower degree of correlation. For this study, the relative humidity was consistently calculated to be greater than 100%.

	RH	ΔT	MM
RH	1	.985	.536
ΔT		1	.617
MM			1

$R^2 = .561$

7. Harbor Freeway, 9-20-72 and 9-27-72

The combined results of the Harbor Freeway gave the following results:

	RH	ΔT	MM
RH	1	.458	.564
ΔT		1	.569
MM			1

$R^2 = .440$

8. Pomona ACHEX 1

These data showed a better correlation between MM and ΔT than between MM and RH. At Pomona, the dew point sensor became dirty very rapidly, and accurate values of RH were difficult to obtain.

	RH	ΔT	MM
RH	1	.815	.639
ΔT		1	.748
MM			1

$R^2 = .563$

9. Point Arguello

The Pt. Arguello data showed essentially no correlation between MM and RH. At Pt. Arguello the calculated humidity was almost always greater than 90%. There is a strong correlation between MM and ΔT, however, only 6 data points were used in the correlation.

	RH	ΔT	MM
RH	1	.177	.020
ΔT		1	.89
MM			1

$R^2 = .812$

A correlation was not made on the Fresno data alone because of insufficient data.

The inside relative humidity was calculated using the dew point temperature and TIN. MM is plotted against the change in RH (based on TIN and TO) in Figure A-13.

A linear correlation was run on MM vs. ΔRH with the following results:

$$MM = 0.264 + 0.00833(\Delta RH) \qquad R_{xy} = 0.826 \qquad F_{ratio} = 70.97$$

The equation is plotted in Figure A-13 as a dashed line (Curve A). This correlation coefficient is about the same as for MM vs. ΔT in case (1). The 95% confidence interval on the coefficient of ΔRH (β) is

$$-0.233 < \beta < 0.250$$

A parabola was also fit to the data and is shown in Figure A-13.

$$MM = 0.320 + 3.94 \times 10^{-3}(\Delta RH) + 6.71 \times 10^{-5}(\Delta RH)^2$$

Since the mismatch should be zero when ΔRH = 0, and since the mismatch parameter is a relative quantity, the curve was shifted down to intersect the origin at ΔRH = 0 (Curve C):

$$MM = 3.94 \times 10^{-3}(\Delta RH) + 6.71 \times 10^{-5}(\Delta RH)^2$$

FURTHER WORK

Further work on this problem could include:

1. Nonlinear correlations between MM and various parameters.
2. A calculation of the inside humidity and a correlation of MM vs. Δ(RH) using ten-minute averages.
3. A study of the overlap region between the Royco 220 and the Royco 245 using the raw MCA counts.
4. A new characterization of the mismatch.
5. Work on the growth of aerosols with changes in RH and the weight fraction of liquid water vs. RH.
6. An analysis of variance on the ten-minute data. Such an analysis could indicate if there were significant differences between the size distributions from different sites and from ACHEX I and ACHEX II based on the mismatch parameter.

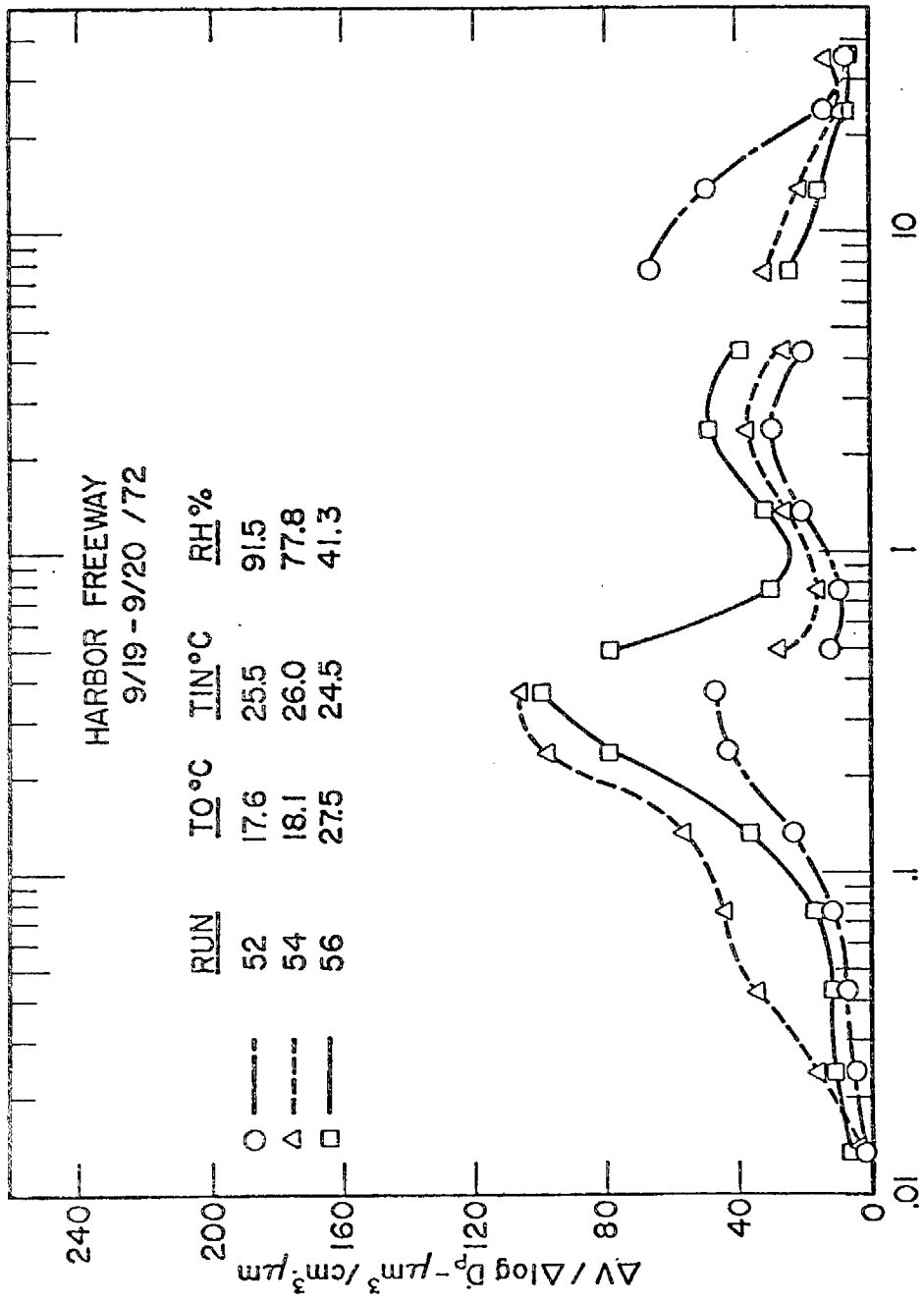

Figure A-1. Mismatch of Volume-Size Distributions at the Harbor Freeway

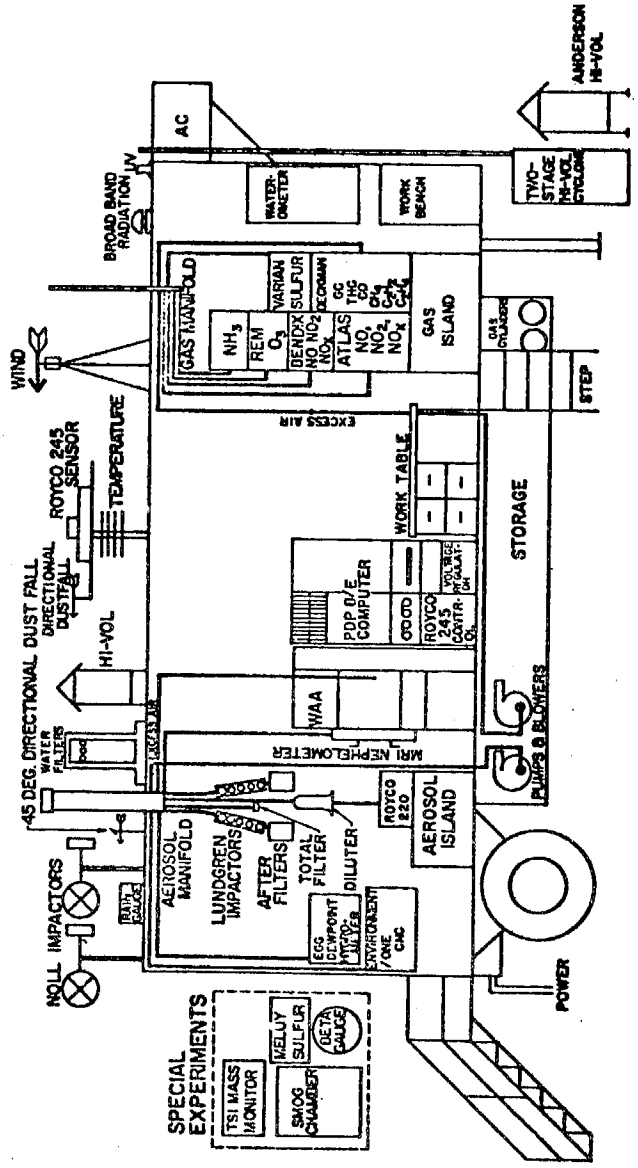

Figure A-2. Sketch of ARB Mobile Laboratory

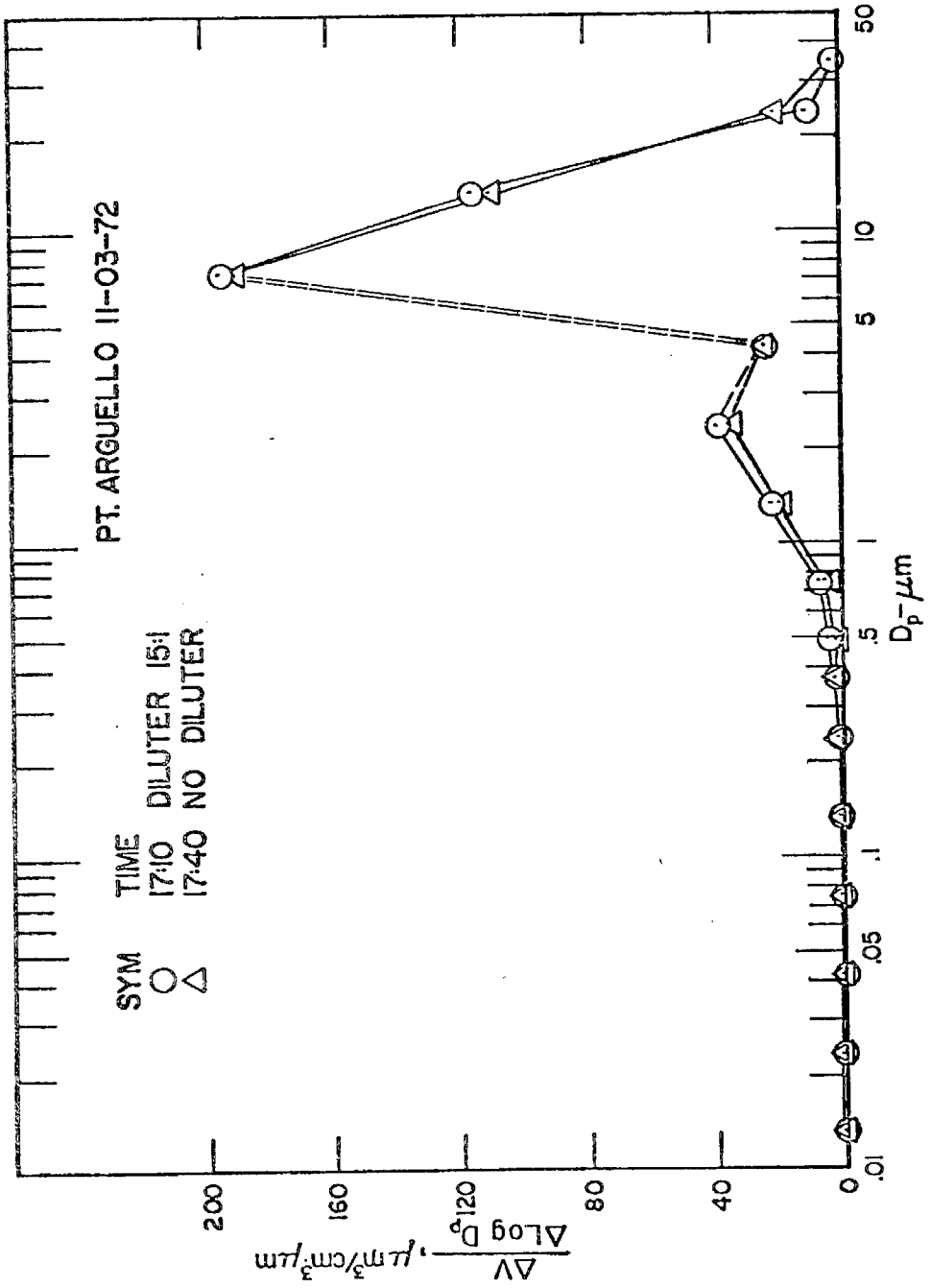

Figure A-3. Effect of Diluter on Volume-Size Distribution Measurement Point Arguello

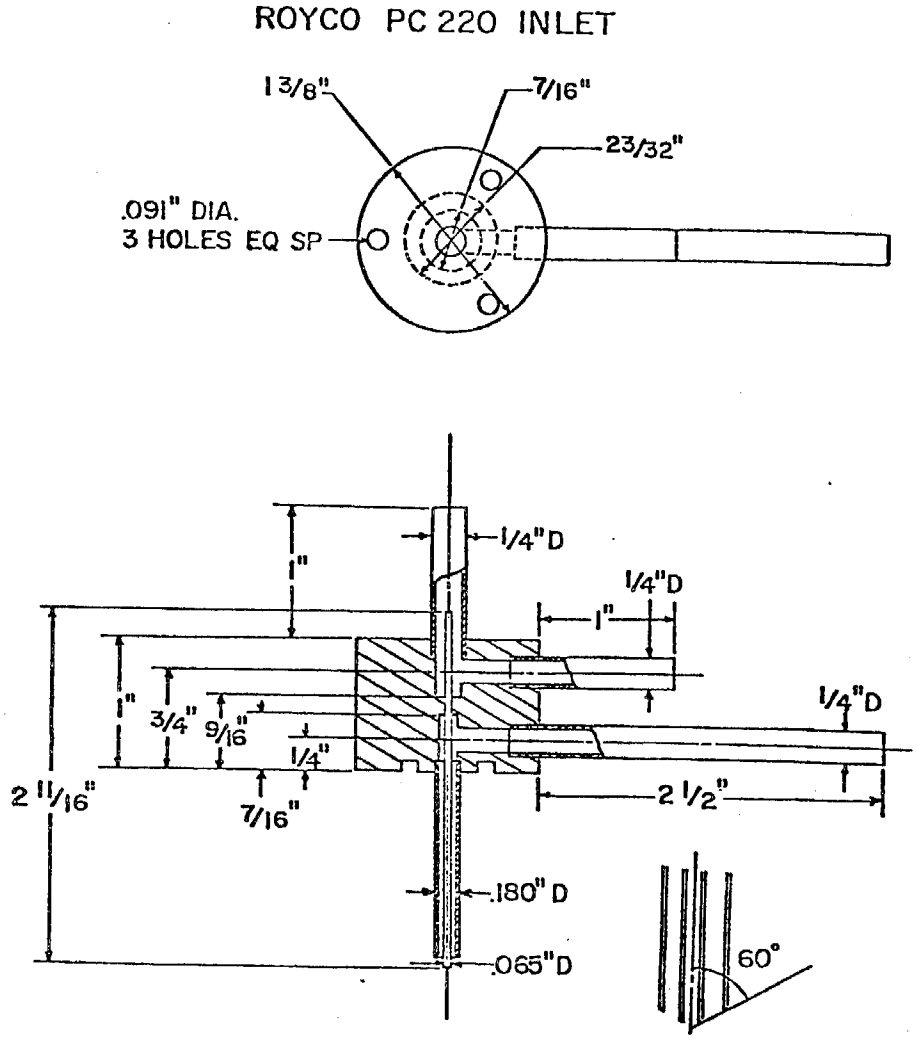

Figure A-4. Sheath Air Sample Inlet for the ARB and EPA Royco PC 220 Optical Particle Counters

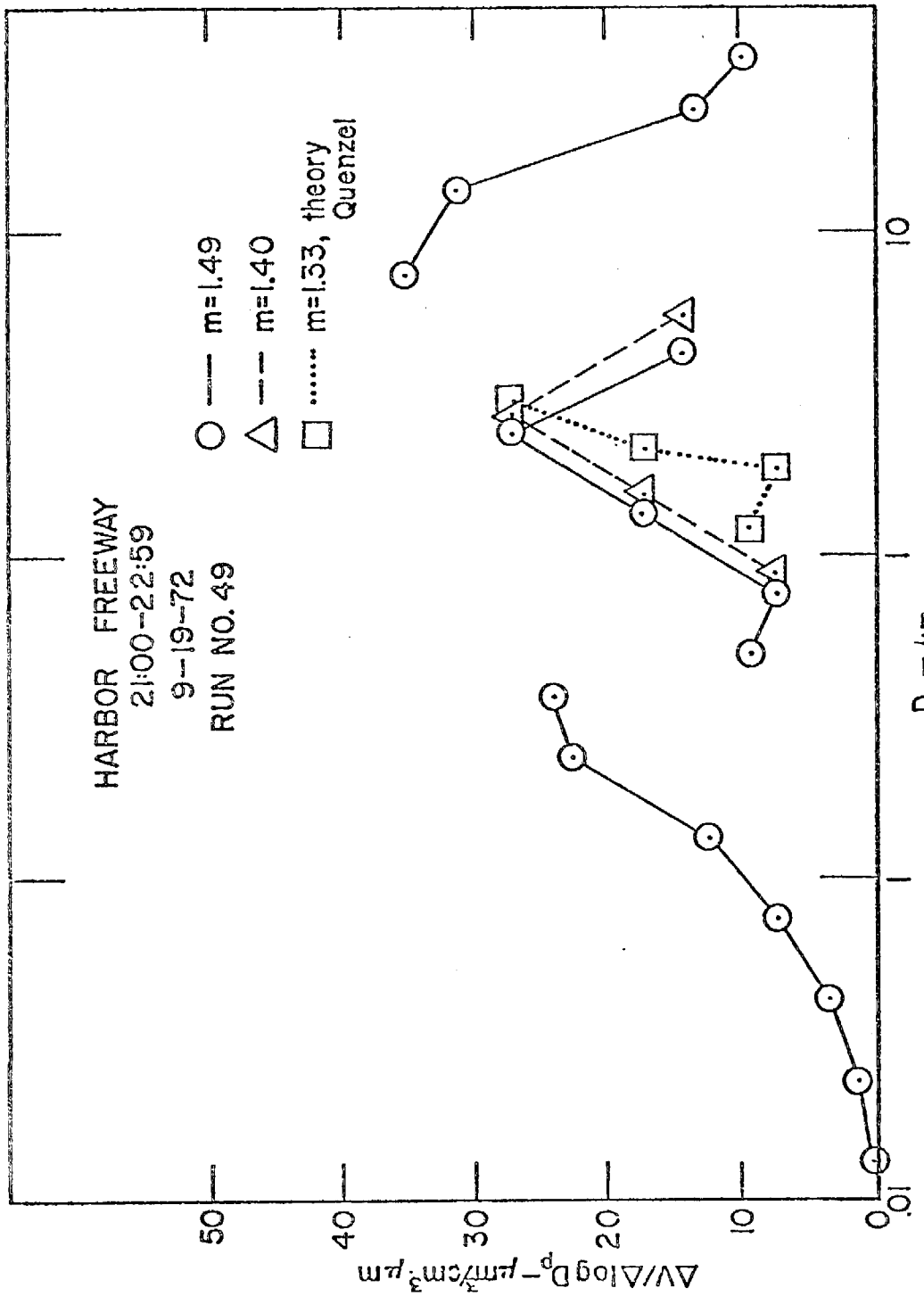

Figure A-5. Results of a Change in Refractive Index for Run 49 at the Harbor Freeway

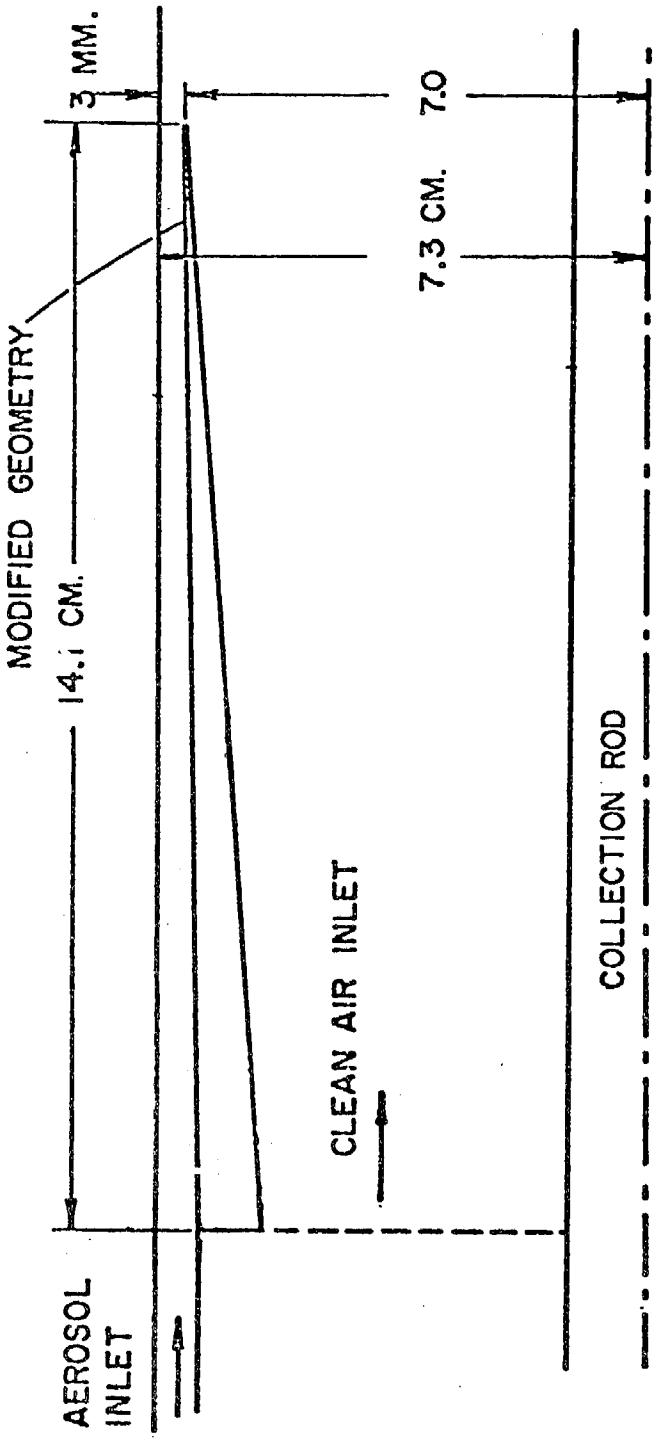

Figure A-6. Aerosol Inlet to Mobility Tube

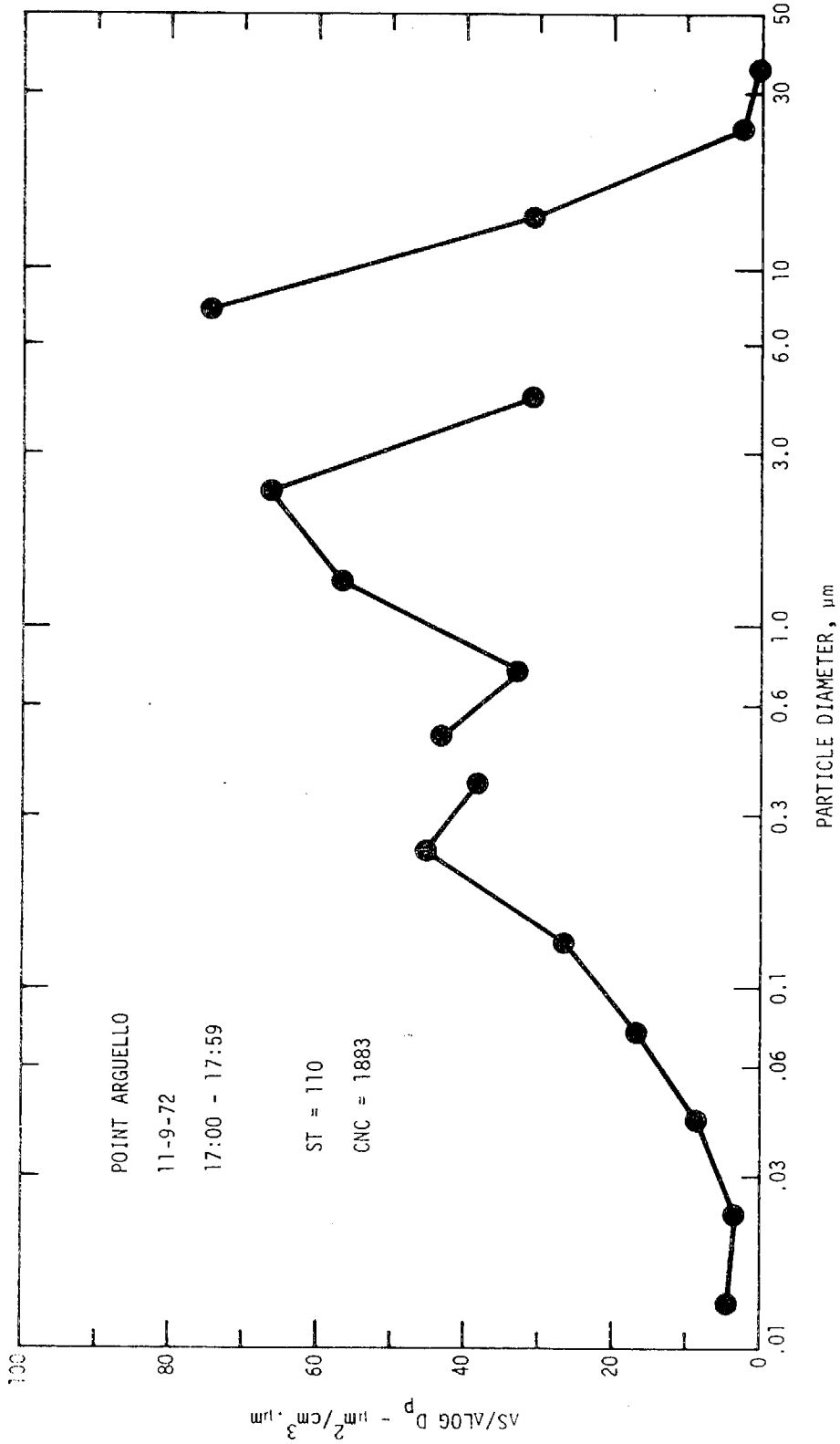

Figure A-7a. Aerosol Surface Distribution at Pt. Arguello

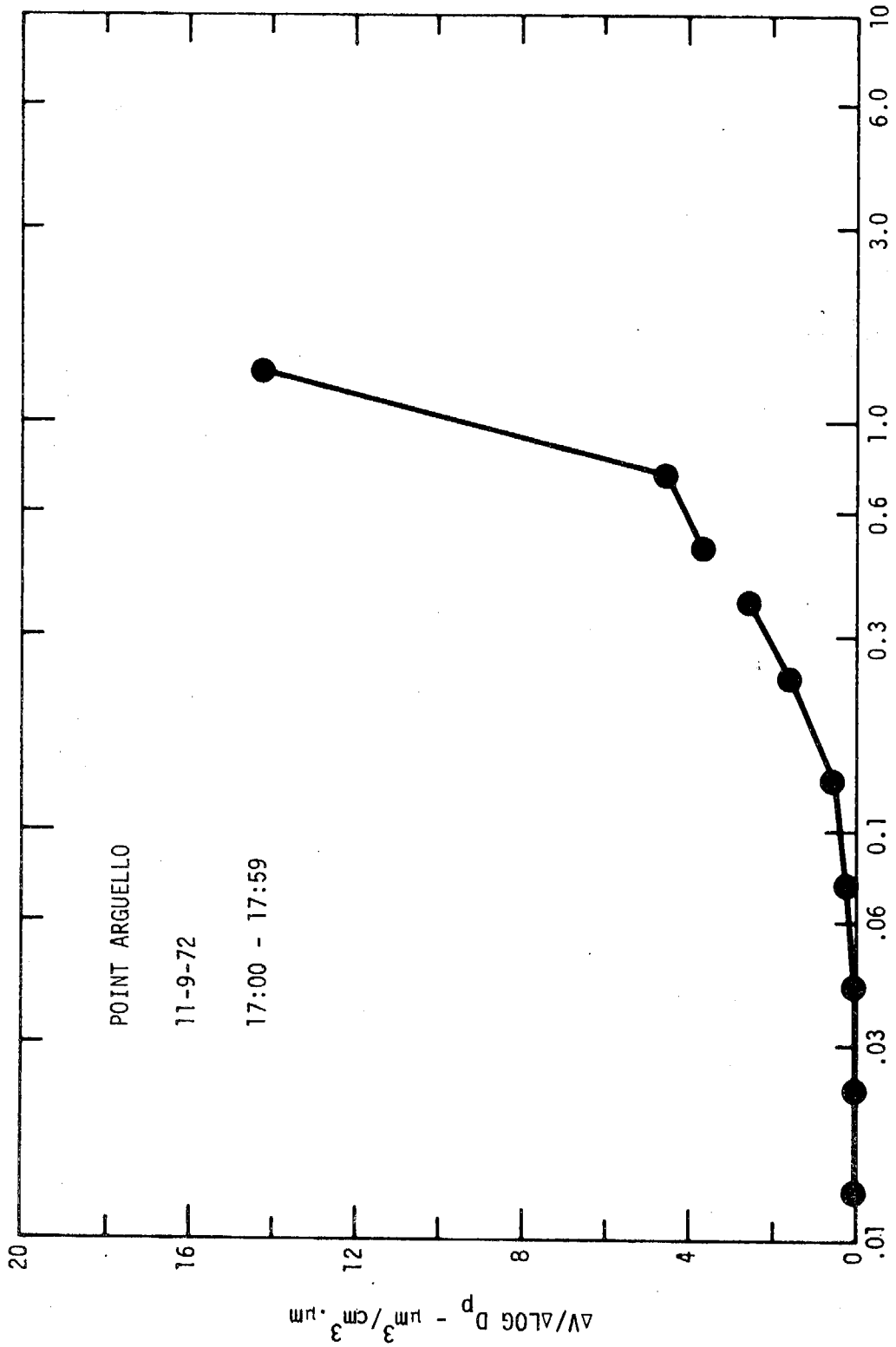

Figure A-7b. Aerosol Volume Distribution at Pt. Arguello

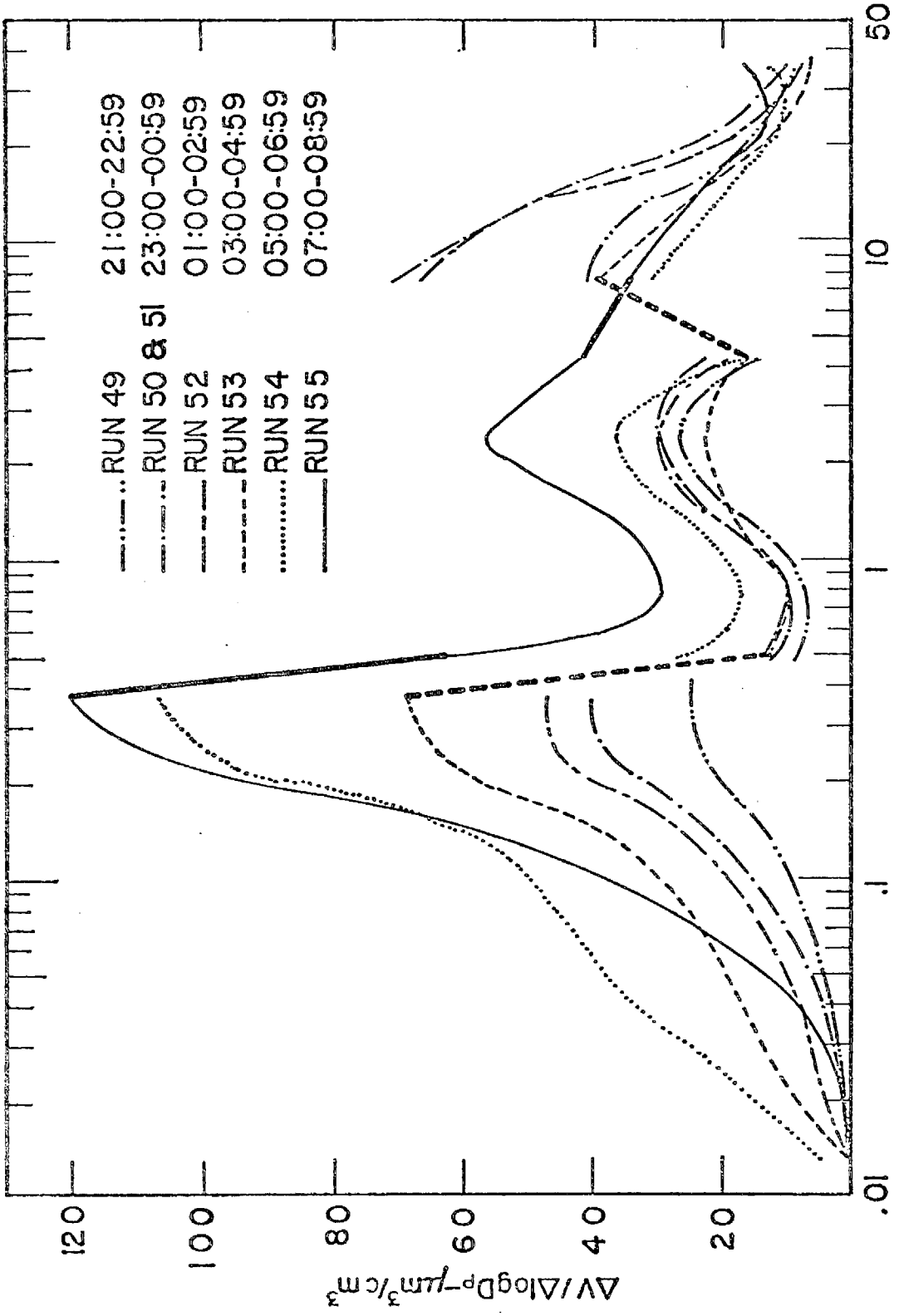

Figure A-8. Mismatch For Runs 49 Through 55

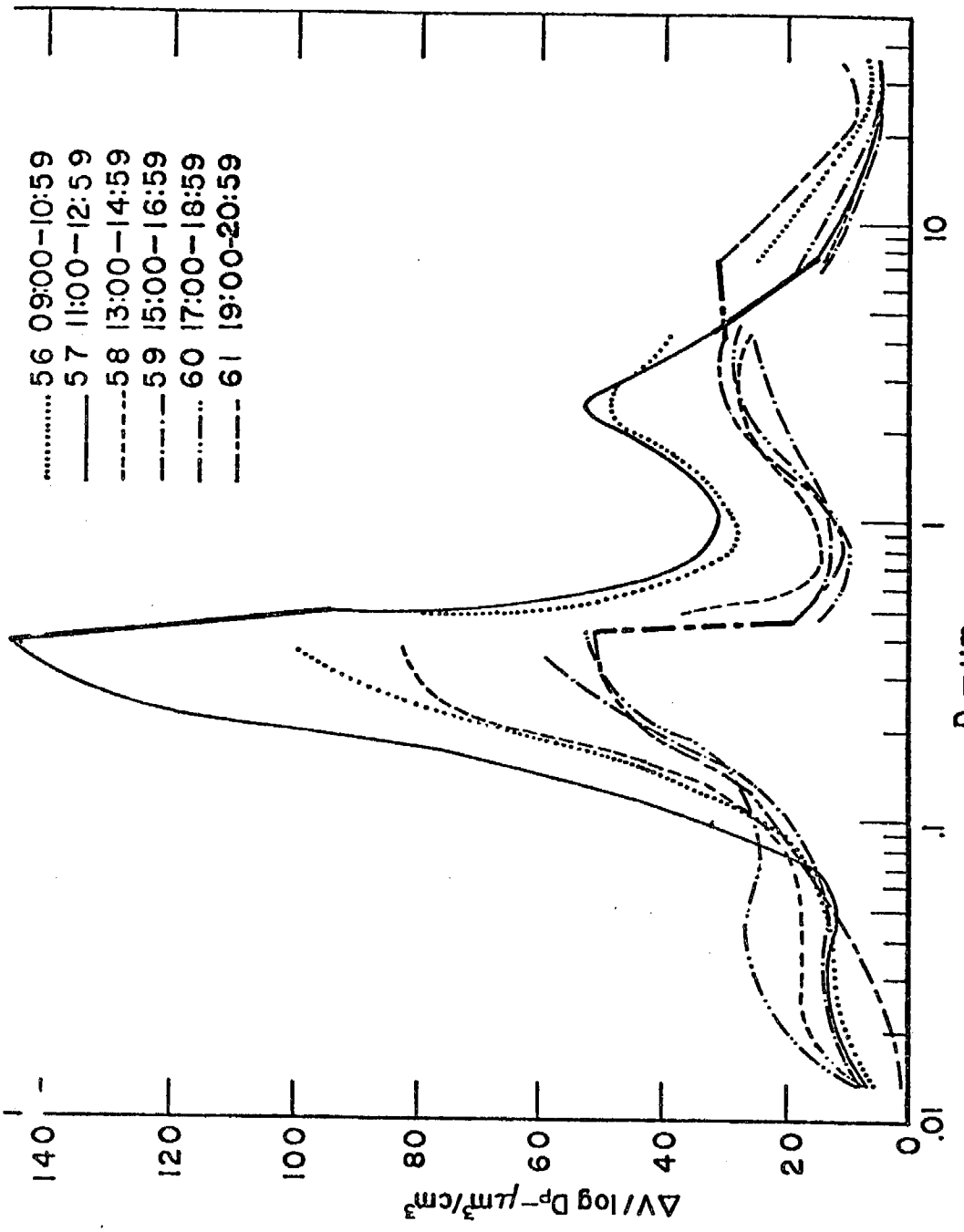

Figure A-9. Mismatch for Runs 56 Through 61

TABLE A-1

ROYCO 220 TEMPERATURES

Time	Room Temp,°C	Sheath Air Temp,°C	Inside Temp,°C	Sheath Air Voltage	Inside Voltage
12:00	Royco turned on				
14:35	21.5	23.1	23.1	.910	.910
14:48	21.8	22.7	24.0	.882	.944
14:55	22	23.3	24.5	.908	.954
15:14	22	23.4	24.4	.915	.953
15:31	22	23.5	24.5	.916	.958
15:55	22	23.5	24.8	.919	.962
16:17	22	23.4	24.7	.914	.960
16:34	22	23.5	24.7	.917	.960
17:00	22	23.7	24.9	.924	.967
18:05	21.5	23.3	24.7	.909	.960
21:40	20	22.2	23.5	.863	.913

- copper-constantan thermocouples
- inside temperature is measured inside the Royco cabinet near the inlet
- sheath air temperature measured in the sheath air line just before re-entering into inlet

APPENDIX B

THE AEROSOL SIZE DISTRIBUTION IN THE MOJAVE DESERT*

ABSTRACT

Recent work in the California Air Resources Board Aerosol Characterization Experiment (ACHEX) in 1972 has shown that reliable instrumentation coupled with a modern data acquisition system enables the researcher to sample a variety of meteorological conditions, gases, and particulates with greater accuracy over a wider range of concentrations. As an example of aerosols sampled, the results obtained at Goldstone in the Mojave Desert are presented. Simultaneously with the taking of filter and impactor samples for chemical analysis, the aerosol particle size distribution was measured with four on-line instruments over the particle size range from approximately 0.003 μm to 40 μm. Plots of $\Delta S/\Delta \text{ Log } D_p$ and $\Delta V/\Delta \text{ Log } D_p$ vs. Log D_p are presented. The lowest volumes ever recorded with the aerosol analyzing system (1.85 $\mu m^3/cm^3$) were obtained at Goldstone. More typical aerosols were also sampled. An incursion of well aged aerosol from the South Coast Basin was also recorded (total volume = 43.1 $\mu m^3/cm^3$). Average nuclei counts ranged from 47 cm^{-3} to 20,000 cm^{-3}.

---

*By George M. Sverdrup, Kenneth T. Whitby, and William E. Clark, Particle Technology Laboratory Mechanical Engineering Department, University of Minnesota. Presented at the 26th Annual Conference on Engineering in Medicine and Biology, Minneapolis, Minnesota, September 30 - October 4, 1973. Submitted to the Journal of Atmospheric Environment.

INTRODUCTION

From July through December 1972, the Particle Technology Laboratory of the University of Minnesota participated in the California Air Resources Board (ARB) Aerosol Characterization Experiment (ACHEX). The main objectives of this study were:

1. To characterize the aerosol in the San Francisco Bay Area, the San Joaquin Valley, and the Los Angeles Basin in terms of the aerosol's physical and chemical properties, its interaction in the atmosphere, and its natural and man-made origins.
2. To evaluate the amount of the atmospheric aerosol in the state's three major basins which can be related to (a) primary emissions, such as auto exhaust or smokestacks, and (b) secondary production due to physical and chemical processes taking place in the atmosphere.
3. To identify those major sources of particles and chemically reactive gases which can be related to aerosol pollution and visibility reduction.

A mobile air pollution laboratory, designed and built by the Particle Technology Laboratory and Thermo-Systems, Inc., under contract with Rockwell International Science Center, played a major role in the project. Measurements included aerosol size distributions, meteorology, gas analysis, and filter samples. The gas instrumentation and filter analysis was performed by the State of California Department of Public Health Air and Industrial Hygiene Laboratory (AIHL), Berkeley, California. The data acquisition software was written by the Rockwell Science Center.

This paper is concerned with the aerosol size distributions obtained from October 31 to November 4, 1972, at the desert site of Goldstone. The site was remote enough so that clean, desert background aerosol could be measured. The lowest volumes ever recorded with the Minnesota Aerosol Analyzing System (MAAS) were obtained (total volume of 1.85 $\mu m^3/cm^3$, nuclei count less than 100). More normal desert background aerosol was also characterized (total volumes of 8 to 13 $\mu m^3/cm^3$ and nuclei count of a few thousand).

SAMPLING SITE

The Mobile Air Pollution Laboratory was located at the Pioneer Station of NASA's Goldstone Tracking Station (see Figure B-1). Pioneer Station is located approximately 200 km northeast of downtown Los Angeles and 58 km north of Barstow, California. Fort Irwin is located 19 km southeast of Pioneer Station. Five other Goldstone stations are located within 16 km of Pioneer to the south. One station is located 4.5 km to the northwest. All stations are connected by a lightly travelled, paved road.

Pioneer Station is located in a basin approximately 3 km by 1 km surrounded by 250m hills to the northwest and 125m hills to the east and south. The mobile laboratory was parked on a paved pad about 125m west of the Pioneer buildings and the paved road leading to the basin. Directly north of the trailer was a dry lake approximately 0.4 km wide and 0.8 km long.

There was a small dump in which open burning took place on the far side of the dry lake north-northeast of the mobile laboratory. Burning was noticed during two periods. During the first, the wind was from the south and during the second period no sampling was taking place. Therefore, it is believed that no combustion aerosols from the dump were sampled.

INSTRUMENTATION

The ARB mobile laboratory was constructed in a forty-foot Fruehauf semi-trailer. The operation of the mobile lab has been discussed elsewhere.[1,2] Figure B-2 shows the location of the instrumentation in the mobile lab. The gas analyzers were located in the front of the lab. The continuous aerosol instrumentation, filters, and impactors were located in the rear. The computer and Whitby Aerosol Analyzer (WAA) were located in the middle of the lab. Whitby et al[3] have listed all major instrumentation along with the individual or group responsible for calibration and maintenance.

METEOROLOGICAL INSTRUMENTATION

The meteorological instrumentation included a Meteorology Research, Inc., (MRI) Model 1074 Ground Based Meteorological Measurement System (wind direction, wind speed, wind sigma), a Rosemount Model 412R Resistance Thermometer (outside temperature), and a Cambridge 880 Dew Point Hygrometer.

Calibration and maintenance of these instruments have been discussed by Whitby et al.[1,3]

Data from instruments whose output is an analog signal (including the meteorological instruments) was collected using software written by Rockwell Science Center.[4] The basic unit of time in the software was 20 seconds. Every 20 seconds a Rockwell-designed multiplexer scanned the analog signals. A voltmeter read each signal, and at the end of the ten-minute cycle an average of the 30 readings for each signal was written on magnetic tape and output on the teletype in engineering units (see Figure B-3).

CONTINUOUS AEROSOL INSTRUMENTATION

The aerosol size distribution system consisted of an Environment One Model Rich 100 Condensation Nuclei Counter (CNC), a slightly modified Thermo-Systems Model 3000 WAA, a modified Royco Model 220 Optical Single Particle Counter (PC), a modified Royco Model 245 PC, and a MRI Model 1550 Integrating Nephelometer.

WAA (WHITBY AEROSOL ANALYZER)

The operating principle of the WAA has been discussed elsewhere.[5] Calibration of the WAA was difficult because of the lack of a suitable standard against which to compare it. The procedures of Husar and Whitby consisted of the following:

1. An experimental determination of the charge on particles of various sizes using the instrument charger and operating conditions for the particular instrument design.
2. A theoretical calculation of the instrument constants using experimental charges and the theoretical relationships between air flows, voltages, particle charge, and fraction charged at the calculated $N_o t$ (ion concentration x charging time) product.
3. An experimental determination of the particle losses in the instrument due to space charge and diffusion.

For the WAA in the mobile lab, the earlier calibration of Husar and Whitby was used. Care was taken to make certain that the instrument was operating at the same conditions of voltage, flow, and geometry that existed when the original calibration was made. Table B-1 shows the particle size range used in

the ACHEX.

A new portable electrical aerosol analyzer (EAA) developed at the University of Minnesota was used at some locations in the ACHEX.[6] The prototype instrument has a total volume of 106 liters and a total weight of 27 kg and is sufficiently portable to be used on small airplanes and ground-based vehicles for mobile air pollution studies. Although the instrument was not used at Goldstone, it was used in conjunction with the WAA in calibrating the CNC. Further studies on its performance apply qualitatively to the WAA.

As a result of recent work at the University of Minnesota using the smog chamber described by Clark[7], an estimate of the relative error in number, surface, and volume vs. particle size for the EAA has been obtained. To do this, 0.23 ppm of SO_2 was illuminated for 17 minutes, the lights turned off, and aerosols allowed to coagulate until practically all of the particles smaller than a few hundredths of a μm had disappeared by coagulation with larger particles and the changes of aerosol surface and volume were linear with time. The change in electrometer current (ΔI) for each size interval was then regressed against time and the standard deviation of the ΔI's about the line of regression was calculated. By multiplying by the appropriate calibration constants, the standard deviation in ΔI was translated into a standard deviation in particle number, surface area, and volume. These results are shown in Figure B-4 as a function of particle size.

It will be noted that the standard deviation of ΔI ($\sigma_{\Delta I}$), ranges from a maximum of about .01 pa at 0.004 μm to a low of about 0.001 pa at 0.4 μm. This is approximately equal to the electronic noise levels at the voltages used for measuring the particular sizes. For these measurements a Doric data acquisition system (Doric Scientific Corporation, San Diego, California) was used, having a filter with an effective averaging time of about 0.25 sec. By using computer averaging of the electrometer output as was done in the ACHEX, the effect of the electrometer noise was reduced even further to values on the order of 0.0005 pa.

In the ACHEX, the WAA was controlled by the computer. While the mobile laboratory was in Minnesota being prepared for the study, it was noted that electronic noise with a period of about 2 seconds was superimposed on the

electrometer signal. Therefore, the computer was used to take a series of readings and to average them over the period of the noise. During the first five minutes of the ten-minute cycle, the WAA was in its first position. After five minutes a series of thirty readings was taken and the average value was used for the first position. The computer then stepped the WAA and after a period of time, took another set of readings. The entire WAA cycle (including some positions which were not used) took five minutes (see Figure B-3 and Table B-1). By averaging the readings at each step, the WAA could be used in regions such as Goldstone where there were relatively few sub-micron particles.

CONDENSATION NUCLEI COUNTER

Past experience has shown that the number of nuclei counted by the WAA is in substantial agreement with that counted by a Pollak counter when the particle size is well above the lower threshold limit of the CNC. The WAA and the EAA were used as reference systems for total nuclei counts. The electrical mobility analyzers have a measurement range of at least 0.006 to 0.6 μm diameter. The accuracy of the electrical aerosol analyzers is best at mid-range with a standard deviation of less than 10.0 for number. Below 0.02 μm the CNC is more accurate for measuring total number concentration NT.

When the CNC was calibrated against the WAA and EAA, aerosols were generated with practically no particles smaller than 0.02 μm and the ΔI's below 0.02 μm were not used in calculating NT. Under these conditions the absolute accuracy of the electrical aerosol analyzers is good and the variability from run to run is on the order of 5 to 10%.

Relatively monodisperse particles in this range were generated by heating rubber tubing with a hair dryer and then removing the small particles through diffusion by passing the aerosol through a 40 cm high rice bed. The aerosols were diluted and aged by coagulation for at least 10 minutes in a 3.5 m^3 bag before they were sampled through the same port by the CNC and the electrical mobility analyzers. The mobility analyzers were connected to a PDP-8E computer which gave the total number count with a small time delay. The CNC was calibrated against the WAA and the EAA at concentrations of 30,000 particles/cc to 80,000 particles/cc in the particle size range of 0.02 to 0.1 μm. Repeated

experiments showed agreement within 20%.

Because the nuclei count was extremely low at Goldstone, extra care was taken in zeroing the CNC. The CNC was run overnight on October 31 to November 1, 1972, with an absolute filter in the sample line. Sixty-five ten-minute averages were used to correct for the electronic offset. The result was the subtraction of 26 particles per cm^3 from each ten-minute average.

OPTICAL PARTICLE COUNTERS

Two optical particle counters (PC) were used in the mobile laboratory. A modified Royco PC 220 was used for the size range 0.422 to 5.62 μm and a modified Royco PC 245 was used for particles with diameters from 5.62 to 38.0 μm.[1,8]

A sheath air sample inlet was installed in the Royco PC 220. The sheath air inlet shown in Figure B-5 removes about 85% of the flow, filters this air, and returns it around the sample stream. The sheath air inlet has four advantages over the original inlet: it (1) dilutes the aerosol so that higher concentrations can be counted, (2) decreases the response time of the optical particle counter by preventing the recirculation of aerosol into the viewing volume, (3) increases the resolution of the optical particle counter by focusing the aerosol sample stream into a more uniformly illuminated portion of the viewing volume, and (4) increases the signal-to-noise ratio by focusing the aerosol sample stream into a portion of the viewing volume which has a higher mean intensity than the original viewing volume. This increase in signal-to-noise ratio and resolution of the Royco PC 220 can be seen in Table B-2 for aerosol particle diameters of 2.98 and 5.81 μm.

The sample flow rate in the Royco PC 220 was determined by plotting the pressure drop in a portion of the sheath air line vs. sample flow maintaining a total flow of 0.1 cfm. The sample flow was found to be 0.0127 cfm (5.99 cm^3/sec). The sample flow was rechecked at Goldstone and found to be 7.43 cm^3/sec. The change was due to the increased resistance to flow through the sheath air line because of particle collection on the sheath air filter in polluted urban areas.

The particle losses in the 0.25 inch diameter by 52 inch long vertical tube leading to the PC 220 sensor were determined using a DOP aerosol with a uranine dye tracer. Using a G. K. Turner Fluorometer it was determined that

for an 8.71 μm particle and a total flow rate of 0.1 cfm, the losses in the sample tube were less than 1%.

The conical sample inlet shown in Figure B-6 was made for the Royco PC 245 to increase the instrument's counting efficiency for particle diameters up to 40 μm. In order to determine the sampling efficiency of the conical inlet, the inlet was stuck through a glass fiber filter at the bottom of a vertical tube and another glass fiber filter was placed at the end of the inlet. DOP aerosols with a uranine dye tracer were generated, and the relative mass collected on each filter and the inlet were determined using a G. K. Turner Fluorometer. The sampling efficiency was then determined by the following equation:

$$\eta = \frac{M_c Q_A}{(M_c + M_I + M_o)\, Q_s}$$

where M_c = relative mass collected on filter after inlet

M_i = relative mass collected on inlet

M_o = relative mass collected on filter at bottom of the vertical tube

Q_A = aerosol flow rate (1.5 cfm)

Q_s = sample flow rate (1.0 cfm)

Figure B-7 is a plot of sampling efficiency vs. particle diameter.

A passive in-line diluter was used for the CNC and Royco PC 220 during the ACHEX.[1] No dilution was necessary at Goldstone.

The outputs of both optical particle counters were calibrated vs. the diameter of a transparent, spherical DOP aerosol with refractive index of 1.49. The DOP aerosols were generated with a vibrating orifice monodisperse aerosol generator described by Berglund (1972).[8] Figures B-8 and B-9 show plots of multi-channel analyzer (MCA) channel number vs. particle diameter. Table B-3 lists the particle size ranges used in the ACHEX.

Polystyrene latex (PSL) aerosols were also generated using a Royco Model 256 aerosol generator to determine a primary field calibration. A primary field calibration was made on both optical counters at Goldstone before any sampling was conducted. A secondary calibration check consisted of

adjusting the gain of the photomultiplier tube in the instrument so that the chopper pulse from the instrument fell in the same MCA channel as it did immediately after a primary field calibration. Secondary calibrations were made twice a day.

When sampling, each optical counter fed pulses to a 256-channel MCA. Because the pulses from the Royco Model 245 were too fast for the MCA, the pulses were first fed into a UM 170-1 pulse converter. The pulse converter was set at a gain af 1 and 50 μ sec delay. During a ten-minute cycle, both MCA's were idle the first minute and accumulated pulses during the last nine minutes (see Figure B-3). Factors such as dilution ratio, sampling efficiency, flow rate, and counting time were taken into account in the computer software.

NOMENCLATURE

Because of the great number of weightings and subranges involved in analyzing aerosol data, the system of nomenclature used is that described in detail in Reference 9. It is also briefly described in the Appendix.

The distributions presented here have been plotted as $\Delta S/\Delta \text{Log } D_p$ and $\Delta V/\Delta \text{Log } D_p$ vs. Log D_p. The area under the curve is then proportional to the surface and volume respectively.

DATA ANALYSIS

During the four days at Goldstone, a variety of aerosols were sampled. The wind direction changed from the north where extremely low aerosol concentrations were observed, to the south where aged aerosol from the south coast basin was sampled. More typical desert aerosols were also sampled.

Figure B-10 is a plot of the diurnal variations of several meteorological and aerosol parameters obtained at Goldstone. The entire sampling period has been divided into nine episodes. Table B-4 lists these episodes and the values of some characteristic parameters.

In an effort to better characterize the aerosol which was sampled, a MRI aircraft was flown during the intensive sampling periods in the ACHEX. The aircraft was a Cessna 205 equipped with gas analyzers, a nephelometer, a CNC, meteorological instruments and an analog data acquisition system. The intensive period at Goldstone was scheduled for 21:00 on November 1 until 21:00 on

November 2, 1972.

Due to a thermal failure in a MCA circuit, all copies of the data acquisition program were destroyed on the morning of the episode. The mobile lab was not in operation until 18:00 on November 2, 1972. Therefore, during the period in which the aircraft was flying and most filter samples were being taken, there are no particulate aerosol data. The one benefit derived from this failure was that the mobile lab stayed an extra day at Goldstone and sampled an incursion of aged aerosol.

CLEAN DESERT AEROSOL - EPISODE A

The period from 13:50 until 16:50 on October 31, 1972 was characterized by the lowest aerosol concentrations ever measured with the MAAS. This episode occurred after a few days of unusual weather conditions. It rained the week before the laboratory arrived at Goldstone. While the lab was at Goldstone a portion of the dry lake directly north of the trailer was covered with water. The day the mobile lab arrived the wind was from the north with gusts up to 80 km/hr. By the time the laboratory was ready for operation at 13:30 on October 31, 1972, the wind was still from the north at 25.2 km/hr blowing across the lakebed.

Figure B-11 shows a volume distribution averaged from 13:50 to 16:50 (19 distributions). The total volume is 1.85 $\mu m^3/cm^3$ with 55% of that below 1 μm. Even though there was a strong wind, the volume of particles greater than 1 μm was only 0.82 $\mu m^3/cm^3$. The nuclei count and BS are baseline values (see Table B-V).

A comparison of the average nuclei count as measured by the CNC (47 cm^{-3}) with the total number NT measured by the WAA (1290 cm^{-3}) in Table B-5 indicates that the WAA does not give reliable results for number in its lower ranges at reduced concentration. Comparing the results in Table B-5 for Figure B-13, as the concentration rises to a few thousand, the ratio of NT/CNC approaches one.

Recent work at Minnesota indicates that two reasons for the discrepancy between the instruments are:

1. As previously described, the WAA is not as accurate as the CNC at the lower size ranges of the WAA. One point below 0.02 μm (.0133 μm) was used from the WAA in the ACHEX.
2. The computer ignored negative ΔI's for the WAA. When the computer encountered such a situation, the number concentration for that size interval was set to zero. Thus any negative ΔN's which would have balanced out the positive fluctuations were not included in the summation.

For these reasons the WAA could be expected to never indicate concentrations of less than one to two thousand for NT.

NIGHT DESERT BACKGROUND AEROSOL - EPISODES B, F, H

These three night episodes represent typical background conditions obtained while the mobile lab was at Goldstone. Total volume was on the order of 8-12 $\mu m^3/cm^3$ with the amount below 1 μm at 3-4 $\mu m^3/cm^3$. The nuclei count varied from 1000 to 6000 per cm^3.

In Figure B-12 a typical Goldstone distribution is compared with the background conditions observed in Ft. Collins, Colorado, during steady periods when there was little evidence of local contamination.

The most striking feature of the volume distributions is in the volume greater than 1.0 μm. At Ft. Collins a high concentration of particles larger than a few microns was observed even under conditions when the anthropogenic contribution was obviously low.[10] The steadiness of the concentration of these large particles suggested that they were not always locally raised dusts, but rather particles settling from higher altitudes. At Goldstone such high concentrations of large particles were not measured.

Episodes B and F were characterized by low wind speed and large fluctuations in wind direction. During Episode H, however, the wind speed was about 15 km/hr from the south for much of the night. This steady wind velocity resulted in an incursion of aged aerosol the next morning. Total surface during Episode H was on the order of 100 to 120 $\mu m^2/cm^3$ compared to 60 to 80 during Episode B. The additional surface appeared in the sub-micron range.

NIGHT AEROSOL - HIGHER VT - EPISODE D

Figure B-11 and Table B-5 show a typical distribution during an evening episode in which VT was about twice as high as other evenings. The total volume in Figure B-11 is 15.2, but was measured as high as 29 $\mu m^3/cm^3$. The volume distribution shows a slight increase in the mode between 0.1 and 1.0 μm and a substantial increase in the mode above 1.0 μm. The increase is probably due to wind blown dust.

Both distributions shown in Figure B-11 are bimodal. The increased volume less than 1 μm for Run 127 is evidence of dilute aged aerosols. This aerosol was sampled when the wind was from a southwesterly direction. The aerosol was probably of anthropogenic origin of some distance away.

DAYTIME AEROSOL AT DESERT LOCATION - EPISODES C, E, G

In Table B-4, parameters representing typical distributions for daytime aerosols are shown. For Episode C the average nuclei concentration was 15,600 per cm^3. The higher nuclei count and increased volume less than 1 μm can be attributed to anthropogenic activity in the surrounding area.

Episode G covers the same time of day as Episode C; however, the nuclei concentration, BS, and sub-micron aerosol volume are considerably less than for Episode C. The nuclei concentration is about the same as during evening hours. The nephelometer was adjusted to read $0.23 \times 10^{-4} m^{-1}$ while sampling clean air to account for Rayleigh scattering. Therefore, the value of $0.259 \times 10^{-4} m^{-1}$ for Episode G is a baseline value. The fact that BS = $0.359 \times 10^{-4} m^{-1}$ for Episode A even though the sub-micron volume was less than that for Episode G ($1.02\ \mu m^3/cm^3$ for Episode A, compared to $2.28\ \mu m^3/cm^3$) suggests that both the nephelometer and the aerosol size distribution instruments were operating at their limits of detection.

INCURSION OF AGED AEROSOL - EPISODE I

From 10:00 on November 3, 1972 until midnight the wind blew steadily from the south at about 15 km/hr. From Figure B-4 it can be seen that as the wind speed increased at about 05:00 on November 4, 1972, the scattering coefficient and sub-micron aerosol volume increased dramatically.

Figure B-13 shows the buildup of the aged aerosol. In a period of 2 hours

VT and BS increased by a factor of 5. The six-fold increase in volume in the 0.1 to 1.0 μm is evidence of well aged aerosol. There was essentially no increase in volume below 0.1 μm. The volume in the 1.0 to 10 μm range increased by a factor of 3. Comparison with Figure B-11, Run 127, indicates little change in volume for particles greater than 1 μm between November 1 and November 4, 1972.

Figure B-11 (Run 127) and Figure B-13 both represent times when the wind had been blowing steadily from the south for a period of time. For Run 127, any aerosol generated within 40 to 50 km to the south of Goldstone would have had time to arrive at Goldstone and yet V3- was only 5.09 $\mu m^3/cm^3$. In Run 171, V3- = 29.9 $\mu m^3/cm^3$. These facts confirm the belief that Figure B-13 represents well aged aerosol from the South Coast Basin.

A comparison of the aged aerosol sampled at Goldstone with smog aerosol in the South Coast Basin is made in Figure B-14. The comparison is made with aerosol sampled at the Los Angeles County Fairgrounds in Pomona eleven days earlier. Total surface is a factor of 3 higher at Pomona, and BS is a factor of 3 higher. Both distributions are similar in shape having a mode at 0.486 μm. The Pomona aerosol has a greater proportion of its surface below 0.1 μm; however, this is to be expected in an urban area.

A chemical analysis of aerosols collected on a total filter also indicates that the aged aerosol was of anthropogenic origin. The filter was a 5 μ, 47 mm Gelman GA-1 cellulose ester filter with an average flow rate of 100 ℓ/min. Three elements known to originate from anthropogenic sources are tabulated in Table B-6 covering a period of about 60 hours. Ratios of bromine, lead, and zinc to total mass, MT, are presented. Just as the ratio of V3/VT increased during the incursion of aged aerosol, the ratios of BR/MT, PB/MT, and ZN/MT increased by a factor of a little over 2.

The lead to bromine ratio has also been tabulated. The lead to bromine ratio, as pointed out by Wesolowski and others, indicates the possible aging of the aerosol based on the removal of bromine from the lead halides from automobile exhaust.[4] There appears to be a systematic difference in the data obtained in the ACHEX with the lead to bromine ratio for fresh combustion aerosol in the range of 2.4 to 3.4 and a much higher ratio for aged aerosol. From

Table B-6, the smallest value of this ratio, 3.3, occurred on November 2, during hours in which Goldstone personnel and the mobile lab crew arrived by automobile. The aged aerosol arrived at Goldstone on November 4, during the same time period, increasing the ratio to 5.8. Thus, the lead to bromine ratio indicates that not only was the aerosol of anthropogenic origin, but that it was aged aerosol.

Four examples of gas concentrations are also tabulated. There was essentially no increase in the concentration of total hydrocarbons, HCTOT, and a small increase in carbon monoxide. Ozone and oxides of nitrogen, tabulated in pphm, showed increases by a factor of about 3. The peak ozone concentration measured was .092 ppm.

PARTICULATE DENSITY

Figure B-15 is a plot of the total mass of particulates obtained from the total filter. Table B-6 shows an estimate of the particulate density at Goldstone. The density was obtained by dividing the mass obtained from the total filter by the total volume obtained with the MAAS. For two periods on November 2, 1972, the density was not calculated since only three ten-minute total volumes were recorded. The average density over a period of about two days was 1.70 g/cm^3 with an uncertainty factor of $\pm$ 0.17 g/cm^3 based on the uncertainty in total mass, and a relative standard deviation of 27.4%.

The value of 1.7 gm/cm^3 is quite reasonable since the absolute value of particle density is probably within the range from 1.5 to 2.5 gm/cm^3. Ho et al[11] have reported that on November 2, 1972 within the limits of detection of the Rockwell waterometer (microwave technique), essentially no liquid water was present in the aerosol. Their conclusion was confirmed by measurement of the water in filter collected aerosols by a gas chromatographic technique.[12]

CONCLUSIONS

From the aerosol size distributions measured in the Mojave Desert at Goldstone, the following conclusions can be drawn:

1. The use of reliable instrumentation coupled with a modern data acquisition system has made possible the sampling of gases and aerosols over a wider range of concentrations with greater accuracy.

2. When the wind was from the north, the lowest volumes ever recorded with the MAAS were obtained. The average total volume over a 3-hr period was 1.85 $\mu m^3/cm^3$. The low volume is probably due to the rain which fell at Goldstone prior to the sampling period. The rain does not explain the low nuclei concentrations (less than 100) which were found. It is speculated that the low nuclei count might have occurred because of high altitude air which was brought down to the earth's surface.
3. The typical background desert condition measured during the sampling period was a total volume on the order of 8 to 13 $\mu m^3/cm^3$ with the amount below μm at 3-4 $\mu m^3/cm^3$. The nuclei count was a few thousand. In contrast with other background data obtained at Fort Collins, Colorado, the volume of aerosol greater than 1 μm was much less, being only 60 to 70% of the total volume. The occurrence of rain just before the sampling period makes it impossible to claim that typical background conditions over a long period of time were measured. Although large amounts of windblown dust had been expected at Goldstone, no evidence of such dust was recorded. The maximum volume greater than 1 μm was about 12 $\mu m^3/cm^3$.
4. Aged aerosol from the South Coast Basin has been measured at a desert location. A total volume of 43.1 $\mu m^3/cm^3$ was recorded with 31.5 $\mu m^3/cm^3$ below 1 μm. Concentrations such as these are of the same order of magnitude as those measured in the South Coast Basin itself on days of light smog.

ACKNOWLEDGMENT

This work was performed in cooperation with Rockwell International Science Center and the Air and Industrial Hygiene Laboratory of the State of California Department of Public Health under Subcontract No. 262-1948 from Rockwell International Science Center, Thousand Oaks, California under Prime Contract No. ARB-358 from the Air Resources Board State of California.

NOMENCLATURE

Inclusive Range	Subrange
0.001 - 0.01 μm	1
0.01 - 0.1 μm	2
0.1 - 1 μm	3
1 - 10 μm	4
10 - 100 μm	5

N = particle number, no./cm^3

S = particle surface, $\mu m^2/cm^3$

V = particle volume, $\mu m^3/cm^3$

T = total number, surface, or volume

V3- = volume in subrange 3 and all smaller subranges

V4+ = volume in subrange 4 and all larger subranges

BS = scattering coefficient, m^{-1}

CNC = condensation nuclei counter

RH = relative humidity, %

WD = wind direction, deg.

WSPD = wind speed, km/hr

BR = Bromine, $\mu g/m^3$

PB = Lead, $\mu g/m^3$

ZN = Zinc, $\mu g/m^3$

HCTOT = Total hydrocarbons, ppm

CO = Carbon monoxide, ppm

O3 = Ozone, pphm

NOX = Oxides of nitrogen, pphm

MT = Total mass, $\mu g/m^3$

REFERENCES

1. K. T. Whitby, Mobile Laboratory Design, Preparation, Operation and Data - ARB Aerosol Characterization Study, Particle Technology Laboratory, University of Minnesota, submitted to G. Hidy, Rockwell International Science Center, March (1973).

2. Operator's Manual, ARB Semi-Trailer Systems, ARB Sampling Systems, Thermo-Systems, Inc., St. Paul, Minnesota, February (1973).

3. K. T. Whitby, W. E. Clark, V. A. Marple, G. M. Sverdrup, G. J. Sem, K. Willeke, B. Y. H. Liu, and D. Y. H. Pui, Size Distributions of Freeway Aerosol, submitted to J. of Atmospheric Environment (1974).

4. G. M. Hidy, Characterization of Aerosols in California, Rockwell International Science Center, SC 524.191R, December (1973).

5. K. T. Whitby, B. Y. H. Liu, R. B. Husar, and N. J. Barsic, The Minnesota Aerosol Analyzing System Used in the Los Angeles Smog Project, Journal of Colloid and Interface Science, 39:136-164.

6. B. Y. H. Liu, K. T. Whitby, and D. Y. H. Pui, A Portable Electrical Aerosol Analyzer for Size Distribution Measurement of Submicron Aerosols, presented at the 66th Annual Meeting of APCA, Chicago, Illinois, June 24-28 (1973) (COO-1248-73).

7. W. E. Clark, Measurements of Aerosols Produced by the Photochemical Oxidation of SO_2 in Air, Ph.D. Thesis, Department of Mechanical Engineering, University of Minnesota (1972).

8. R. N. Berglund, Basic Aerosol Standards and Optical Measurements of Aerosol Particles, Ph.D. Thesis, Department of Mechanical Engineering, University of Minnesota (1972).

9. K. T. Whitby, R. B. Husar, and B. Y. H. Liu, The Aerosol Size Distribution of Los Angeles Smog, Journal of Colloid and Interface Science, 39:177-204.

10. K. T. Whitby, R. B. Husar, and A. K. Rao, Size Distributions of Non-Urban Colorado Aerosols, submitted to J. of Atmospheric Environment.

11. W. Ho, G. M. Hidy, and R. M. Govan, Microwave Measurements of the Liquid Water Content of Atmospheric Aerosols, J. Appl. Meteor. 13, 871 (1974).

12. R. A. Meyer, G. M. Hidy, and J. H. Davis, Determination of Water and Volatile Organics in Filter Collected Aerosols, Environmental Letters, 4:9-20 (1973).

TABLE B-1
PARTICLE SIZE RANGES AND TIME AT EACH STEP FOR WAA

Step	D_p, μm	D_{pi}, μm	Time at Step
1	.01	.0133	5 min.
2	.01778	.0237	40 sec.
3	.0316	.0422	40 sec.
4	.0562	.075	20 sec.
5	.100	.133	20 sec.
6	.1778	.237	20 sec.
7	.316	.365	20 sec.
8	.422		20 sec.

TABLE B-2
MEAN AND RELATIVE STANDARD DEVIATION OF PARTICLE VOLTAGE PULSES FROM THE ARB ROYCO PC 220 (SERIAL NO. 431) OPTICAL PARTICLE COUNTER WITH THE ORIGINAL AND SHEATH AIR SAMPLE INLETS

	D_p = 2.98 μm		D_p = 5.81 μm	
Inlet	Mean (Volts)	Relative Standard Deviation	Mean (Volts)	Relative Standard Deviation
Original	1.29	0.197	3.59	0.168
Sheath Air	2.89	0.073	7.66	0.065

TABLE B-3

PARTICLE SIZE RANGES FOR THE OPTICAL SINGLE PARTICLE COUNTERS

Royco Model 220		Royco Model 245	
D_p, μm	D_{pi}, μm	D_p, μm	D_{pi}, μm
.422	.487	5.62	7.50
.562	.750	10.0	13.33
1.00	1.33	17.78	23.7
1.78	2.37	31.62	34.7
3.16	4.22	38.0	
5.62			

D_p = particle diameter at boundary of size range.

D_{pi} = particle diameter at midpoint of size range.

TABLE B-4

SUMMARY OF AVERAGED DATA FOR GOLDSTONE

Episode	Date	Time	WD deg	WSPD Km/hr	RH %	BS $m^{-1}\times10^{4}$	No./cm^3		Surface, $\mu m^2/cm^3$					Volume, $\mu m^3/cm^3$					Remarks
							CNC	NT	S2	S3	S4	S5	ST	V2	V3	V4	V5	VT	
A	10/31/72	1350-1650	360	16.2	36.0	.359	47	1,290	4.61	21.4	1.21	.075	27.3	.04	.98	.602	.221	1.85	Wind from north across dry lake bed; low volumes & nuclei
B	10/21-11/1	1700-0600	228	6.31	62.9	.441	-	6,906	17.6	44.3	8.16	.40	70.4	.15	2.06	4.61	1.06	7.88	Typical continental background
C	11/1	0600-1700	199	12.4	31.9	.642	15,640	18,123	42.0	134	10.8	.35	187	.36	5.80	5.93	.95	13.1	Daytime aerosol
D	11/1-11/2	1700-0600	231	3.30	68.1	.579	3,582	9,365	40.5	115	14.4	1.64	173	.39	5.01	9.39	4.45	19.3	Night aerosol; high VT
E*	11/2	0600-1700	230	7.08	23.8	.632	1,570	4,252	21.1	82.6	11.4	.30	116	.22	3.73	6.35	.82	11.1	Daytime aerosol
F	11/2-11/3	1700-0700	204	1.23	66.5	.425	3,445	10,317	26.3	69.4	6.18	0.22	102	.23	3.20	3.59	.57	7.58	Night aerosol
G	11/3	0700-1700	213	12.7	38.9	.259	2,815	8.039	20.9	46.9	4.33	.16	72.3	.18	2.10	2.45	.41	5.14	Daytime aerosol
H	11/3-11/4	1700-0500	200	10.2	48.9	.531	2,277	6,489	30.9	65.8	4.47	.21	101	.31	2.82	2.48	.57	6.18	Night aerosol; high S3-
I	11/4	0500-0900	207	16.3	63.0	2.02	4,630	8,332	45.6	392	20.7	.41	459	.50	22.5	8.51	1.06	32.5	Incursion of well-aged aerosol

*Only 6 ten-minute averages from 0800-1000.

SC524.25FR

Science Center
Rockwell International

TABLE B-5

AEROSOL AND METEOROLOGICAL PARAMETERS FOR ASSOCIATED PLOTS IN FIGURES B-11 - B-14

Site	Run	Date	Time	Meteorology WD deg	WSPD Km/hr	RH %	BS $m^{-1} \times 10^4$	No./cm^3 CNC	NT	Surface, $\mu m^2/cm^3$ S3-	S4	S5	ST	Volume, $\mu m^3/cm^3$ V3-	V4	V5	VT	Figure
Goldstone	-	10/31/72	1350-1650	360	16.2	36.0	.359	47	1,290	25.9	1.21	.075	27.3	1.03	.602	.221	1.85	11
Goldstone	127	11/2/72	0000-0100	223	1.39	69.0	.567	3,000	6,010	145	12.1	1.0	158	5.09	7.30	2.77	15.2	11
Goldstone	108	11/1/72	0110-0200	172	5.18	70.6	.410	-	5,635	56.1	8.63	.49	65.3	1.96	5.00	1.31	8.27	12
Ft. Collins	1-22	08/5/70	0039-0740	147	3.04	43.0	-	6,087	7,422	46.9	9.03	-	57.4	1.81	7.91	-	13.2	12
Goldstone	-	11/4/72	0500-0510	195	8.87	68.0	.599	1,620	6,112	136	5.53	.31	142	4.72	2.97	.75	8.44	13
Goldstone	-	11/4/72	0540-0550	188	15.4	66.7	1.14	5,180	5,378	329	15.3	.39	344	15.9	7.08	1.0	24.0	13
Goldstone	-	11/4/72	0750-0800	217	17.7	62.1	2.78	9,140	8,225	575	28.7	.36	604	31.5	10.7	.89	43.1	13
Goldstone	171	11/4/72	0700-0800	204	19.6	62.6	2.57	6,160	10,550	552	26.1	.39	578	29.9	10.1	1.0	41.0	14
Pomona	76	10/24/72	1200-1400	253	5.57	51.8	7.79	71,600	69,500	1,650	130	1.62	1,780	88.3	41.6	4.66	135	14

TABLE B-6

PARTICLE DENSITY, CHEMISTRY, AND GASEOUS CHEMISTRY AT GOLDSTONE

			Particle Density				Particle Chemistry				Gas Chemistry			
Run	Date	Time	VT $\mu m^3/cm^3$	MT $\mu g/m^3$	Density g/cm^3	RH %	BR $MT_3 \times 10^3$	PB $MT_3 \times 10^3$	ZN $MT_3 \times 10^3$	PB/BR	HCTOT ppm	CO ppm	O3 pphm	NOX pphm
124-127	11/1-11/2	2100-0100	16.13	30.5	1.89	62.9	.770	3.84	.528	4.98	1.82	.667	2.38	.263
128-131	11/2	0100-0500	14.67	20.6	1.40	71.1	.720	4.17	.680	5.73	1.89	.577	2.69	.521
132	11/2	0500-0900	11.6*	42.3	-	-	1.10	3.62	.329	3.30	1.75*	.708*	3.65*	.341*
133	11/2	0900-1700	10.7*	6.91	-	-	.509	2.65	.713	5.20	1.77*	.740*	4.18*	.295*
134-136	11/2	1700-2100	7.38	18.9	2.56	38.6	.582	2.03	.465	3.50	2.14	.561	3.63	.325
137-146	11/2-11/3	2100-0700	7.64	10.0	1.31	67.1	1.27	5.42	.637	4.27	2.20	.523	1.28	.536
147-153	11/3	0700-1400	5.09	7.64	1.50	32.0	.967	4.15	.415	4.29	1.81	.449	3.93	.359
154-160	11/3	1400-2100	5.34	6.50	1.22	35.9	1.31	5.74	.491	4.38	1.65	.387	4.53	.426
161-170	11/3-11/4	2100-0700	7.26	15.7	2.16	56.2	1.50	8.34	.745	5.57	1.70	.528	4.06	-
171	11/4	0700-0830	41.77	65.5	1.57	60.7	1.97	11.4	1.32	5.78	1.96	1.18	9.18	1.09

* Only three ten-minute averages recorded.

SC524.25FR

Science Center
Rockwell International

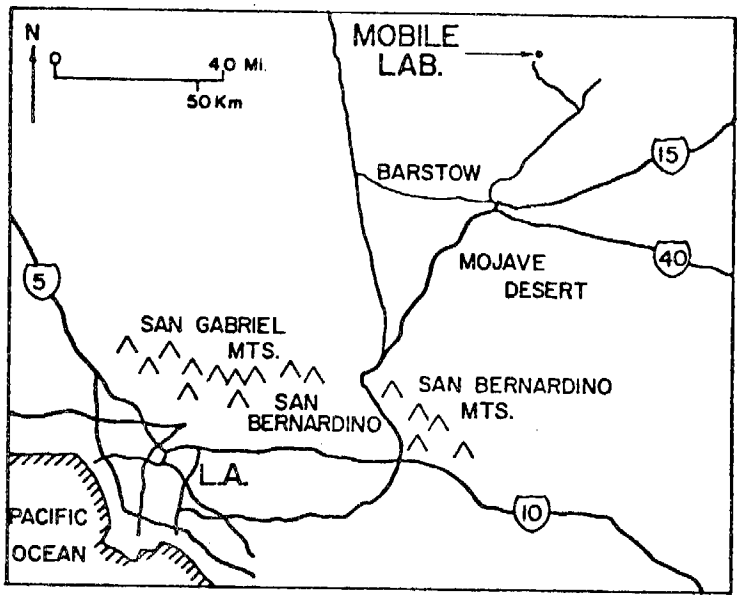

Figure B-1. Location of the Mobile Laboratory.

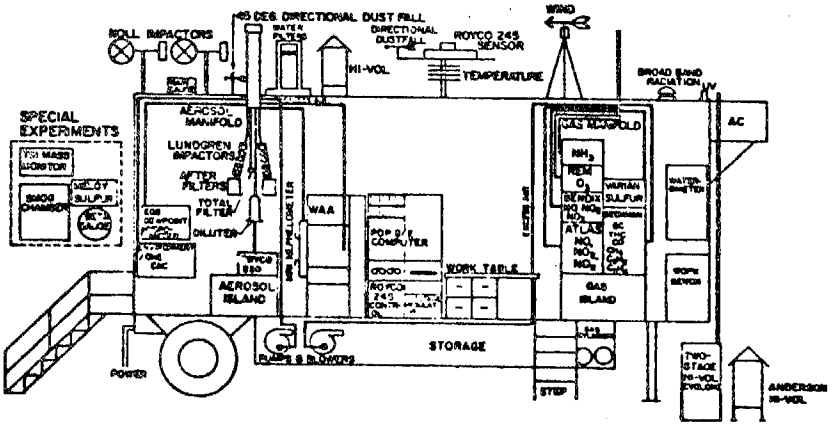

Figure B-2. Location of Instrumentation in the Mobile Laboratory

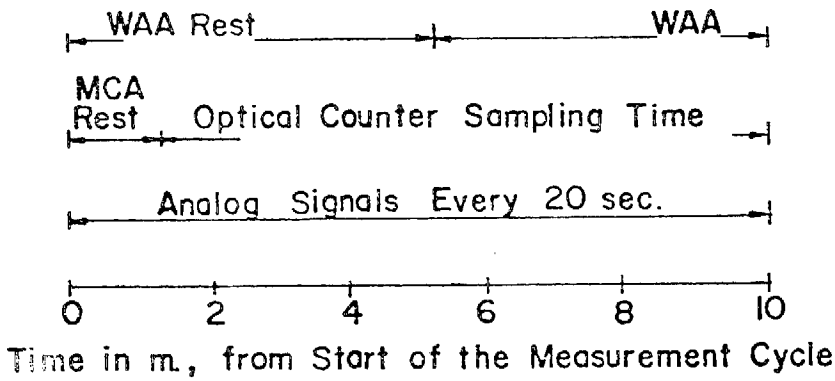

Figure B-3. Sampling and Recording Times in the Ten-Minute Cycle

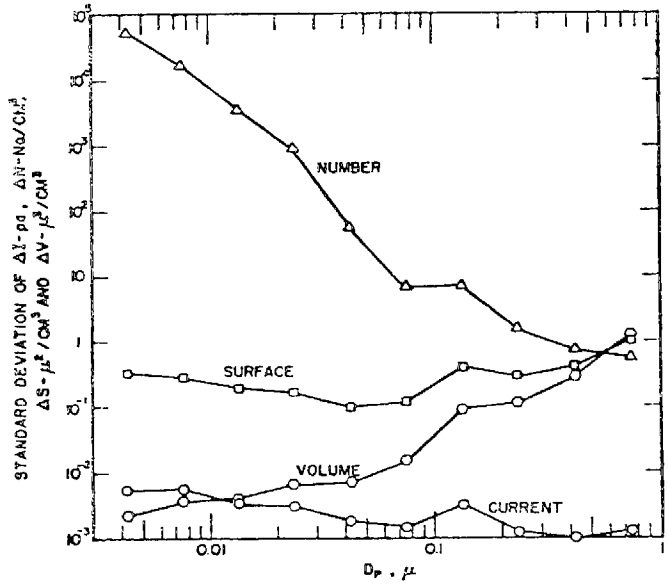

Figure B-4. Variability in Electrometer Current, Particle Number, Surface Area, and Volume Due to Instrument Noise

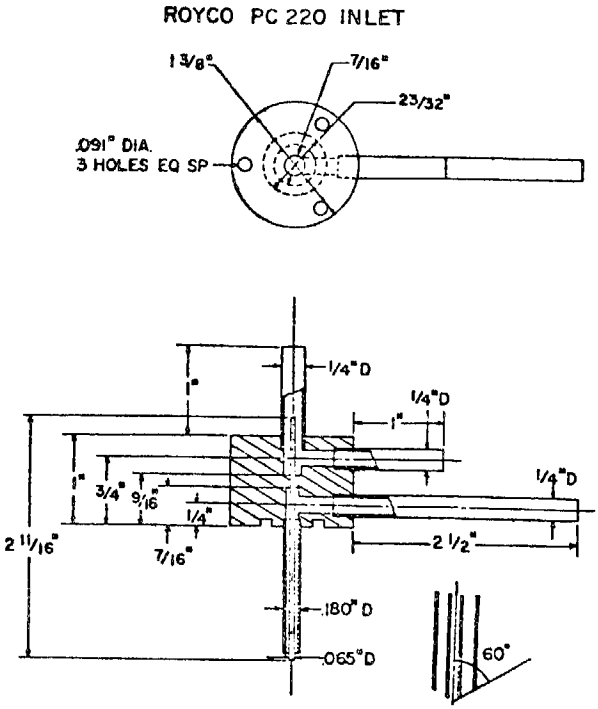

Figure B-5. Sheath Air Sample Inlet for the Royco PC 220 Optical Particle Counter

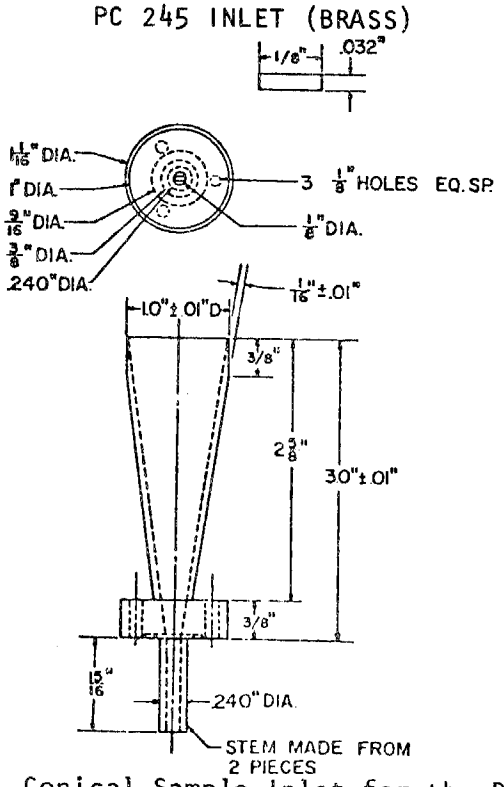

Figure B-6. Conical Sample Inlet for the Royco PC 245 Optical Particle Counter

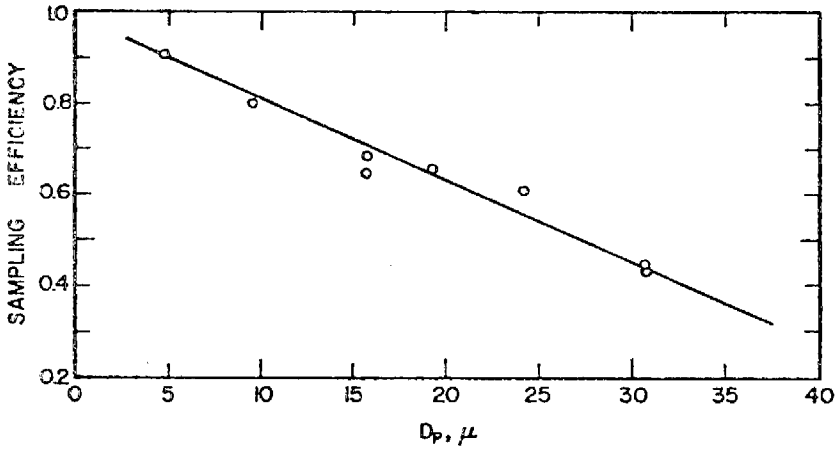

Figure B-7. Sampling Efficiency of the Conical Inlet vs. Particle Size

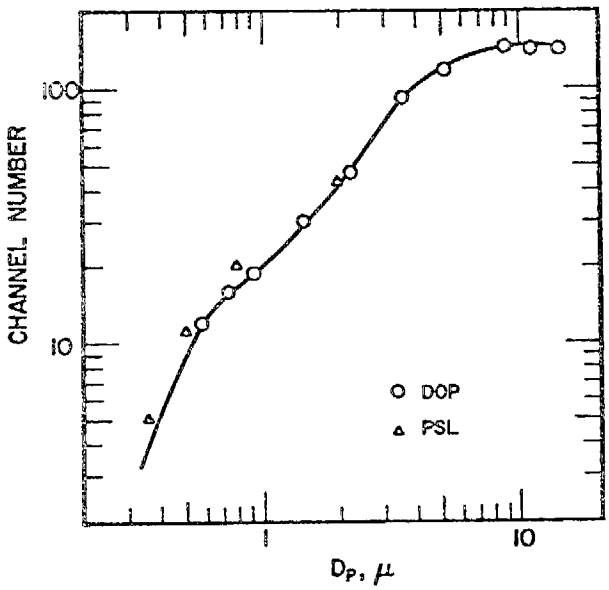

Figure B-8. MCA Channel Number vs. Particle Diameter for the Royco PC 220 Optical Particle Using DOP Aerosols with a Refractive Index of 1.49

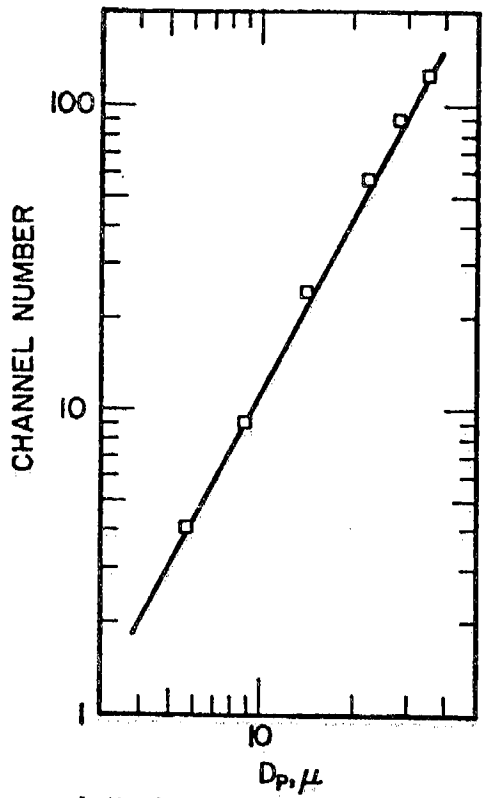

Figure B-9. MCA Channel Number vs. Particle Diameter for the Royco PC 245 Optical Particle Counter Using DOP Aerosols with a Refractive Index of 1.49

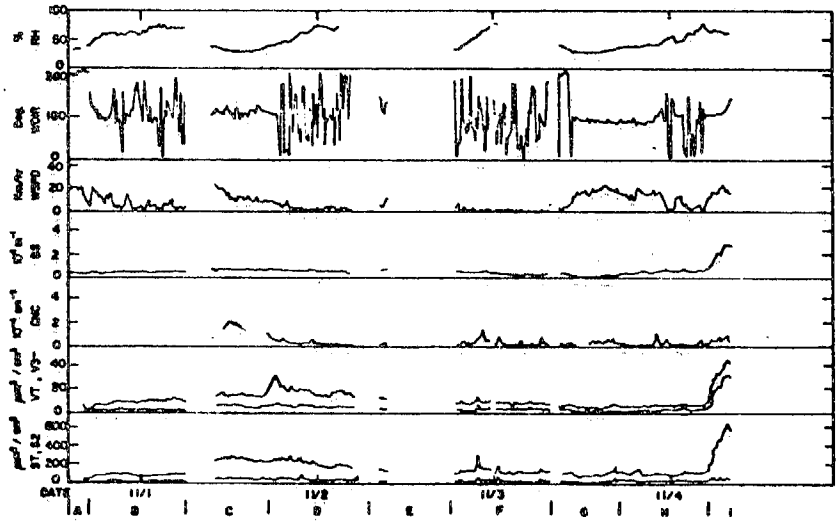

Figure B-10. Plot of the Diurnal Variation of Selected Ten-Minute Averages Obtained at Goldstone

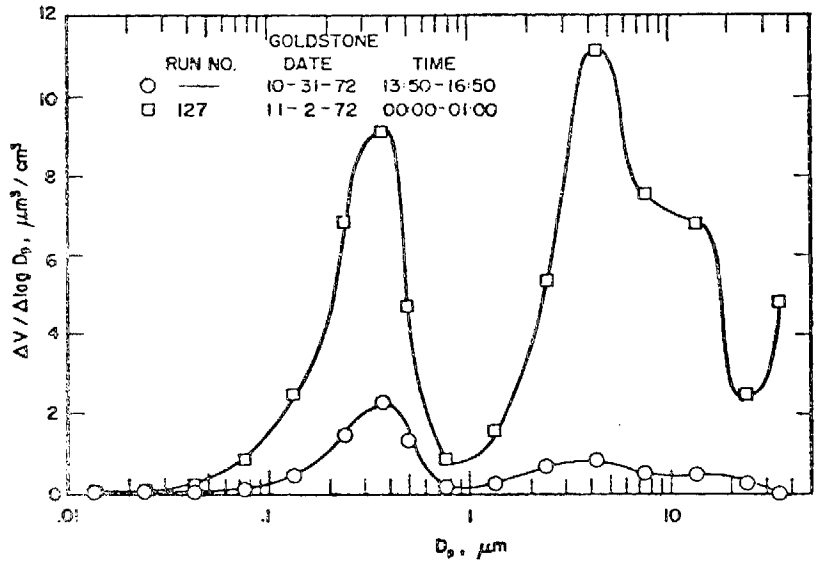

Figure B-11. A Comparison of the Background Volume Distributions During A Very Clean Period and an Evening with Higher Total Volume

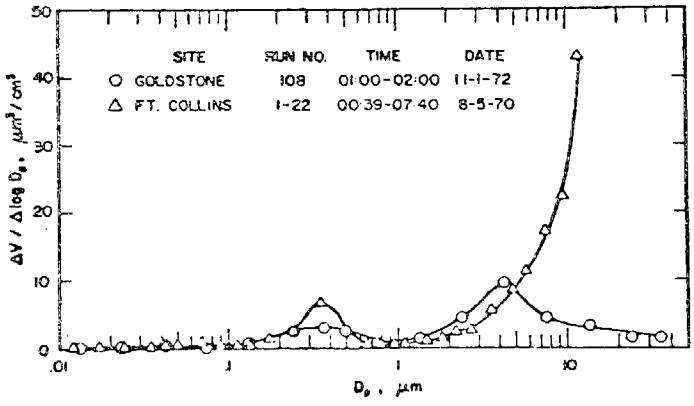

Figure B-12. A Comparison of the Volume Distributions of Background Aerosols Sampled at Goldstone and Fort Collins, Colorado

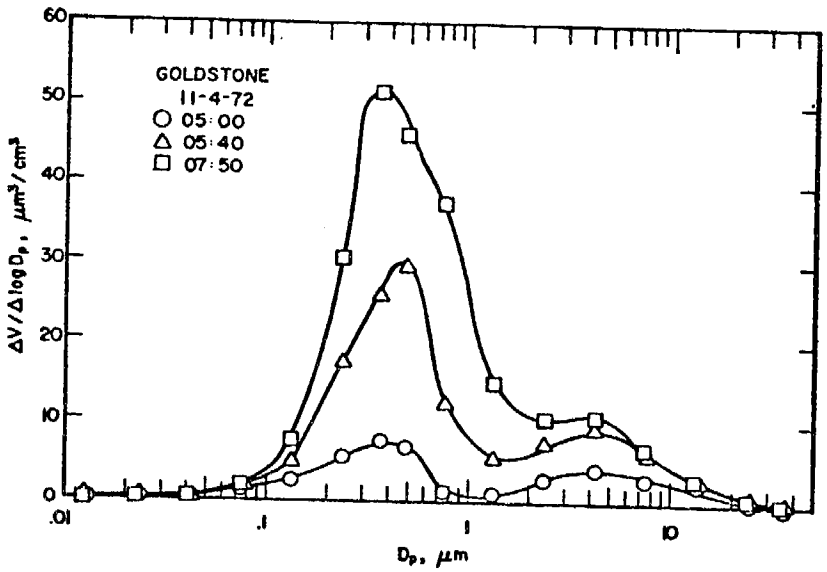

Figure B-13. Incursion of Aged Aerosol From the South Coast Basin

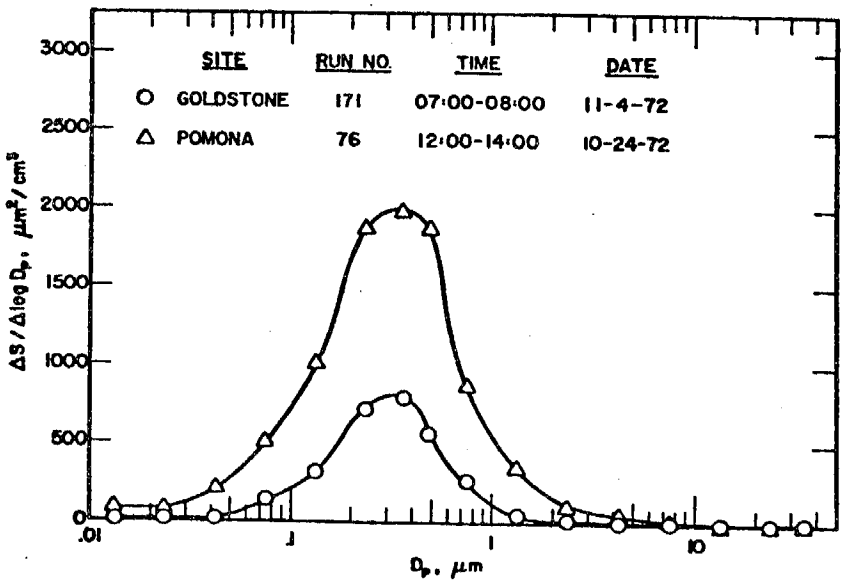

Figure B-14. A Comparison of the Aged Aerosol Sampled at Goldstone and Pomona

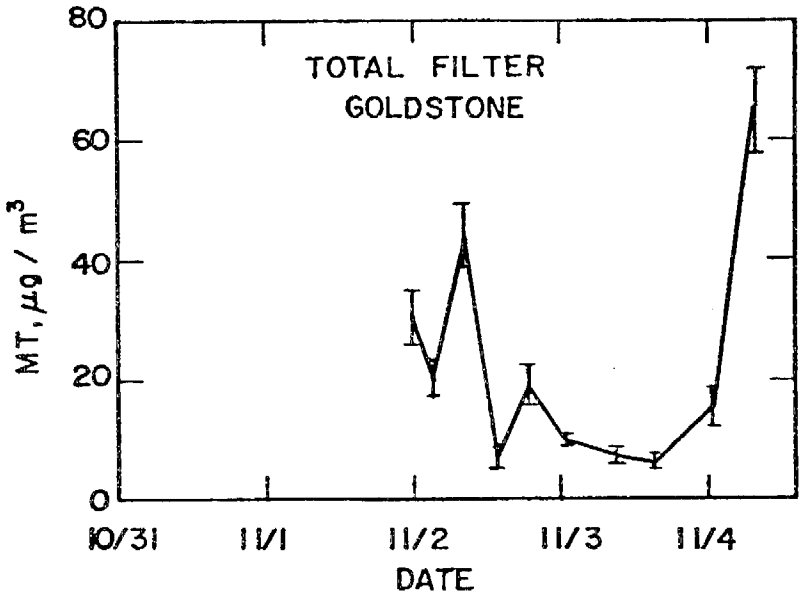

Figure B-15. Total Mass of Aerosol at Goldstone Determined From the Total Filter

APPENDIX C

CONDENSATION NUCLEI COUNT VS. V3-/b_{scat}*

INTRODUCTION

The work reported here was performed to further investigate the relationship between the scattering coefficient, b_{scat}, and sub-micron aerosol volume, V3-, as an aid for the characterization of background aerosols. The present preliminary report examines the relationship between the condensation nuclei concentration, CNC, and the ratio V3-/b_{scat} (K). This is only one way of examining the interrelationships between these variables. Earlier work involved an examination of the correlation of V3- with b_{scat} using an estimate of the geometric mean size of the sub-micron volume mode of the aerosol.

This work is preliminary in nature. First, the final data tapes are not yet available. Therefore, all the data taken were not used. This is especially significant with regard to the non-urban sites at Goldstone and Point Arguello. Secondly, most of the averages which were used for the present work were averages over filter chemistry times which are not appropriate for this study. The data used represent times ranging from 10 minutes (San Pablo) to 14 hours (Goldstone). Thirdly, there has not been sufficient time to investigate the influence of other variables on K.

GENERAL CORRELATION OF CNC VS. K

Figure C-1 shows a plot of condensation nuclei concentration vs. K with certain classifications superimposed on the data. Figure C-2 shows the ACHEX II data plotted on a separate graph with the same scale for clarity. The CNC ranges from about 50 to 5×10^6 per cm^3. K ranges from 2 to 60. V3- ranges from 0.74 to 159 $\frac{\mu m^3}{cm^3}$ and b_{scat} from 0.21 to 20.9 $\times 10^{-4} m^{-1}$.

---

*George M. Sverdrup and Kenneth T. Whitby, Mechanical Engineering Department, University of Minnesota, August 12, 1974.

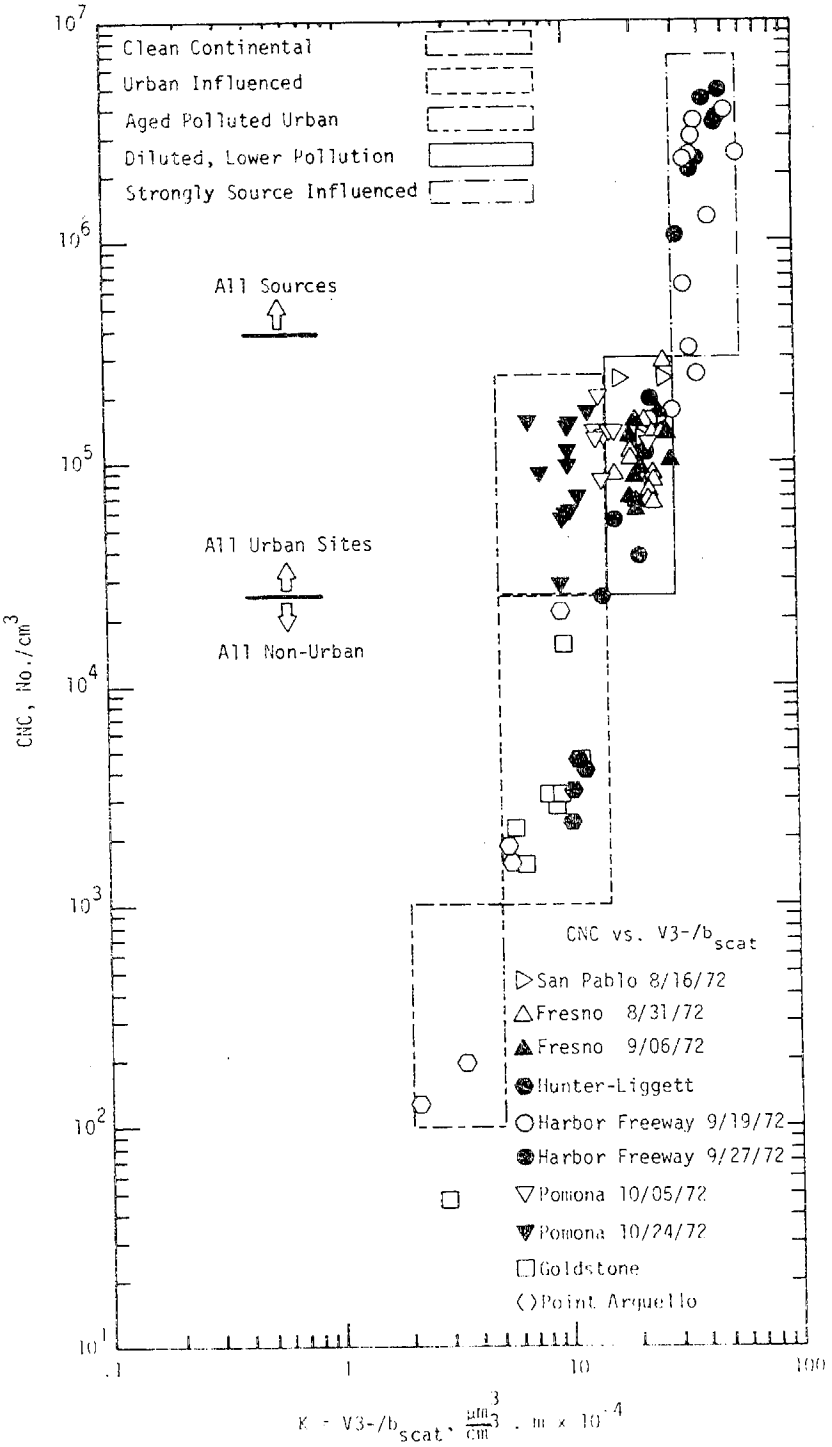

Figure C-1. Condensation Nuclei Concentration vs. K with Superimposed Aerosol Classifications for ACHEX I Data.

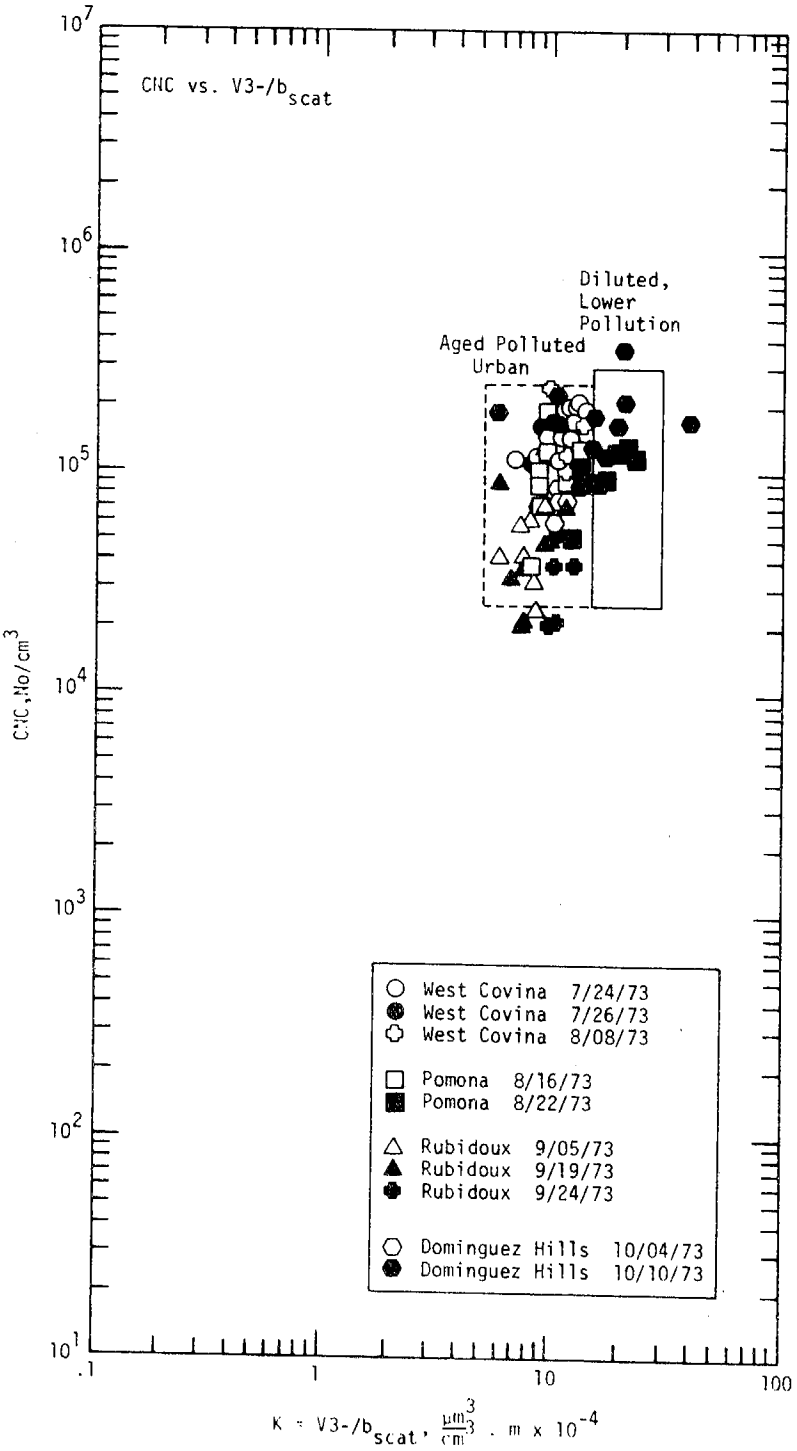

Figure C-2. Condensation Nuclei Concentration vs. K for ACHEX II Data

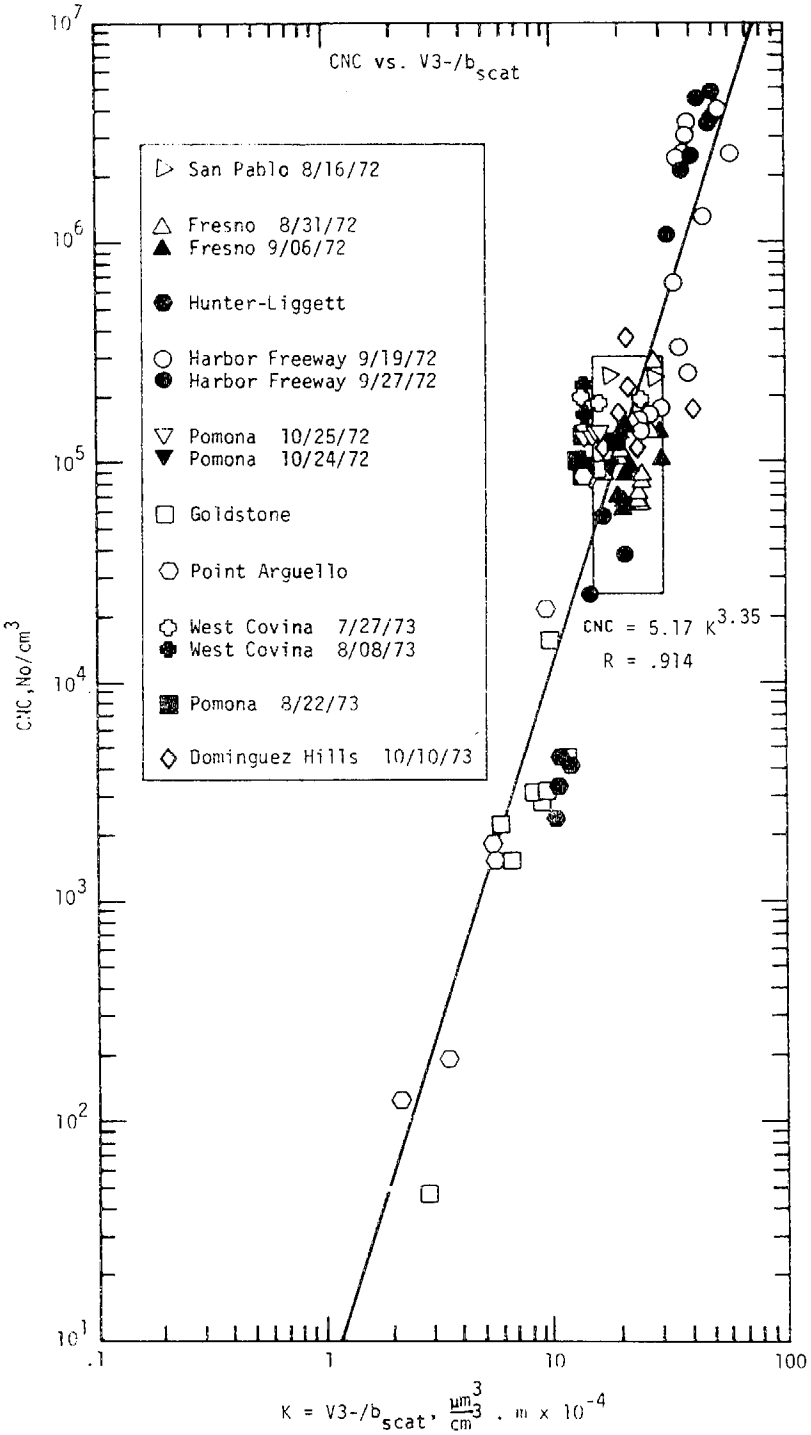

Figure C-3. Condensation Nuclei Concentration vs. K for ACHEX I and II Data, Except Aged Polluted Urban Category With K < 13

TABLE C-1

IDENTIFIABLE CATEGORIES OF URBAN AND NON-URBAN CONCENTRATIONS OF CNC AND K = V3-/BS

Category	$\frac{\mu m}{cm^3} \cdot m \times 10^{-4}$ K(V3-/BS)	No./cc CNC
Clean Continental	2 - 5	100 - 1K
Urban Influenced (Urban District)	5 - 15	1K - 25K
General Urban		
Aged Polluted	5 - 15	25K - 250K
Diluted, Lower Pollution	15 - 30	25K - 300K
Strongly Source Influenced	30 - 60	300K - 7000K

It appears that there is a general and significant correlation between CNC and K. An overall power fit to the 169 data points resulted in the following equation with a correlation coefficient of .746:

$$CNC = 236\ K^{2.25}$$

Referring to Figure C-1 it is seen that the line K = 15 divides the two categories labelled Aged Polluted Urban and Diluted, Lower Pollution. After some work with the data, it was felt that a K = 13 line might be more appropriate although it is still rather arbitrary. Hence, Figure C-3 shows a plot of the ACHEX I and II data neglecting those data in the Aged Polluted Urban category with K < 13. A curve was fit to the 93 data points resulting in the following equation:

$$CNC = 5.17K^{3.35}$$

The correlation coefficient was 0.914.

In order to determine what effect relative humidity (RH) might have played, the data were plotted as in Figure C-1 and C-2, and marked according to three R.H. categories which characterized them:

$$RH < 50\%$$
$$50\% < RH < 75\%$$
$$75\% < RH$$

No systematic variation of CNC vs. K with RH was detected.

AEROSOL CATEGORIES

From Figure C-1 it can be seen that the data fall into groupings which can be identified with general location. The categories are listed in Table C-1 along with appropriate values of K and CNC.

The data from ACHEX I can be divided into urban and non-urban categories by a nuclei concentration of 25,000 per cm^3.

Clean Continental

Clean continental conditions were rare during the ACHEX. From Figure C-1 it is seen that such conditions were encountered at Goldstone (C-1) and Point Arguello. Table C-2 shows the range, mean, and percent standard

TABLE C-2

THE RANGE, MEAN, AND PERCENT STANDARD DEVIATION OF
BSCAT, V3-, AND VT FOR CATEGORIES OF CLEAN CONTINENTAL AND URBAN CONDITIONS

		$m^{-1} \times 10^4$				$\frac{\mu m^3}{cm^3}$				$\frac{\mu m^3}{cm^3}$			
		BSCAT				V3-				VT			
	No. Pts.	Min.	Max.	Avg.	% Std. Dev.	Min.	Max.	Avg.	% Std. Dev.	Min.	Max.	Avg.	% Std. Dev.
Clean Continental	3	.350	.362	--	--	.74	1.85	--	--	1.85	8.16	--	--
Urban Influenced	14	.259	2.02	--	--	2.28	23.	--	--	5.14	76.0	---	--
Aged Polluted Urban	74[1]	.211[2]	20.9	6.26	63.5	1.73[3]	159.	58.5	54.5	21.1	450.	119.	59.7
Diluted, Lower Pollution	60[4]	.482	4.66	1.57	66.8	7.19	79.6	29.7	56.8	17.4	138.	66.6	42.
Strongly Source Influenced	16	.663	2.62	1.19	46.2	31.8	96.6	50.4	40.1	44.4	134	80.3	34.9
Denver City Maintenance Yard	13	.14	2.4	--	--	1.0	32.8	--	--	3.6	207	--	--
Denver Welby	4	.99	2.91	--	--	11.5	56.1	--	--	47.2	466	--	--

[1] 61 Runs for VT

[2] Only two runs below $1.3 \times 10^{-4} m^{-1}$

[3] Only two runs below 10 $\frac{\mu m^3}{cm^3}$

[4] 58 runs for VT

deviation of V3-, b_{scat}, and VT for each category. The mean was not calculated for categories in which there were few data points and in which the data were already averaged over significantly different time periods.

The boundaries for this category are very tentative. Values of K are somewhat uncertain since the baseline value of the nephelometer was $.23 \times 10^{-4} m^{-1}$, and the b_{scat} values for this category were not much above that value.

Urban Influenced

This category includes the Urban District category proposed by Whitby in another classification scheme. The CNC ranges from 1K to 25K per cm^3 and K ranges from 5 to 15. Data were obtained from Hunter-Liggett, Goldstone, and Point Arguello. The data are significant because it appears that much of the background aerosol in Southern California is influenced by urban sources.

General Urban Aerosol

The lower limit of CNC for aerosols sampled in urban locations was about 25K per cm^3. From Figure C-1 it is seen that except at the Harbor Freeway site an upper limit of $2.5\text{-}3 \times 10^5$ per cm^3 was obtained. This limit, established by coagulation, is in agreement with values reported previously for Los Angeles[C-2].

The general urban aerosol has been divided into two categories depending on the value of K.

Aged Polluted Urban

The Aged Polluted Urban category has K values ranging from 5 to 15. That these are the same K values as for the Urban Influenced category is reasonable since aged aerosols would also be expected to make up the Urban Influenced category. The lower limit of nuclei concentration overlaps into the Urban Influenced category for the Rubidoux data. Rubidoux generally had a lower nuclei concentration. The difference between an Aged Polluted Urban aerosol and an Urban Influenced aerosol can be simply the degree of dilution.

The highest mean values for b_{scat}, V3-, and VT were obtained for the Aged Polluted Urban category.

Figure C-1 shows that all Pomona data taken on October 24, 1972 fall into this category. Data from Pomona on October 5, 1972, a day during which

Santa Ana conditions prevailed, is in the transition zone between the two urban categories.

Diluted, Lower Pollution

This category has K values from about 15 to 30. Mean values of V3-, b_{scat}, and VT were lower than for the Aged Polluted Urban category.

All Fresno data fall into this category as well as data from Pomona taken during relatively clean conditions. Data from the Harbor Freeway site taken during periods when the wind was not from the freeway or when there was little traffic also fall into this category[C-3].

Strongly Source Influenced

Figure C-1 shows that this category has the largest K values ranging from 30 to 60. The CNC ranges from 3×10^5 to 7×10^6 per cm^3. All data are from the Harbor Freeway site. Table C-2 indicates that b_{scat} was only slightly greater than that for the Urban Influenced category while V3- and VT were much greater.

REFERENCES

C-1. G. M. Sverdrup, K. T. Whitby, and W. E. Clark, The Aerosol Size Distribution in the Mojave Desert, submitted to J. of Atmospheric Environment (1974).

C-2. K. T. Whitby, R. B. Husar, and B. Y. H. Liu, The Aerosol Size Distribution of Los Angeles Smog, J. of Colloid and Interface Science, 39, 177-204 (1972).

C-3. K. T. Whitby, W. E. Clark, V. A. Marple, G. M. Sverdrup, G. M. Sem, K. Willeke, B. Y. H. Liu, and D. Y. H. Pui, Size Distribution of Freeway Aerosol, submitted to J. of Atmospheric Environment (1974).